A concept design for the removal of concrete legs of gravity based structures

Master of Science Thesis

J.A. Vogel

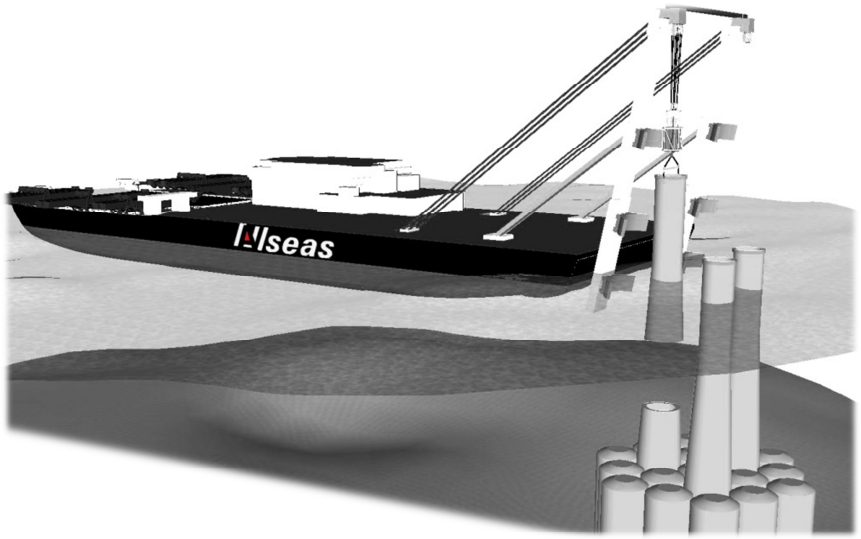

Allseas

TU Delft

A CONCEPT DESIGN FOR THE REMOVAL OF CONCRETE LEGS OF GRAVITY BASED STRUCTURES.

Master of Science Thesis

For the degree of Master of Science in Offshore and Dredging Engineering at
Delft University of Technology

Graduate student:	Juri Vogel
Date:	30-9-2015

Graduation committee

Prof. dr. A.V. Metrikine	Delft University of Technology
Dr.ir. K.N. van Dalen	Delft University of Technology
Ir. J.S. Hoving	Delft University of Technology
Ir. H. Hendrikse	Delft University of Technology
Ir. O. Kooy	Allseas Engineering B.V.
Ir. M.J. van Kampen	Allseas Engineering B.V.

Preface

This report is the Master Thesis of Juri Vogel, student at Delft University of Technology, Faculty of Civil Engineering and Geosciences.
This thesis project is the last part of my studies in Offshore and Dredging Engineering. The project has been carried out under the guidance of Allseas Engineering, Delft. The subject of this report is the concept design for the removal of concrete legs of gravity based structures.

I am very pleased that I got the opportunity to carry out my thesis research at Allseas Engineering. Allseas is well known for its pioneering work and their ability to surpass technical boundaries. I could get involved in the most challenging offshore project at the moment, namely the preparation of the Pioneering Spirit, one of the world's largest vessels, for installation and removal of huge offshore structures and for advanced pipe laying. Of course many challenging research items arise in the realisation of these tasks. My research item was concentrated on the lifting phase of the concrete legs of an offshore platform.

At first I concentrated my attention on the broader context, because the research solution for one component will influence the possibilities for the design of other components in the total removal concept. After mastering the possibilities and challenges of the removal concept, I directed my further research attention to the lifting procedure. I carried out detailed studies on a crucial part in the lifting process, the initial lifting phase. I found out that fast lifting is essential in the initial lift phase and I concentrated my design activities on this part.

Acknowledgements

First of all I would like to thank the members of my graduation committee for their comments and support during my graduation project. The members of this committee are:

- Prof. dr. A. Metrikine
- Ir. J.S. Hoving
- Dr.ir. K.N. van Dalen
- Ir. H. Hendrikse
- Ir. O. Kooy
- Ir. M.J. van Kampen

I would like to thank Allseas and its Innovations department for the inspiring time, help and advice during my graduation.
Furthermore, I would like to thank my family and friends for their support during the years I spent in Delft.

Abstract

During the early 1970s the offshore market in the North Sea was growing rapidly. Due to discoveries of natural reserves and development of the oil price, the oil and gas industry developed and deployed many bottom founded offshore structures in the North Sea. Apart from steel jacket structures, many concrete gravity based structures (CGBSs) were constructed.

In the coming decades many of the fields with these CGBSs approach the end of their lifetime and must be decommissioned. However, currently no solid solution for the removal of these concrete substructures is available. The introduction of Allseas' *Pioneering Spirit* and her capabilities could provide new possibilities for the decommissioning of CGBSs.

The *Pioneering Spirit* is designed for the decommissioning of platforms and its substructure using a unique "single lift" technique. A complete removal of the concrete substructure using this single lift technique is, due to its constructive condition, a perilous operation. However, the decommissioning regulations allow a partial removal of the concrete legs above a water depth of 55 meters. At this water depth a cut is made in the legs and after cutting the *Pioneering Spirit* can perform a lift of the leg using the Jacket Lift System (JLS). During this removal operation various problems may arise.

In this study the main technical difficulties of the partial removal operation are identified. A focus is laid on the difficulties during the lifting phase. The hoisting speed of the JLS is relatively slow compared to the ship motions. This can result in a rebound of the leg during the initial lifting phase. Damage to the leg and a probable damage to the part of the GBS where the oil storage was located may then occur. The objective in this study is to design a solution for the initial lifting phase and analyze the feasibility of this concept.

An adequate fast lifting solution after cut-off could overcome the problems associated with the rebound of the concrete legs. The designed solution for fast lifting is based on the concept of a passive heave compensator (PHC).

The basic working principle of the concept resembles a pre-tensioned spring. The PHC will function as a spring, the pretension on the system will be provided by pressurized gas in a connected accumulator. The end of the cylinder of the PHC is connected to the main hoist and the piston rod is connected to the concrete leg. After the cut has been

made in the leg, the pressure of the accumulator will automatically push the piston and consequently the concrete leg, to a higher point. Ultimately, this results in a device which provides fast lift capabilities for loads with high mass uncertainty and prevents large load variances in the main hoist ropes.

To gain insight into the feasibility of this concept a model has been made in MATLAB/Simulink. Input data for the simulation model are mechanical dimension parameters and physical pressure parameters. By altering the parameters an estimation of the motions of the leg and hence the feasibility of the concept is determined.

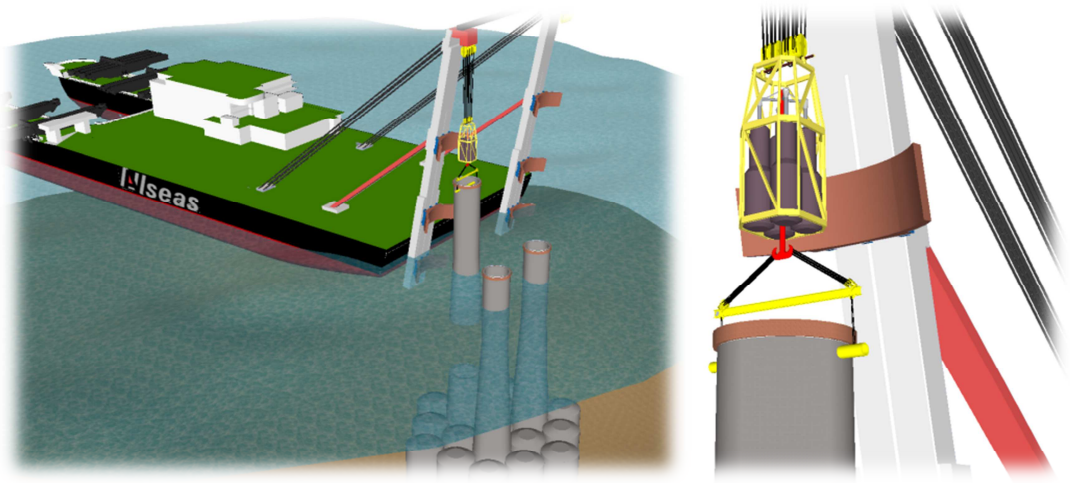

Contents

List of Abbrevations

CGBS	-	Concrete Gravity Based Structure
CoG	-	Centre of Gravity
HLV	-	Heavy Lift Vessel
JLS	-	Jacket Lift System
OSPAR	-	Oslo-Paris Convention on the protection of the marine Environment of the North-East Atlantic
HC	-	Heave Compensator
PHC	-	Passive Heave Compensator
PS	-	Pioneering Spirit
TLB	-	Tilting Lift Beam
TLS	-	Topside Lift System

ROV	-	Remotely Operated Vehicle

List of Symbols

Δp_w = Flow resistance [N/m^2]

d_i = Internal diameter [m]

ρ = Density [kg/m^3]

λ = Friction factor [-]

V_m = Flow velocity [m/s]

Re = Reynolds number [-]

υ = Viscosity [m^2/s]

p = Gas pressure [N/m^2]

V = Volume [m^3]

n = Amount of moles of the gas [-]

R = Universal gas constant [-]

T = Temperature [K]

κ = Adiabatic gas constant [-]

c_{pipe} = damping coefficient [kg/s]

d_i = Internal diameter [m]

A = Surface area [m^2]

c = friction coefficient [Ns/m]

k = spring stiffness [N/m]

Q = Flow [m^3 / s]

D = Diameter [m]

m = Mass [kg]

g = gravitational acceleration [m/s^2]

F = Force [N]

u = Displacement [m]

ΔL = Elongation [m]

h = Height [m]

n_H = Number of reevings of the hoist wire configuration [-]

EA = Effective wire rigidity [N]

L = Length [m]

1 INTRODUCTION

1.1 Allseas

In 1985 Edward Heerema founded the Swiss-based Allseas Group S.A., a company specialized in offshore pipeline construction. Currently Allseas is a global leader in the offshore pipelay and subsea construction industry employing over 2000 people worldwide and operating seven in-house designed special purpose vessels of which 4 are specialized in pipelaying. Most of the projects' engineering is done from the Allseas Engineering BV office in Delft, The Netherlands.

In this 30 years of Allseas' engineering, it has become a tradition to pioneer and surpass technical boundaries as was done over the years introducing pipelay on dynamic positioning and laying pipelines in ever deeper waters. Since the founding of the company a reliable solution for the installation and decommissioning of platforms was found in the so called "single lift" technology.

This technical step in platform installation and decommissioning has been reflected in Allseas latest vessel, the Pioneering Spirit (PS). This vessel encompasses all innovations that have been developed by Allseas over the last 30 years. (Fig. 1-1)

Figure 1-1 "Pioneering Spirit"

The PS, with its length of 382 meter and a breadth of 124 meters is one of worlds' largest vessels. This dynamically positioned platform installation, removal and pipelay vessel has been designed as a worldwide operational multi-purpose lift and transportation vessel.

The most common type of offshore structure in service today is the jacket structure. The PS is designed for the removal of the complete platform topside + jacket structure. Currently jackets are removed by Heavy Lift Vessels in modules, the steel structure is cut into smaller parts. This involves a lot of offshore time and risks.

With a game changing single lift technology the PS is capable of installing and removing topsides as well as steel jackets structures in one single lift, as showed in Fig. 1-2.

Figure 1-2 – Impression of the Pioneering Spirit

1.2 Concrete gravity based structures

During the early 1970s, the offshore market in the North Sea was growing rapidly. Due to discoveries of natural reserves and development of the oil price, the oil and gas industry developed and deployed many offshore structures in the North Sea.

The North Sea area is ideal for the application of fixed offshore structures, because of the relatively shallow water and its harsh environment. Besides steel jacket structures, many concrete gravity based structures (CGBSs) were constructed.

A CGBS is generally a very large and extremely heavy reinforced concrete structure which is placed on the seabed. An example of a CGBS is shown in Fig. 1-3. It withstands the extreme environmental forces in the North Sea, by virtue of its own weight and inherent strength. Furthermore, a CGBS is ideal to support the very high topside weight of the processing facilities of high production rate fields.

Figure 1-3 "Brent Bravo CGBS"

In the early 1970s, the pipeline infrastructure to transport the crude oil to shore was rare and insufficient. The large storage capacity within the base of these CGBSs could compensate for the lack of infrastructure for the transportation of the crude oil. CGBSs provided development solutions to a large scale of oil fields.

Since 1973 a total of 27 CGBSs have been installed in the North Sea area. Coming decades many of these fields approach the end of their lifetime and must be decommissioned because of OSPAR regulations.

1.3 Installation

Concrete offshore platforms of the gravity-base type are almost always constructed in their vertical attitude. After constructing the base of the concrete substructure, which is composed of a cell structure that can be used for the storage of oil, the concrete legs are built on this base. This generally takes place in a sheltered fjord, due to the depth of the structure, and this allows the inshore installation of equipment. Transport of the whole structure to the installation site is done by towing the floating substructure to its final location. By ballasting the base of the structure, it will be sunk to the seabed. The so-called skirts, which are located beneath the cell structure, are sunk into the soil. This will provide a firm foundation of the structure.
The weight, size and presence of these skirts make it too risky to use a reversed installation, a refloat, as the applied removal procedure.

Currently no solid solution for the removal of these concrete substructures is present. The introduction of the Pioneering Spirit and her capabilities could provide new possibilities for the decommissioning of concrete GBSs.

1.4 OSPAR

When the economic end of the production phase of a field is reached, the platform will be shut down. After decades of production the heavy concrete construction has to be removed from the seabed, which is a precarious operation.

There are four main ways of decommissioning offshore structures. Currently they are either completely removed, partially removed, disposed of at sea or left in place with only the topside removed.

The Oslo-Paris Convention (OSPAR) on the protection of the marine environment of the North-East Atlantic in 1998 states that platforms need to be removed completely. OSPAR Decision 98/3 provides the regulatory framework [1].

- All topsides of all structures are to be removed and brought to shore for reuse, recycling or disposal.
- All sub-structures or jackets weighing less than 10,000 tons must be totally removed and brought to shore for re-use, recycling or disposal.
- For sub-structures weighing over 10,000 tons, there is a presumption to remove them totally but with the potential of a derogation being agreed on whether the footings might be left in place.
- Derogation may be considered for the heavy concrete gravity based structures as well as for floating concrete installations and any concrete anchor-base.

The OSPAR decision recognizes that there may be technical difficulties and major environmental/safety risks in removing some support structures, and therefore some exceptions may be granted, known as “derogations”.

An example of a relevant decommissioning project is the Frigg field. In the end of 2012 the Frigg field was decommissioned. The five topsides and steel substructures were removed in parts, but the concrete substructures were left in place. The alternatives for the removal of these constructions were considered too risky and an exemption for derogation of the OSPAR regulations was made. As a solution navigation aids were installed on the concrete constructions.

Summarizing, international legislation requires topsides to be fully removed. For a concrete installation an exemption or derogation may be sought to be ‘dumped or left wholly or partly in place’ where it can be shown that ‘there are significant reasons why an alternative disposal method is preferable to re-use or recycling or final disposal on land’. Significant costs make the decommissioning a considerable phase of the offshore platform life cycle.

1.5 Overview of CGBSs

An overview of the installed CGBSs will provide a scope for upcoming removal projects. A similarity in the design of CGBSs can give opportunities for the applicability of a removal concept.
Since the 1970s until 1999 a total of 27 CGBSs had been installed in the OSPAR Maritime Area. With depths ranging from 42 to 303 meter and weights of the substructure from 46 to 830 ton, different types of CGBSs were constructed. They can be divided into three main types depending on the design of the concrete base or caisson:

- concrete base with a single caisson extending above sea level (surface piercing).
- concrete base consisting of storage cells, with one or more concrete shafts extending above sea level
- concrete base supporting steel legs.

The most common type with a number of 20 installed CGBSs in the OSPAR area is the design with concrete shafts on a concrete base; the Condeep design.

Figure 1-4 "Overview CGBSs outside OSPAR region"

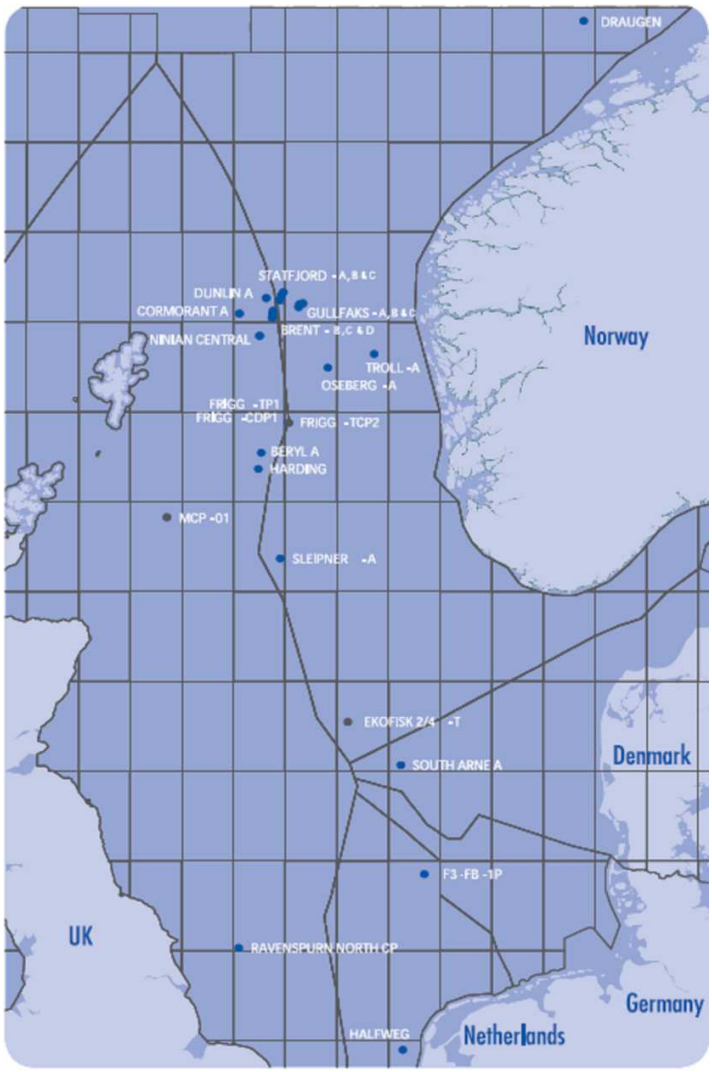

Figure 1-5 "Overview CGBSs OSPAR region"

1.6 Decommissioning Scope

Summarizing; coming decades many of these fields approach the end of their lifetime and must be decommissioned. Decommissioning plans are even accelerated due to the dropping oil price. However, currently no solid solution for the removal of these concrete structures is available. The introduction of the Pioneering Spirit and her capabilities could provide new possibilities for the decommissioning of concrete GBSs.

A complete removal of the concrete substructure is, due to the constructive condition, a perilous operation. Therefore, OSPAR regulations allow a partial removal of the concrete legs above a depth of 55 meters below LAT.
In the coming years decommissioning of fixed platforms will proceed. This will include projects concerning concrete gravity based structures. Some projects are already in the preparatory phase. This prospect creates the need for a safe, practical and feasible solution for the removal of CGBSs. Since complete removal is considered as too risky and therefore not feasible, partial removal of the substructures could provide a feasible solution.

The majority of the concrete support structures of GBSs in the OSPAR region are of the Condeep design, shown in Fig. 1-6. Determination of a method to remove these legs partially will allow initiation of future decommissioning projects.

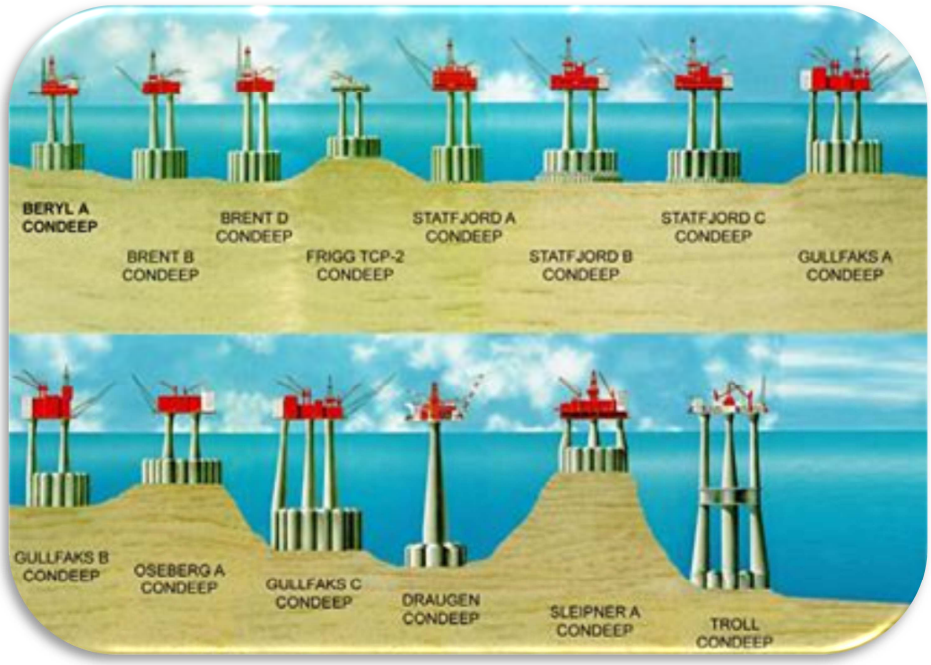

Figure 1-6 - "Condeep design CGBSs"

2 PROBLEM DEFINITION

2.1 General

The partial removal of concrete substructures of GBSs is a wide ranging topic. The removal of a CGBS has never been done before; therefore, many uncertainties are present with respect to this topic. New concepts have to be developed which are not based on proven technology.

The design of a complete removal solution involves an extensive design process. The implementation of the complete design process is too extensive for this study. Therefore one component of the removal process will be designed. For the design of this component, but also for the complete removal design, all operational demands need to be defined.

A description of the complete operation will identify the major technical difficulties and the process can be divided into comprehensible parts. Each phase of the removal operation will be analyzed. In this way the required components can be defined.

The components in the total design have a strong coherence; a solution for one component will influence the possibilities for the design of other components of the total removal concept.

Identifying the technical difficulties of each phase will result in the major challenges of the total operation. A solution for one of these major problems will affect the shape of the total concept for the partial removal of the concrete substructure.

In the design process, shown in Fig. 2-1, a number of feedback loops can be recognized. This approach is regarded as an integral design. A design process of the components with open models and flexible algorithms is required. This allows straightforward adaptation of model boundary conditions or system parameters. The feedback loops, as part of this integral design, will be illustrated in chapter 2.3

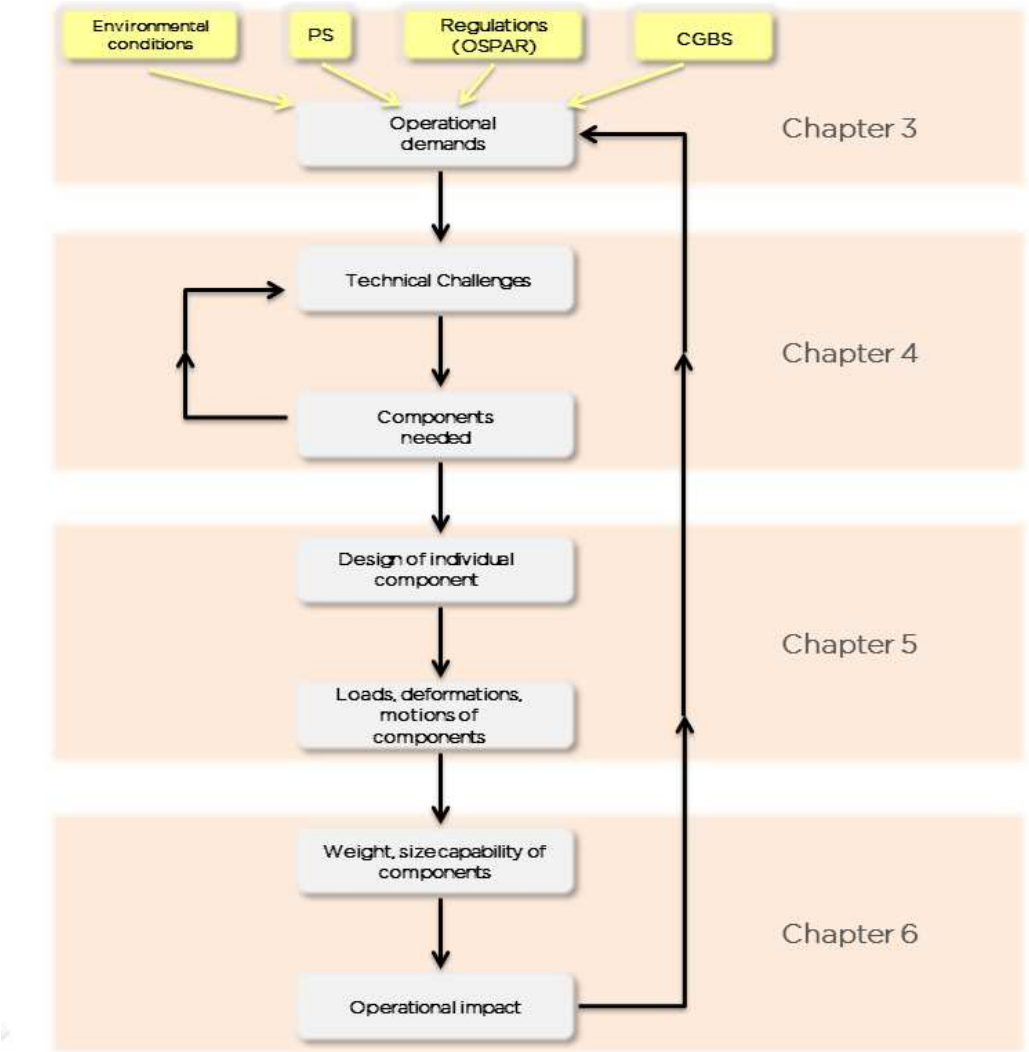

Figure 2-1 "Design Process"

The majority of the installed CGBSs in the OSPAR region are of the Condeep design. In this thesis a case study is done on the Brent Bravo CGBS. This structure is also designed by Condeep and is therefore in many ways similar to most of the installed CGBSs.

2.2 Thesis Objective

In this study the main technical difficulties of the partial removal operation for different phases in the process will be identified, defining the components needed for the complete operation. A focus will be laid on the difficulties during the lifting phase.

The removal operation will take place in open sea. Since the North Sea can have very harsh seastate conditions, this offshore operation could be confronted with less favourable conditions. It is therefore important to know the dynamic behaviour of the Pioneering Spirit and the concrete shaft at all different phases of the lift procedure.

One of these phases can be defined as the initial lifting phase, the phase were the cut part of the substructure will be disconnected from the bottom founded part.
In this study focus will lay on the start of the lifting operation, the initial lifting stage, with the main objective:

Design a solution for the initial lifting phase and analyze the feasibility of this concept.

An important technical challenge in the total removal process is the avoidance of a rebound of the lifted part of the concrete leg with the remaining bottom founded structure during the initial lift phase.

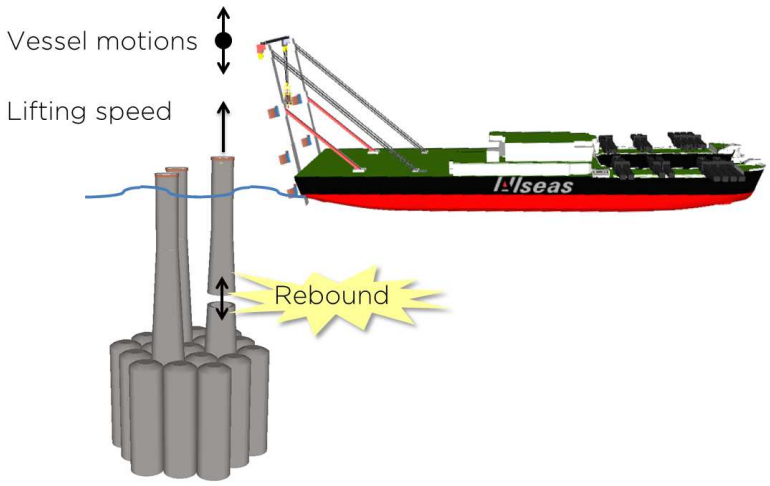

Figure 2-2 "Rebound during lift"

A simplified heavemotion of the PS with lifting speed of JLS is illustrated in Fig. 2-3. To prevent a rebound the timing of the start of the lifting operation is essential.

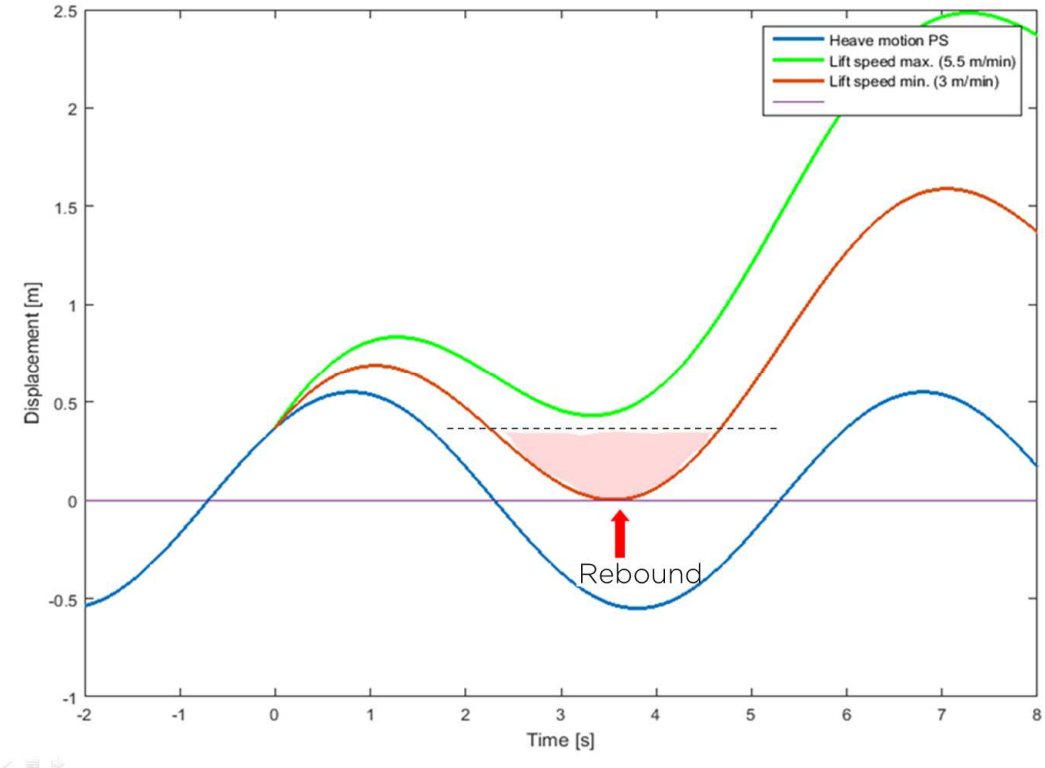

Figure 2-3 - Lift speed vs. heave motions PS

This challenge to avoid rebound can be solved by fast lifting the concrete leg.
In this thesis a component with heave compensation and a fast lift capability will be designed. The various dynamical effects during the lifting phase, such as vessel motion and lifting speed, will be modelled.
The input data for the design of this model are the dimensions of the hydraulic lifting tool. Altering these dimensions will give different responses to the motions of the lifted leg.

The responses of this model are the input for the heave compensating solution to be designed. In this way it can be determined whether the concept is technically possible. By changing these dimensions and by making an estimation of the motions of the leg, the feasibility of the concept can be determined.

2.3 Methodology

In this thesis a concept for the removal of the concrete legs with the JLS is analyzed. By means of a model the requirements and assumptions for a concept design for a lift system will be set. In the analysis the technical and operational feasibility for the solutions are determined and the risks are discussed in order to obtain a reliable solution for the operational removal process.
The problem will be approached using the design process, as shown in Fig 2-1. In this thesis one component of the entire removal procedure will be designed.

Operational demands in Fig. 2-1 has four inputs: The environmental conditions, Pioneering Spirit, OSPAR regulations and the CGBS as concerned.

In this thesis a case study of the Brent Bravo is carried out. An overview of the specifications of the concrete substructure, the vessel and its equipment and the environmental boundaries for which the system has to be designed is given. This will be covered in chapter 3: “Operational demands”.

To gain insight into the technical demands and their mutual interrelationship, an understanding of the complete removal procedure is necessary.

Different phases of the process will be determined providing insight into the technical demands. This will be discussed in chapter 4: “Procedure and technical challenges”.

For each phase the main technical challenges are identified. These challenges are interconnected within the operational procedure. Solutions to these challenges should be found in the design of a component. An adequate solution may influence the technical demands, as illustrated in the feedback loop in Fig. 2-4.

One important technical challenge is the avoidance of a rebounce of the lifted part of the concrete leg with the remaining bottom founded structure during the initial lift phase. The design of a component needed for the initial lifting phase will be presented in chapter 5: “Component design”.

The feasibility of the designed component and the operational impact of the designed component will be discussed in chapter 6: “Feasibility of the lifting tool”. After this phase in the design process a feedback loop can be made. The designed component will

influence the operational demands. However, in this study only one component of the complete system will be designed. The feedback loop will not be considered.

Based on the component design and feasibility study, conclusions and recommendations regarding the initial lifting phase are made for further consideration or investigation. Conclusions and recommendations are presented in Chapter 7.

3 OPERATIONAL DEMANDS

In this chapter all the systems involved in the removal process are described.
In this thesis a case study is done for the Concrete GBS of the Shell operated Brent Bravo platform in the North Sea. This structure has the typical Condeep design for CGBSs. This is the most common design of CGBSs in the OSPAR region. The Brent Bravo platform has an average size in the "family" of the Condeep designed CGBSs.

3.1 Brent Field

The Brent field lies 186 km offshore, north-east of Lerwick, Scotland, at a water depth of 140m, and has four platforms, Alpha, Bravo, Charlie and Delta, as presented in Fig. 3-1. The substructure of the platforms consists of respectively a steel jacket structure and three large concrete gravity based structures.

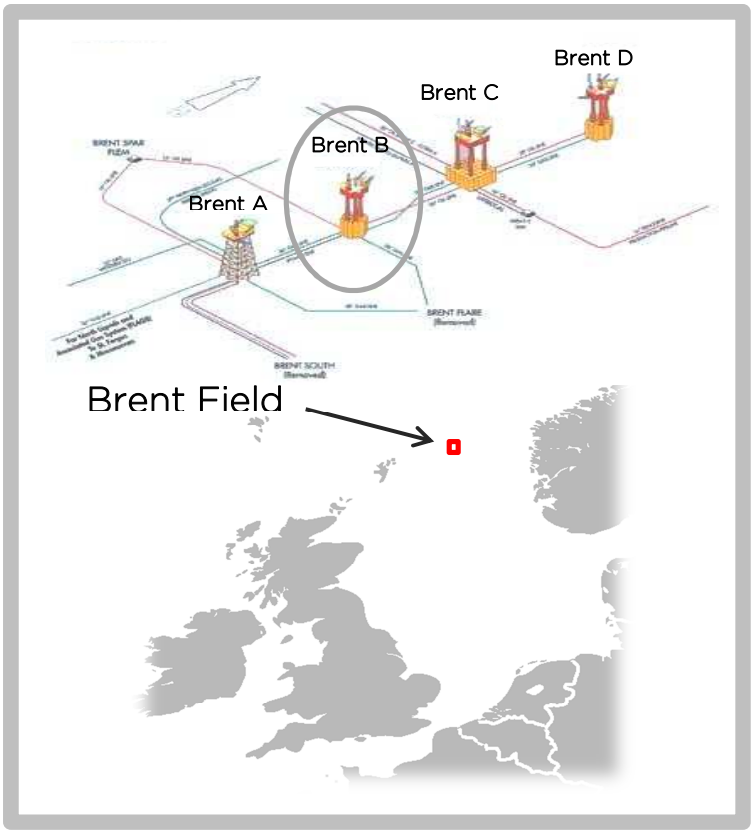

Figure 3-1 – the Brent Field

After more than 35 years of production the field will be shut down. Currently the last phase of the field development will commence: the decommissioning.

Allseas have been awarded by Shell to undertake the removal project the lifting, transportation and quayside load in of the Shell Brent topsides, as part of the Brent field decommissioning project. The PS with its "single lift" technology provides the solution for a safe removal of the topsides, as illustrated in Fig. 3-2. However, a solution for the removal of the concrete support structures has not yet been found.

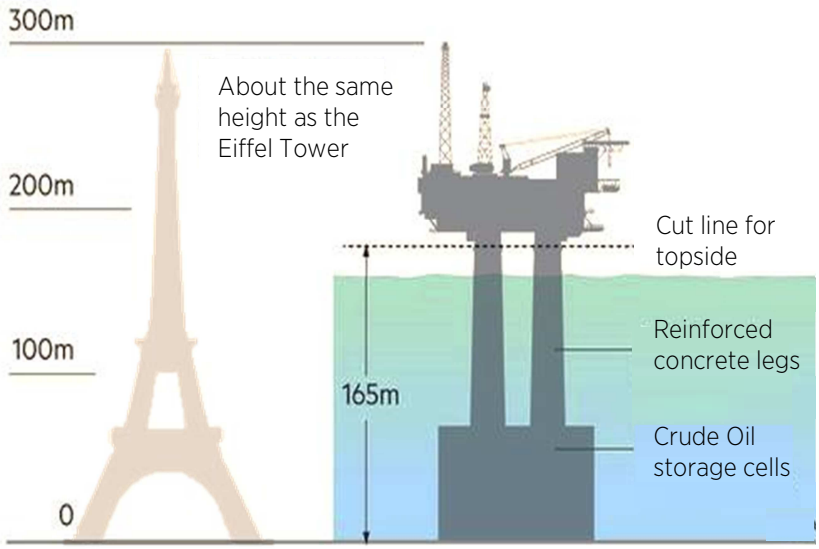

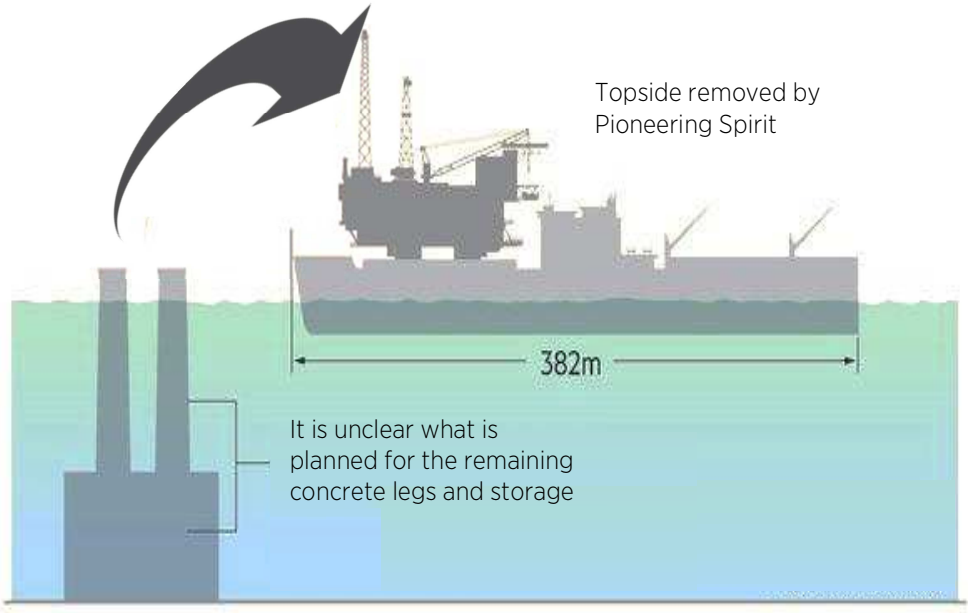

Figure 3-2 "CGBS topside removal"

3.2 Brent Bravo

In 1975 the Brent Bravo platform was installed. This three-legged concrete GBS is similar to the Brent Delta of the Condeep design. Brent Bravo, presented in Fig. 3-3, has a base comprising 19 reinforced concrete cells arranged in a hexagonal-shaped honeycomb caisson, secured to the seabed. Three of the cells extend upward to form the leg bases, while the other 16 are capped off below sea level and are used for oil storage. (surface area of approximately 6,200 m^2).

Figure 3-3 - Brent Bravo

The 16 caissons function as storage cells, which store the crude oil that is drilled. When the oil is pumped in the cells the same amount of water is displaced through pipes located at the bottom of the cells. When oil is exported through the pipes located at the top of the cells, a same amount of seawater is let in. The cells will operate in four different groups. One group fills with oil, one group exports the oil and two groups are used for settling. At the bottom of a storage cell there is sandy ballast.

The remaining content of these caissons cause a high environmental risk. At all costs potential damage to this structure must be avoided during the removal process.

For a partial removal of the concrete leg, the part from -55 m LAT is the most interesting. This part can be modelled by a cylinder with a varying diameter, as shown in Figure XX. In this study this simplified model will be used for calculations.

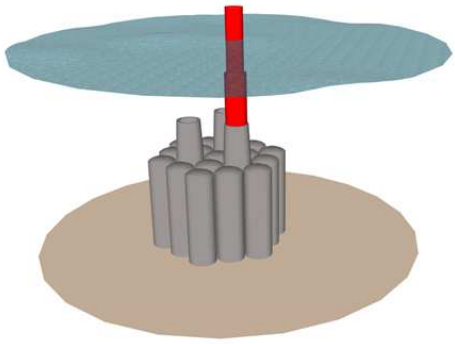

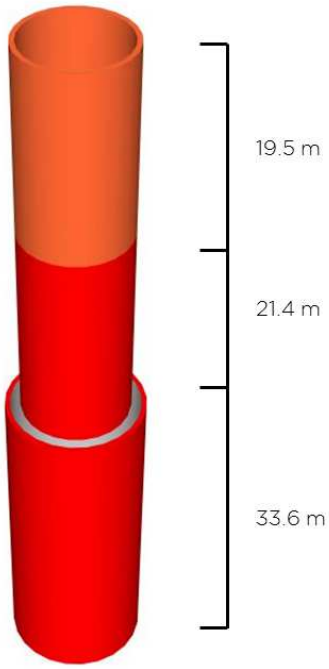

Utility leg		
Height (m)	D_in (m)	D_out (m)
19.5	11.2	12.2
21.4	11.2	12.2
33.6	13.3	14.3
	Total weight (t)	3870
	MN	38.

Figure 3-4 - Simplified model of the Brent Bravo leg

3.3 Environmental conditions

For this study the environmental conditions are of great importance. The environmental conditions influence vessel motions, forces on the concrete structure and eventually the operational limit of the operation.
Operational conditions have been defined as a significant wave height of 2.5m with a zero mean up-crossing period of 12s. A lift will take a maximum of 12h. The environmental conditions are presented in Table 3-1.

Item	Value(s)	Unit
Significant wave height, H_s	2.5	[m]
Wave period (zero mean crossing), T_s	12	[s]
Wave direction, μ	0-360	[-]
Wind	-	[m/s]
Current	1	[m/s]
Spectrum type	JONSWAP	[-]

Table 3-1 - Environmental conditions

3.4 Pioneering Spirit

Allseas' flagship, the Pioneering Spirit, with its length of 382 meter and a breadth of 124 meters is one of worlds' largest vessels. This dynamically positioned platform installation, removal and pipelay vessel has been designed as a worldwide operational multi-purpose lift and transportation vessel.

With a game changing single lift technology the Pioneering Spirit is capable of installing and removing topsides as well as steel jackets structures in one single lift. Key to this technology is the striking hull shape of the vessel. The two bows of the Pioneering Spirit form a giant slot in front of the vessel. In this slot, topsides can be lifted by the Topside Lift System (TLS). For lifting substructures a Jacket Lift System (JLS) is located at the aft of the vessel.

Besides the installation and removal of platforms, the Pioneering Spirit is capable of laying pipelines. The vessel can be converted to lay pipe, by installing a 170 meter stinger in the slot between the bows. With four tensioners of 500 [ton] each pipelines

with a diameter of 68" could be installed with the vessel. In Table 3-2 some specifications of the vessel are shown.

Name	Pioneering Spirit
Length (incl. tilting lift beam protrusion and stinger)	431 m
Length (excl. tilting lift beam protrusion and stinger)	382 m
Breadth	124 m
Slot length	122 m
Slot width	59 m
Topside lift capacity	48000 t
Jacket lift capacity	25000 t
Maximum speed	14 knots
Total installed power	95000 kW
Accomodation	571 persons

Table 3-2 "Pioneering Spirit specifications"

For this study the relative heave motions of the PS for the required seastate are of importance. These relative motions for the tip of the TLB are calculated by the AQWA-model as shown in Fig. 3-3.

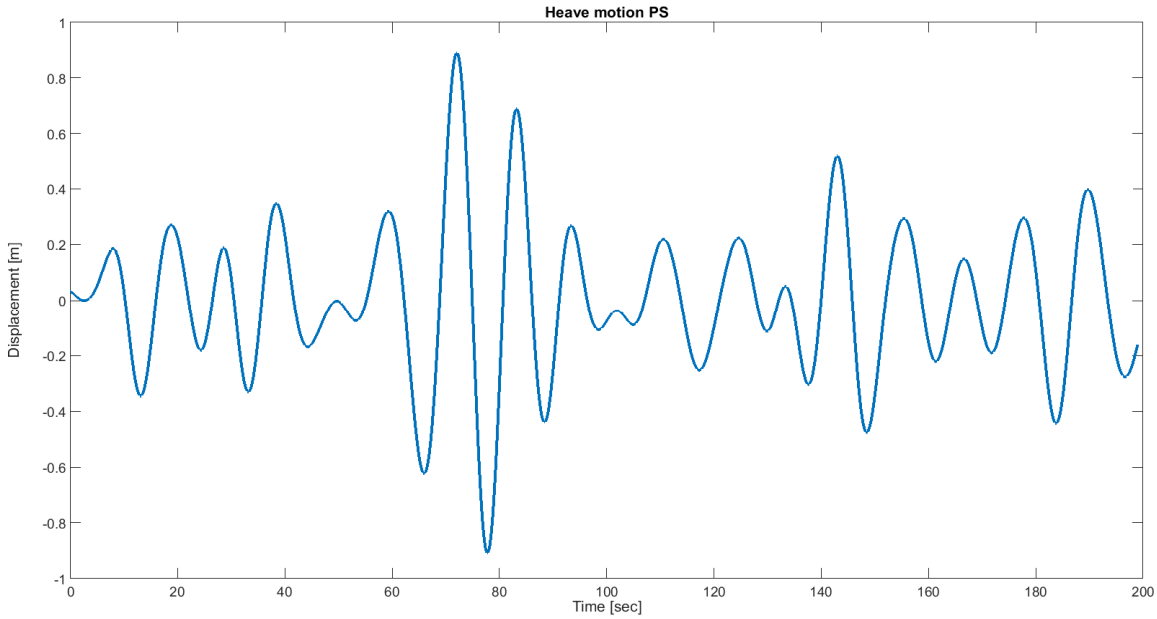

Figure 3-5 – "Heave response PS, Hs=2.5, Ts=12 , Head=0, Pos=Hammerhead"

3.5 JLS

The JLS is located on the stern of the PS. The JLS consists of two tilting lift beams (TLBs), connected over at the top by a beam and is designed to lift jackets up to 25,000 tons and of over 200 meters in length. During transit, the TLBs are supported at the hang-off frame, the upend skid and the derrick hoist skid. The TLBs are upended using a two-step hydraulic push-up system. The outside upenders push the TLB upwards over an angle of 25.6 degrees, the inner upenders upend the TLB from 25.6 to 97 degrees. At the angle of 97 degrees, the center of gravity of the TLB shifts outboard and the TLB rotation is controlled by the derrick hoist cables. The main hoisting blocks are located at the top part of the TLB, called the hammer head. The factored load of a single hoist block is 4,200 tons and the blocks can be combined to a double or triple block. Each TLB is limited to a factored load of 14,400 tons. The JLS has a maximum lifting speed of 5.5 m/min and its slow lifting speed is 3 m/min.

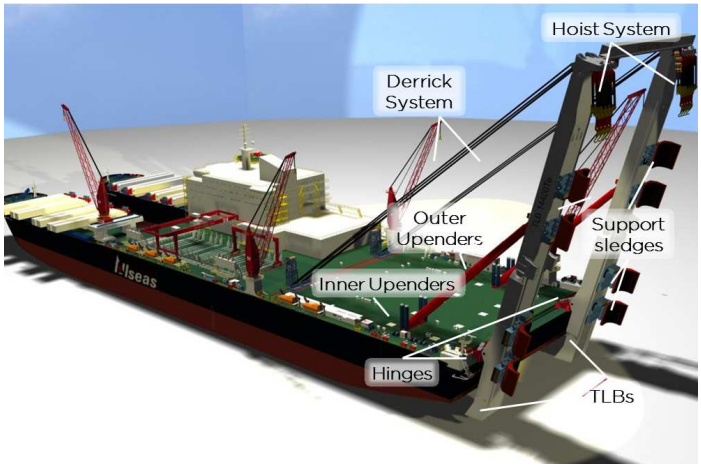

Figure 3-6 - JLS nomenclature

The maximum heavemotions for 2,5m significant wave height for different wave headings of the PS are illustrated in Fig. 3-5. The hoist speed of the JLS is also plotted. It can be clearly seen that this hoist speed, in most situations, cannot keep up with the heave motions of the vessel. This may result in a rebound during the initial lift and undesired slack wires during lifting operations.

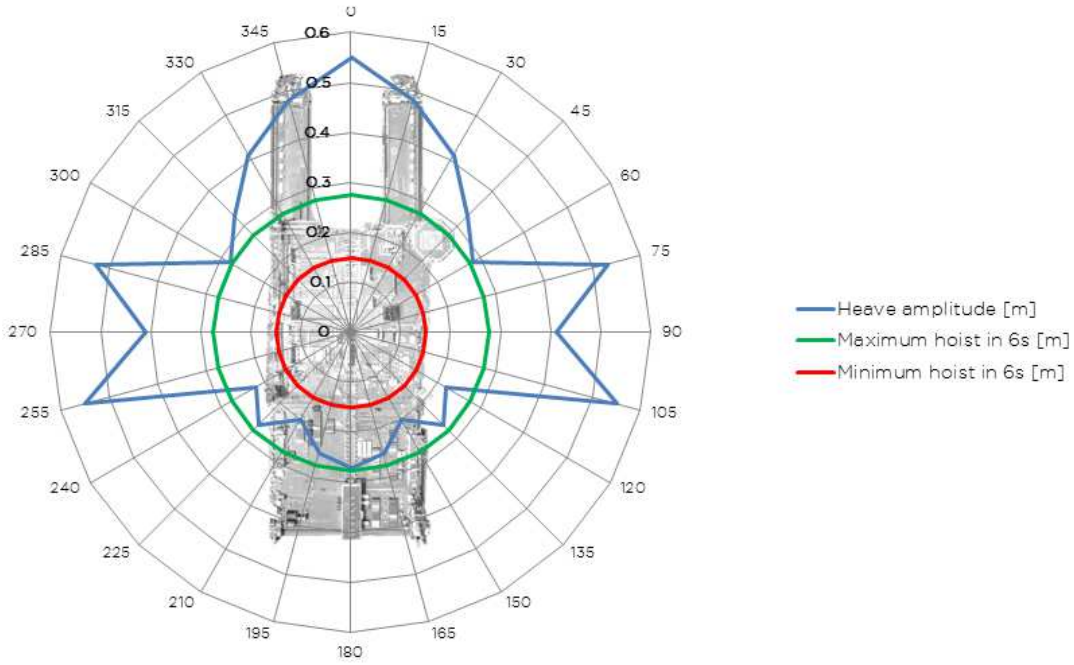

Figure 3-7 - "Heave amplitude per heading and lifting speed"

4 REMOVAL CONCEPT

This chapter describes the removal concept of the GBS legs of Brent Bravo using the JLS of the PS. The concept removal procedure of a concrete support structure will be defined.

4.1 Partial removal

Since current regulations state topsides are under no circumstances to be left offshore for derogation, this will also apply to the Brent B topside.
As was stated in the Offshore-mag about the decommissioning of this Brent platform: "The removal of the platform is expected to be one of the most technologically demanding abandonment projects ever attempted"
For the removal of the topside most of these technological challenges are tackled by the revolutionary single-lift technology onboard the PS, which ensures a safe and cost effective method of removing a topside of this size.
Regulations regarding concrete support structures are less stringent. These state that all installations less than 10.000 tons and with a water column less than 55 meters above the structure should be completely removed. Since the foundations of the Brent B platform weighs much more than 10.000 tons, these regulations do not necessarily apply. However, a section of at least 55 meters below sea level shall have to be removed. For the lower sections of the foundations there is room for debate.

As similar concrete gravity-based structures at the Frigg field have received permits to leave the section underneath the 55 meter water column in place, it is to be expected that the same permits will be issued for the Brent B platform. This means that it is possible to only remove a section of 55 m below sea level and leave the rest in place.
Whether this is legally and environmentally responsible is yet another question. If the storage cells are properly cleaned, partial removal is advised. The costs and risks of removing a larger section outweigh the environmental benefits. Leaving a "clean" concrete structure on the sea bed poses few environmental risks.

Partial removal is the preferred way of decommissioning the columns of Brent B. A section of 55m below sea level will be cut and transported onshore for demolition.

4.2 Removal procedure

In this master thesis the partial removal of a concrete substructure is analyzed.
This partial removal operation of the concrete support structure can be divided into several phases: Preparation, cutting phase, lifting phase and transportation.

To provide a proper insight into this operation the whole conceptual removal process is described in this section.

4.2.1 Preparation

After the topside has been removed from the support structure, the remaining concrete pillars must be prepared for the cut. The support structure of the Brent B platform consists of three concrete legs. Two of the shafts were used as drilling shafts. The conductors inside those shafts have to be cleaned and removed properly. The inside of the legs is shown in Fig. 4-1.

Apart from the platform consisting of a topside and support structure, subsea infrastructures, such as pipelines, are installed. The installed cables and pipes need to be removed as a preparation for the removal procedure.

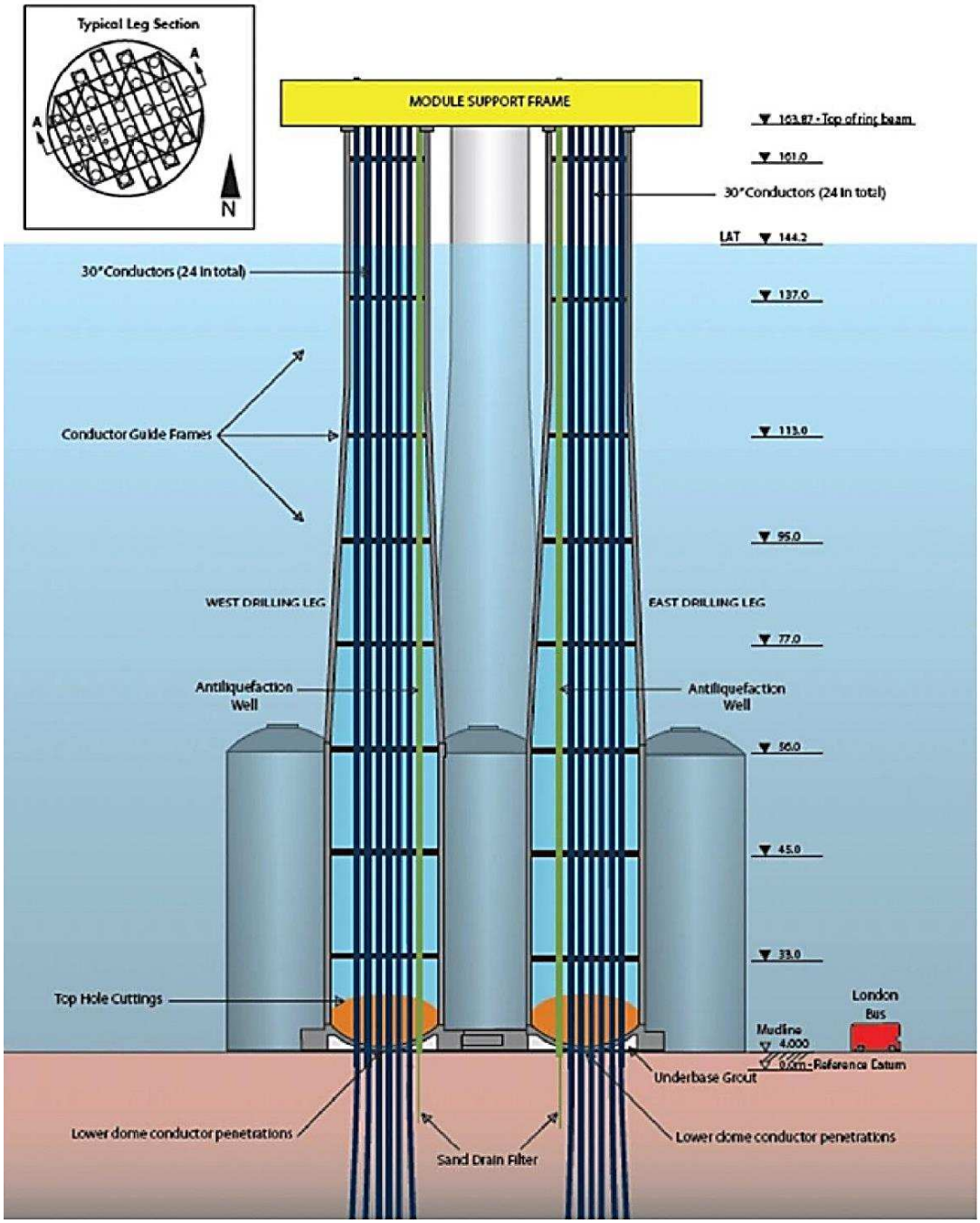

Figure 4-1 - "Brent Bravo leg section"

A following step in the preparatory phase is the installation of lift points on the concrete legs. The firmness of the concrete structure needs to be determined when installing the lift points and when hoisting on the installed lift points.

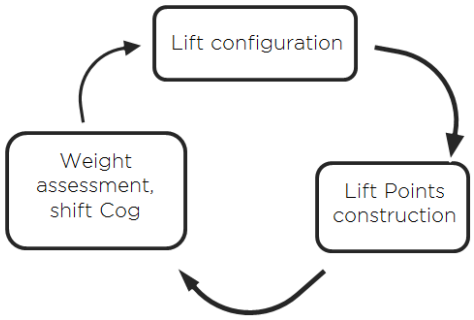

A next step in the preparatory phase is an examination of the stability of the leg. As a swinging or tilted leg is undesirable during lift operation, an assessment of the weight, a detailed study on the CoG of the cut part of the leg, and the influence of the lift operation have to be made.
Consequently, a determination of the lift configuration, that is, the interface between the rigging and the GBS legs, has to be made.
As illustrated in the diagram, the final lift points construction can be deducted from this lift configuration.

In this preparatory phase it is also necessary to take into account the various stability solutions during and after cutting of the leg. These solutions usually require additional connection points or constructions on the leg. Moreover, the positioning of these additional structures requires a clear insight into the dynamics of the legs during lifting.
Finally, it has to be stated that an analysis of the Load-on phase may result in additional constructive elements.

It should be noted that it is preferred to perform the preparation activities when the legs are still accessible from the topside.

Summarizing, apart from the more evident activities as the cleaning of the leg itself, there are 3 main technical challenges during the preparation phase:

- Lift configuration
- Lift point construction and a structural analysis of the GBS.
- A detailed assessment of the stability and the CoG and include effect of the CoG

The design of these elements are out of the scope of this thesis.
It should be noted that the preparation of the constructive elements on the leg is dependent on the selected lifting procedure, the cutting method and the lift configuration itself.

4.2.2 Cutting

The cutting itself can be done with different cutting methods. An overview of different cutting techniques is given below in Table 4-1.

Method	Application	Advantages	Disadvantages	Comments
Diamond wire cutting	Abrasive cutting	Controlled cuts, Remote operation. Guaranteed cut, no bridges of left material after cut. No restrictions on the axial load	Wire can jam or break	Commonly used offshore. Proven technology for cutting large steel and concrete structures.
Ring- and chainsaw	Abrasive cutting	Mounted on tracks, remote operation possible, controlled cuts	Blade can jam in cut. Axial load will restrict the use of a saw	Commonly used onshore, without large axial forces
Stitch drilling	Abrasive cutting	Remote operation possibility	Long cutting time. Cut needs to be stabilized during cutting process	Only practical use is for small segments
Pressure cutters	Pressure demolition	Non	Only operates on a free edge. Concrete thickness too large	Only proven technology onshore
Explosives	Pressure demolition	Short cutting time. Low cost	Large environmental impact. Cannot be used with a crane attached. More or less prohibited by OSPAR	Non proven method for concrete structures offshore
Thermal lance	Heat cutting	Efficient for steel rebar, not so much for concrete	Divers to be present at cut Long cutting time. Inaccurate cut.	Safety hazard for operator.
Water Jet cutting	Abrasive cutting	Remotely operated	Cutting depth not large enough. Needs pre mounted tracks. Can leave bridges of uncut material.	Not tested in deep cuts in subsea areas

Table 4-1 - "Cutting methods"

Cutting method

Selecting the right cutting method is influenced by many factors and considerations

Moreover, the structural integrity of the concrete after 40 years of operating in a marine environment is unknown; this has to be taken into account when selecting a cutting technique.

The cutting phase is also related to the workability. The cutting of the leg will be a time consuming activity, moreover, the different cutting techniques can be weather dependent. The North Sea environment can have very harsh conditions. A workable weather window for both cutting and lifting could be very rare. To minimize the required weather window and optimize the workability of the operation, the cutting and lifting phase should be separated. This way both operations will have their own weather window, resulting in a higher workability. To allow this separation of the phases, stability of the cut part must be ensured. The design of the component ensuring this stability determines to what extent this separation is feasible.

Stablity after cut.

One of the main issues in the decommissioning process of the Brent B foundations, is the stability of the cut section during and after the cut. When the cut is started the stability of the structure will no longer be guaranteed.
During the cutting phase the leg has to withstand the environmental forces, namely the wave forces and the current forces. For the leg of the Brent Bravo these forces are calculated and illustrated in Table 4-2

Forces	Sliding		Toppling	
Drag force from current	0.91	MN	67.8	MNm
Wave Forces	5.86	MN	316	MNm
Total	6.77	MN	383.8	MNm

Table 4-2 - Forces on the Brent Bravo leg

To ensure the cut section does not collapse or move during the cut, a number of concepts have been developed. The difficulty in doing this lies in the fact that the cut section does not stay stable after the cut has been made. Due to forces that are being excited on the structure by waves and currents, the structure will slide or topple if nothing is done. The concepts described below either increase the toppling and sliding capacity or apply forces to keep the structure stable.

- Collar around the cut zone

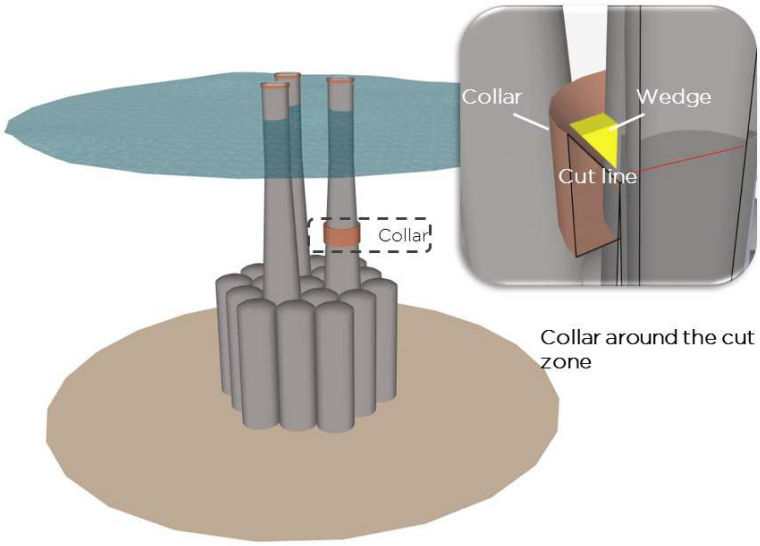

Figure 4-2 - "Collar around the cut zone"

A wedge is driven between the collar and the wall of the leg, as shown in Fig. 4-2.
This construction possibly prevents toppling of the leg after cut.
It is uncertain whether the wall of the leg is able to withstand the stresses.

- Tied down with cables

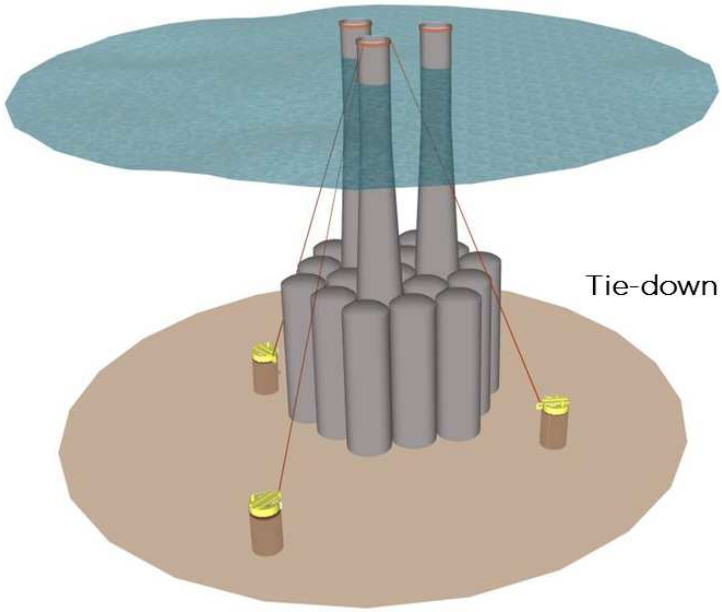

Figure 4-3 - "Tied down with cables"

As shown is Fig. 4-3, tendons running from the top of the leg to suction piles in the seafloor could prevent toppling. For lifting a release mechanism at the top is required. A perfectly timed release can be obtained by this mechanism.

- Weighed down

If a heavy collar is placed above the cutting zone, hanging from the top of the leg, the leg could also be weighed down by internal ballast inside the leg. Due to this ballast the leg would be weighed down creating additional stability.
However, this concept will consequently lead to a higher load to be lifted.

- Non horizontal cutting

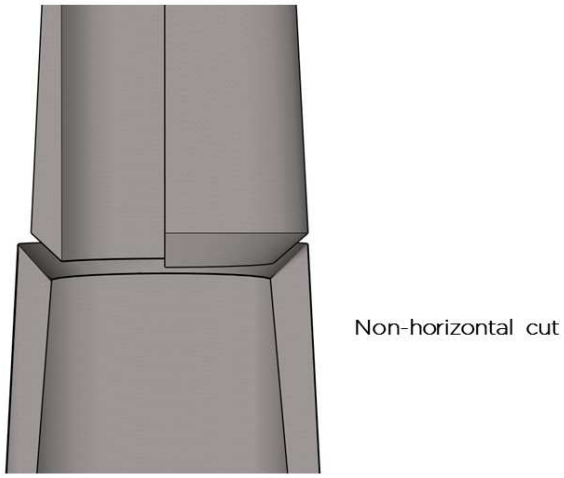

Figure 4-4 - "Non horizontal cutting"

If some tension is applied to the top of the leg, which can prevent the leg from toppling, the non-horizontal cut can withstand the horizontal forces. This non-horizontal cut is shown in Fig. 4-4.

- Partial cutting

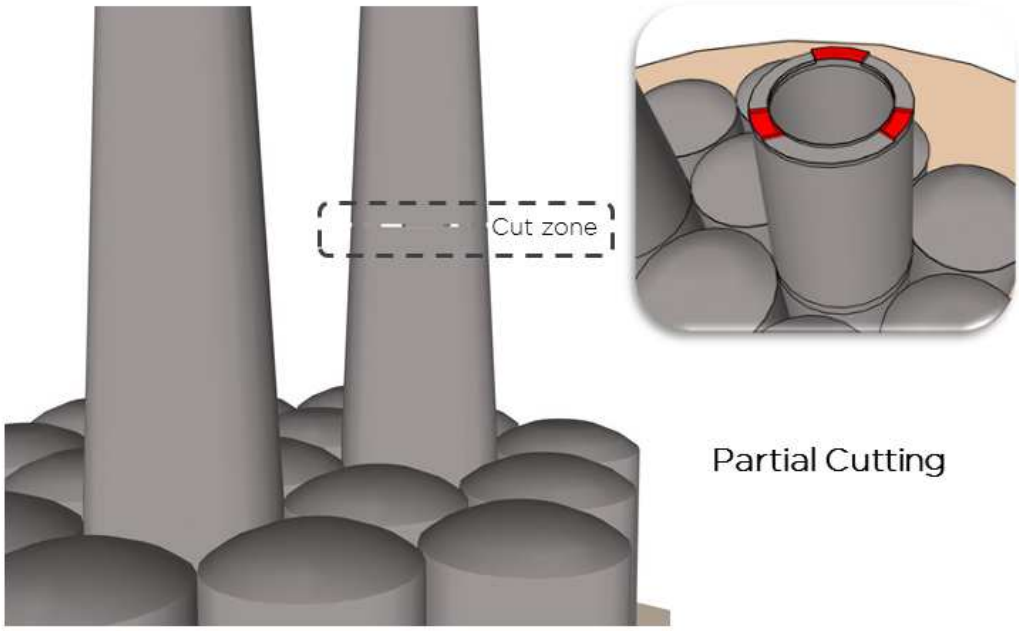

Figure 4-5 - "Partial cutting"

By using the concept of partial cutting, as presented in Fig 4-5, three sections can be left uncut. These sections will also act as supports and stabilizers. At the moment of lifting, the final cuts are made after which a fast lift can be carried out. Therefore interaction between the cutting phase and the lifting phase is of great importance.

In Table 4-3 the advantages and disadvantages of the concepts are summarized.

Concept	Advantages	Disadvantages
Weighed down	Easy installation	More lifting capacity required, Horizontal forces
Collar around the cut zone	Controlled horizontal forces	Difficult installation
Tied down with cables	Horizontal and vertical forces, leg can be pretensioned	Installation of suction piles, cables
Non horizontal cutting	Cost effective	Cutting technique, limited horizontal forces
Partial cutting	Cost effective, vertical force/ allows pretension	Cutting and lifting phase are not separated, lower workability

Table 4-3 - "Concept evaluation"

Summarizing, the main technical challenges during the cutting phase are the following:

- Interaction between cutting and lifting
- Cutting method
- Stability after cut

These technical challenges are coherent.

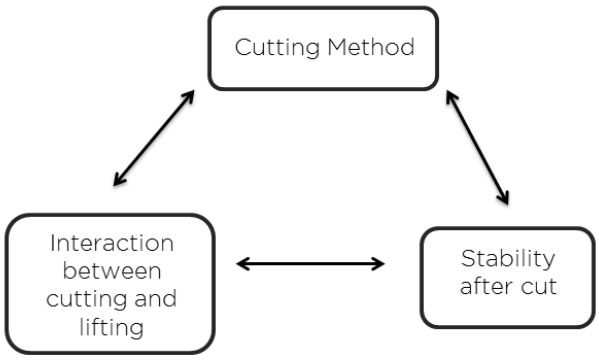

Finally, the cutting phase has a strong impact on the lifting phase

4.2.3 Lifting

After cuts have been made in the leg at a depth of 56 meters, the upper part of the substructure can be lifted by the JLS.

Initial lift – rebound

One of the main technical challenges is the rebound during the initial lifting phase. Due to the vessel motions and a relatively slower lifting speed, the lifted part of the concrete structure can slam onto the gravity based bottom part. This can result in damage of the substructure and consequential the caissons on the seabed. A partial higher lifting speed can prevent this rebound.

Lifting phase – slack wires

Since the hoisting speed of the JLS is not high enough to keep up with the heave motions, the tension in the rigging will vary. If the motions are too strong, the wires will go slack and after that snap tight. This snapping is uncontrolled behaviour and snap-loads are strongly discouraged by the manufacturers of steel wires. There are some options to prevent snap-loads, most of which rely on some kind of heave compensation, constant tension and/or elastic rigging. As another option slack loads can be reduced by reducing snap distances.

Forces on the TLB

The TLBs will be used to tilt the GBS leg on deck of the PS. In the final lifting phase, before tilting the leg, an interaction between the TLB and the leg will occur. The impact loads on both of the structures should be examined ensuring no potential damage on the structures. A saddle construction on the sledges embracing the concrete structure, could minimize the impact loads.

Lift capacity – lift block configuration

The components involved in the total removal operation, will influence the lift capacity. The below formulas will be used for calculating the lifting weights:

- Rigging weight = rigging weight factor x dry weight including weight contingency
- Lifting weight = ((dry weight x weight contingency) + rigging weight + marine growth) x tilt factor x DAF

It can be concluded that:

- The initial lift just after the final cut-off is the crucial part in the removal process.
- A rebound of the structure is not allowed
- Fast lifting in this phase is a requirement
- The stability of the structure and the avoidance of slacking wires have to be taken into account in a solution for fast lifting

These technical challenges have a strong interaction with each other.

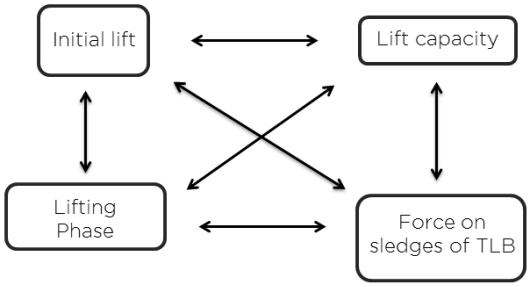

It should be noted that fast lifting will have a major impact on the whole approach of the removal process. Controlling the moment of final cut-off will be of crucial importance.

4.2.4Load on

To transfer the GBS leg on the PS, the GBS leg must be tilted on the vessel. This will lead to an interaction between the TLBs and the concrete structure. The impact loads, on both structures, should be examined ensuring no potential damage on the structures. Moreover, the structural integrity of the leg in horizontal position has to be considered, since the structure has been designed for vertical operations. In this phase additional strengthening might be needed.
A saddle construction on the sledges, embracing the concrete structure, could minimize the impact loads.

4.2.5Transportation

Once loaded on the deck, the concrete shaft can be transported to shore for disposal. However, a barge transfer has to be foreseen as the Pioneering Spirit has a relatively large draft. In order to transport the GBS leg to shallow water disposal yards, the leg must be transferred to the dedicated cargo barge by use of support towers. This is the preferred transfer and load-in method. This operation will be undertaken in a sheltered water location. The cargo barge will then be towed to the quayside of the nominated facility to commence the load-in of the leg. During this barge transfer, the following must be taken into consideration.

- Stability of the barge
- Load onto barge
- Sea fastening

4.3 Discussion

This removal process contains many uncertainties, which have to be tackled in order to complete a successful removal operation.
For most of the challenges several concepts can be developed which will lead to a successful removal operation. However, most challenges have a strong correlation to each other; the application of one concept may exclude the possibility of using a solution for another challenge.

An important challenge in the lifting phase is the avoidance of a rebound of the cut-off section of the leg with the remaining bottom founded structure. Contrary to other challenges only one technique can offer a solution. It can be stated that fast lifting is an essential method to avoid a rebound. Therefore, a fastlift is an essential aspect for successful removal and would be applied in every total removal concept. Designing a fastlift solution would provide demands and requirements for the solutions of other challenges.
The design for the initial lifting phase, as the focus in this study, is depending on a number of conditions:

- The weight of the part of the leg to be removed
- The lifting speed of the JLS on the PS
- The vertical movements of the PS-platform in relation to the sea-state
- The application of non-vertical forces after cut-off
- The final cutting method

- The primarily feasibility of the concept
- Leg behaviour after cut-off
- Slack wires

The weight of the part of the leg to be removed

As described in chapter 3.2, the weight of a leg of the Brent Bravo is about 4000 tons.. During this study a number of buoyancy solutions have passed. Buoyancy solutions inside the leg and around the leg can be considered. In general they lower the load to be lifted. Their volume has to be extreme to really diminish the load in a substantial way. Moreover, their connection to the leg is dependent on the individual leg structure. Both developing and subsea mounting can be time-consuming and expensive. However, in the design possible buoyancy solutions are taken into account. In the models to be designed, they only change the effective load to be lifted.

The lifting speed of the JLS.

The maximum lifting speed of the JLS is 5.5 m/min, which corresponds to 0.275 m/s.
In chapter 3.3 is stated that the heave response of the PS is 0.55m and has a period of 6 sec. This results in a mean downward velocity due to this motion of 0.37 m/s. Since this is only the mean downward velocity, it is clear that in order to avoid a rebound, additional and faster initial lifting is anyhow required.

Vertical movements of the leg

The knowledge of the vertical movements of the leg in amplitude and time is essential for the final tuning of the fast lifting device to be designed.
The leg may respond to wind, waves and current with motions on different time scales. The response of the platform to the sea state is complex. The sea state itself is specified by a wave frequency spectrum with a given significant wave height, a representative frequency, a mean propagation direction and a spreading function.

Non-vertical forces

A solution in avoidance of a rebound can be suggested by a fast horizontal displacement of the upper part of the leg, directly after cut-off.
Applying these forces on the bottom part of the leg, just above the cutting place, can be accomplished by subsea vehicles or with longer lines from a ship on a relatively large distance from the spot of lifting. From a practical point of view, these solutions are high demanding.
The main problem is the fact that the leg starts to turn on his point of gravity. Taken into account that the size of the leg is about 75 m vertical by 12 m horizontal, it is obvious that the edges of the bottom part of the leg will collapse against the remaining bottom founded structure.
A horizontal clearance of at least 12 meters in 6 seconds has to be made in order to prevent a rebound. This will result in a horizontal force around $80*10^5$ N, which is unlikely to achieve with ROVs. Therefore, also these approaches require an initial fast vertical lifting.

Final cutting

There are a large number of cutting methods.
For the fast lifting device it is important that during the final and last cut the cutting machine is no longer connected to the part of the leg to be lifted. The cutting specialists have solutions for this problem available.
An alternative approach is that the leg is held in place by cables or a structure. Just after cut-off this additional devices will be removed and the initial lifting has to start.
The advantage is that there is a better control of the moment in time of complete separation.

Primary feasibility

Fast lifting at a non- defined moment of complete cut-off requires a system under pretension. The speed of the lifting has to be under control. Wires have to be held under tension and the vertical displacement has to be controlled in time.

A kind of spring system in the most general way can allow for these requirements. In literature and also in common practice, solutions for faster lifting of loads can be found in pneumatics, hydrodynamics and electro/mechanics.

Hydraulic systems are in principle capable of handling very high pressures, up to 1000 bar. In pneumatic systems the system pressure is limited to much lower values, such as

16 bar. Hydraulic systems have a substantially higher energy density than electro-mechanical systems. With smaller systems much more power can be achieved.

The challenging lifting problem in this thesis is an extreme.
The load is extremely high and a displacement of the load to be accomplished over 1 or 2 m in a very limited time is high demanding.

In this thesis the hydraulic approach is applied, taken into account that the spring type solutions can be described by the same set of formulas. The choice for hydraulic solutions also match with common practice. In the high end of the market for faster lifting of heavy loads a hydraulic solution is the feasible approach.

Leg behavior after cut-off

Just after cut-off uncontrolled movements of the leg in both vertical and horizontal direction can be expected. Uncontrolled movements can be initiated by waves and currents influencing the position of the upper part of the leg.
As those uncontrolled movements can cause unwanted rebound, an approach for stabilization is required.
The uncontrolled movement in a vertical sense is related to the vertical movements of the PS. It is regarded as impractical to couple the upwards movement of the PS with the final moment of cut-off. Moreover, the following downwards movement of the PS results in a slacking of the wires and again an uncontrolled situation.
The solution in mind is the application of pretension on the head of the leg. This will result in a fast displacement of the lower part of the leg from the cut-off position.

The uncontrolled movements in a horizontal sense are related to the fact that the disconnected leg does not have a stable vertical position. Due to the fact that the leg is partly above sea level and for a larger part under water and the corresponding points of gravity of the total body of the leg and the “buoyancy” body are displaced to each other tumbling of the leg may occur. Probably the edges of the bottom part of the leg will collapse against the remaining bottom founded structure .
Again a pretension applied on the head of the leg will prevent these unwanted horizontal movements and their expected damage by a rebound.
With pretension the required stabilization is accomplished.

Slack wires

The hoisting speed of the JLS cannot keep up with the stronger heave motions to be expected. If the motions are too strong, slacking and uncontrolled behavior of the wires will occur. One of the solutions can be found in a heave compensation approach.
In the design of the system this will be taken into account.

4.4 Conclusions

The components in the removal process are described and their interrelationships are depicted. Their technical challenges are addressed.
For most of the challenges several concepts can be developed which will lead to a successful removal operation. However, most challenges have a strong correlation to each other; the application of one concept may exclude the possibility of using a solution for another challenge.
An important challenge in the lifting phase is the avoidance of a rebound of the cut-off section of the leg with the remaining bottom founded structure. Contrary to other challenges only one technique can offer a solution. It can be stated that fast lifting is an essential method to avoid a rebound. Therefore, a fastlift would be applied in every total removal concept. Designing a fastlift solution would provide demands and requirements for the solutions of other challenges; consequently giving direction to a solution for the general problem: the removal of the concrete leg.

The effects of destabilisation, rebound and wire slacking are described in their effects on the initial lifting procedure.

The most important factors for a reliable initial lifting are:

- Fast lifting
- Pretension
- Stability after cut-off

In chapter 5 these factors will be incorporated in the design of the component which enables the initial lifting

5 COMPONENT DESIGN

In chapter four it has been concluded that for all lift configurations, important factors for a successful lift operation are:

- The heave compensation related to the vertical movement of the tip of the JLS.
- The realisation of an initial fast lifting system that prevents a rebound.

In this chapter a component will be presented which will account for the above stated factors.

5.1 Concept

A solution can be found in heave compensation. Passive Heave Compensation (PHC) systems are used in lifting and drilling operations in order to reduce the influences of waves. The PHC systems are based on storing impact energy from external forces such as waves and current, while dissipating them or releasing them at a later time. It consists of hydraulic cylinders which are connected to pressurized air volumes via accumulators. A PHC system basically acts as a gas loaded spring system. Due the passive nature of the system, it does not require an external power supply, which makes it a relatively fail safe system.

An example of passive heave compensation systems is the Cranemaster lifting unit, shown in Figure 5.1. Cranemaster units are used for the reduction of forces and motions, based on passive heave compensation and shock absorption between a crane-hook and the load. Cranemaster units are supplied in many different forms and sizes, serving applications such as transfer lifts, splash zone crossing, landing speed reduction, subsea resonance avoidance and shock absorption.

Figure 5-1 - " Cranemaster Passive Heave Compensator"

The basic working principle of a PHC is the use of a large volume of gas under a certain pressure. This volume of gas is connected to a cylinder with a piston. The end of the cylinder is usually connected to the main hoist and the piston rod to the load. As the piston moves due to motions of the vessel, the volume of gas will change and thus the pressure will change as it is a closed system. If the gas volume is large enough, the volume change due to the movements of the vessel will induce only a relatively small volume change of the gas, thus resulting in only a small pressure change. As the pressure is directly related to the force acting on the piston, the force exerted on the load will remain almost constant. This means that the object will remain still.

A solution for the initial fast lift, preventing the leg from a rebound on the cut part, can be found in a sudden release of a pre-tensioned spring. In this case, the PHC will act as the pre-tensioned spring.
To perform a fast lift with a massive load like a concrete leg, a huge amount of energy is required. Hydraulic systems can cope with these demands in a relatively not too large and heavy set-up. The basics for a temporary demand of huge energy supply can be found in a pressure storage reservoir in which a non- compressible hydraulic fluid is held under pressure by an external source. A hydraulic accumulator can act as such an energy storage device.

By combining the hydraulic accumulator and the PHC, the stored energy from the accumulator can initiate the fast lift by pushing the piston of the PHC. Forcing the

vertical lifting cylinder to its most retracted position will result in a fast-lift and will consequently help to bring the load away from the rebound zone.

The combination of a PHC and a hydraulic accumulator the application of "pre-tenioned" fast lift, results in a unique concept, as illustrated in Fig. 5-2, 5-3 and 5-4.

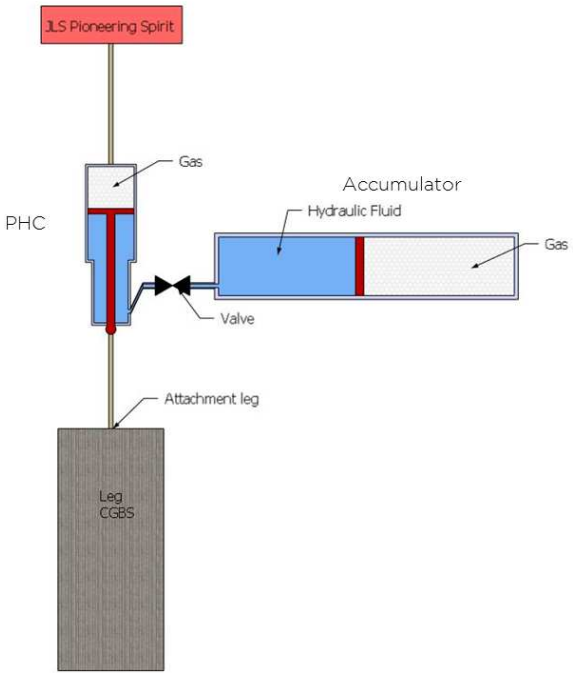

Figure 5-2 - "Fast lift system, initial state"

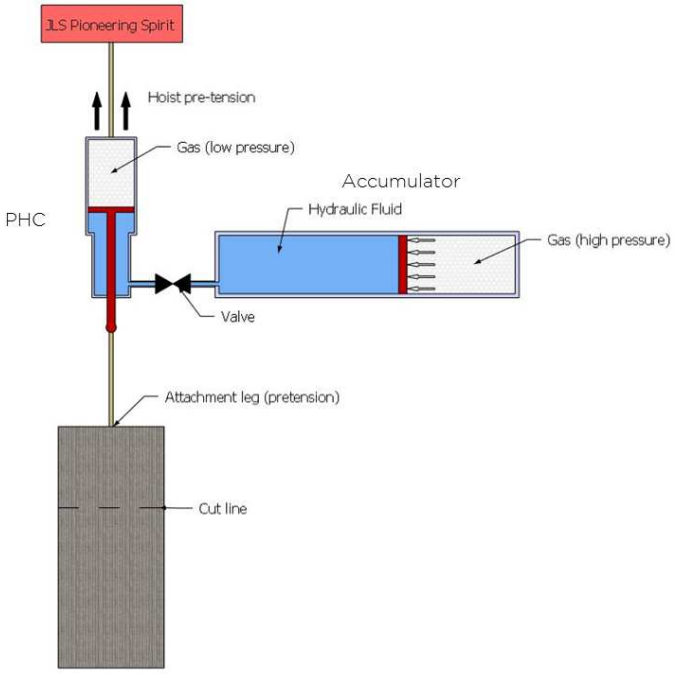

Figure 5-3 - "Fast lift system, building pretension"

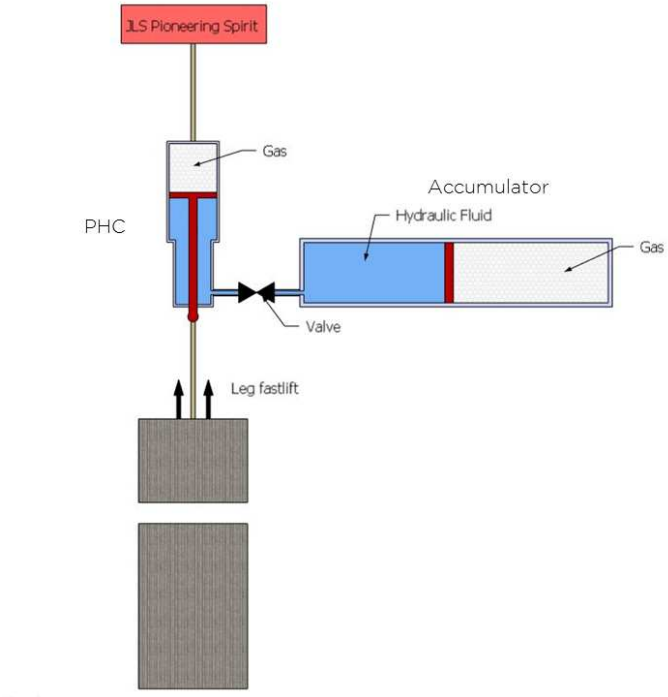

Figure 5-4 - "Fast lift system, lifting"

The major differences between this concept and a traditional PHC are that the pressure in the accumulator will not be the pressure just right for the load, but it will be higher; in that way the PHC will actually lift the load to a higher position. Furthermore, instead of creating an as large as possible gas volume in the cylinder, the gas volume can be kept relatively small. This provides a spring with a non-constant spring coefficient to the system, which can cause a desirable effect.
The system must comprise the following properties:

- Initially the pressure acting on the piston should be high, in order to perform a fastlift. As soon as a certain height, outside the rebound zone, is reached, it should equal the mass of the load as otherwise the piston would hit the end of the cylinder.

- The mass of a load is quite uncertain. Ideally this concept can be used to lift concrete legs with different dimensions and be applicable to multiple projects. This means the pressure has to vary to accommodate mass uncertainties.

- Perfect heave compensation is not necessary; the only limitation to the load variations is the capacity of the wire rope to handle varying loads.

The result is a PHC that provides fast lift capabilities for loads with high mass uncertainty, while preventing large load variances in the main hoist ropes.

5.2 Hydraulic lifting tool

To get a general understanding of the system and to get an idea of the feasibility of the system, a basic scale model, as shown in Fig.5-5, was designed and tested at Allseas Engineering.

Figure 5-5 - "Scale model test for fastlift concept"

The results of the test were satisfying, a fast lift was performed. This test could be seen as a proof of concept.
To gain insight into the feasibility of this concept, a model has to be made to give an idea of the dimensions of the system. The dimensions of the hydraulic lifting tool will give an idea about the technical feasibility. The size can be compared to existing hydraulic systems to evaluate the feasibility of the concept. Furthermore, the dimensions of the hydraulic lifting tool will influence the hoist capacity of the JLS system and consequently the feasibility of the concept.
The costs of this concept will determine the financial feasibility. Since the dimensions are closely related to the costs, an estimation on the financial feasibility can be made when knowing the dimensions of the hydraulic lifting tool.

Several parameters in the model will influence the response of the system. Parameters for the model are the dimensions of both the accumulator and the hydraulic cylinder, resulting in the dimensions of the lifting tool.

5.3 Initial model

An understanding of the different dynamical effects during the lifting phase will be obtained by an initial model. This model simulates the motions of the fast lift system and the leg.
Since the leg will be lifted vertically and the vertical motions of the leg will determine whether a rebound will occur, these heave motions are the governing motions. The

horizontal motions will have a relatively small impact on the initial lifting phase and are therefore neglected in this model.
When the concrete leg is lifted and a smaller part of the leg will be submerged, the buoyancy of the leg will consequently decrease. The further the leg will be lifted, the heavier it will become to lift. Since the initial lifting phase is considered in this study, focus will lay on only the first meters of the leg to be lifted. The relative load increase in this stage will be in the order of 1 percent of the total weight and can therefore be neglected in the model.
The hydraulic friction of the leg due to its motions is also neglected in this model.
In this initial model the motions of the PS are considered as 0. These motions will be applied at a later stage. This model is introduced in chapter 5.5.

This concept can be modelled as a mass-spring-damper-system with 3 degrees of freedom.
The 3 degrees of freedom are u_1, u_2 and u_3. Where u_1 is the vertical motion of the PHC, u_2 is the motion of the piston of the PHC and u_3 is the motion of the concrete leg.
A schematic figure of the model is shown below in Fig. 5-5.

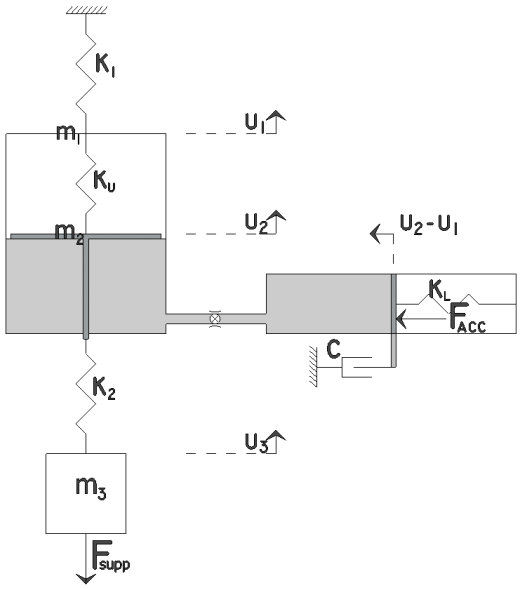

Figure 5-6 - "Schematic model"

The hoist cables between the JLS are modelled as a linear spring k_1. The cables connecting the piston to the leg of the CGBS are also modelled as spring k_2.
The compressed gas in the PHC is modelled as a spring k_u. The gas in the accumulator is corresponding to spring k_L.

The system is damped by the pressure drop in the valve and the pipe connecting the accumulator to the hydraulic cylinder. This damping is modelled as damper c. The magnitude of damping c is dependent on the velocity of the hydraulic fluid through the pipeline and valve, which is correlated to the relative velocity between u_1 and u_2.
The masses of the PHC, the piston and the leg of the CGBS are corresponding to m_1, m_2 and m_3.
The force F_{supp} corresponds to the force due to the pretension. This can be addressed to the tensile force in the leg's reinforcement or a retaining system. After the cut has been made, this force decreases to zero. This will initiate the upward motion of the leg.
The compressed gas in the accumulator causing an upward pressure on the piston is modelled by F_{acc}.
In this model the hydraulic fluid is considered to be incompressible.
Noticeable is the notation of the displacement of the piston in the accumulator. Since the hydraulic fluid is assumed to be incompressible, the relative motion of the piston in the PHC is equal to the motion of the piston in the accumulator. Note that this displacement needs to be factored for the difference in diameter of the pistons. In this model the diameter of both pistons are assumed to be equal.

For the determination of the equations of motion the displacement method is used. This can be found in Appendix D. This results in the following equations of motion.

$$
\begin{aligned}
&m_1\ddot{u}_1 + c(\dot{u}_1 - \dot{u}_2) + k_1 u_1 + (k_u + k_l)(u_1 - u_2) = 0 \\
&m_2\ddot{u}_2 + c(\dot{u}_2 - \dot{u}_1) + (k_u + k_l)(u_2 - u_1) + k_2(u_2 - u_3) = F_{acc} \\
&m_3\ddot{u}_3 + k_2(u_3 - u_2) = -F_{\sup}
\end{aligned}
$$

Equation 5-1

This can be expressed in the following matrix form:

$$
\begin{pmatrix} m_1 & 0 & 0 \\ 0 & m_2 & 0 \\ 0 & 0 & m_3 \end{pmatrix}
\begin{pmatrix} \ddot{u}_1 \\ \ddot{u}_2 \\ \ddot{u}_3 \end{pmatrix}
+
\begin{pmatrix} c & -c & 0 \\ -c & c & 0 \\ 0 & 0 & 0 \end{pmatrix}
\begin{pmatrix} \dot{u}_1 \\ \dot{u}_2 \\ \dot{u}_3 \end{pmatrix}
+
\begin{pmatrix} k_1 + (k_u + k_l) & -(k_u + k_l) & 0 \\ -(k_u + k_l) & k_2 + (k_u + k_l) & -k_2 \\ 0 & -k_2 & k_2 \end{pmatrix}
\begin{pmatrix} u_1 \\ u_2 \\ u_3 \end{pmatrix}
=
\begin{pmatrix} 0 \\ F_{acc} \\ -F_{\sup} \end{pmatrix}
$$

Equation 5-2

Since the displacement of the leg of the CGBS on t_0 = 0 and the system is in rest, the following initial conditions can be drawn:

$$t = t_0$$

$$u_1 = \frac{-\mathrm{m}_1 \cdot g \cdot \mathrm{k}_2 + (F_{acc} - m_1 \cdot g - m_2 \cdot g) \cdot (k_u + k_l)}{k_1 \cdot k_2 + k_1 \cdot (k_u + k_l) + k_2 \cdot (k_u + k_l)}$$

$$\dot{u}_1 = 0$$

$$u_2 = \frac{(F_{acc} - \mathrm{m}_2 \cdot g) \cdot \mathrm{k}_1 + (F_{acc} - m_1 \cdot g - m_2 \cdot g) \cdot (k_u + k_l)}{k_1 \cdot k_2 + k_1 \cdot (k_u + k_l) + k_2 \cdot (k_u + k_l)}$$

$$\dot{u}_2 = 0$$

$$u_3 = 0$$

$$\dot{u}_3 = 0$$

Equation 5-3

An overview of all the input parameters of the model is presented below in Table 5-1.

m_1	mass of the PHC [kg]
m_2	mass of the piston [kg]
m_3	mass of the concrete leg [kg]
k_1	spring-stiffness of the hoist cable [N/m]
k_2	spring-stiffness of the connecting cable [N/m]
k_u	spring-stiffness of the compressed gas in the PHC [N/m]
k_L	spring-stiffness of the compressed gas in the accumulator [N/m]
c	damping coefficient due to the valve [Ns/m]
F_{sup}	Support force (retaining force) [N]
F_{acc}	Pressure force accumulator [N]

Table 5-1 - "Input parameters"

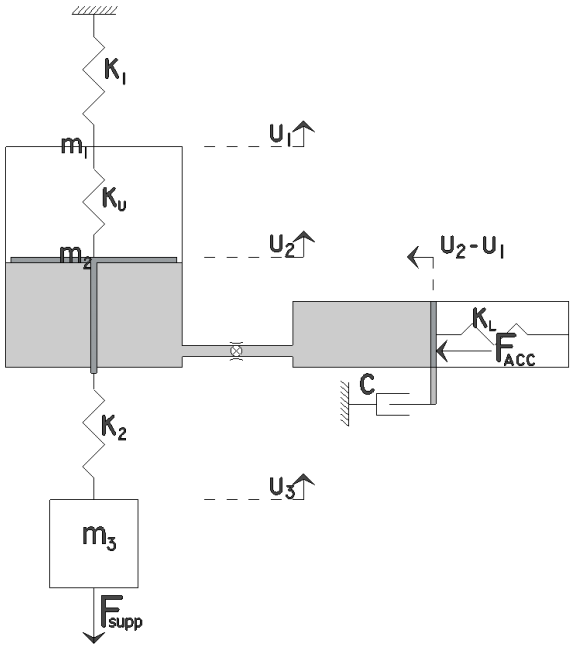

5.3.1 MATLAB/Simulink model

In order to investigate the responses of this model during the initial lifting phase, the initial model has been simulated in Matlab/Simulink. This model is based on the introduced system and analyzed in the time domain. In this basic model some assumptions were made:

- Spring stiffness in the PHC and accumulator are modelled as linear springs
- Weight of the moving hydraulic fluid is neglected
- The diameters of the pistons are equal. Therefore, the motions of the pistons will be the same.

This model will be validated by a hand calculated/Maple model.

MATLAB/Simulink

An input sheet for the model, with some calculations is made in MATLAB. This sheet will run and refers to the actual model which is made in Simulink. Simulink is a graphical programming environment for modelling, simulating and analyzing dynamic systems. The model in Simulink is presented in Fig. 5-7.

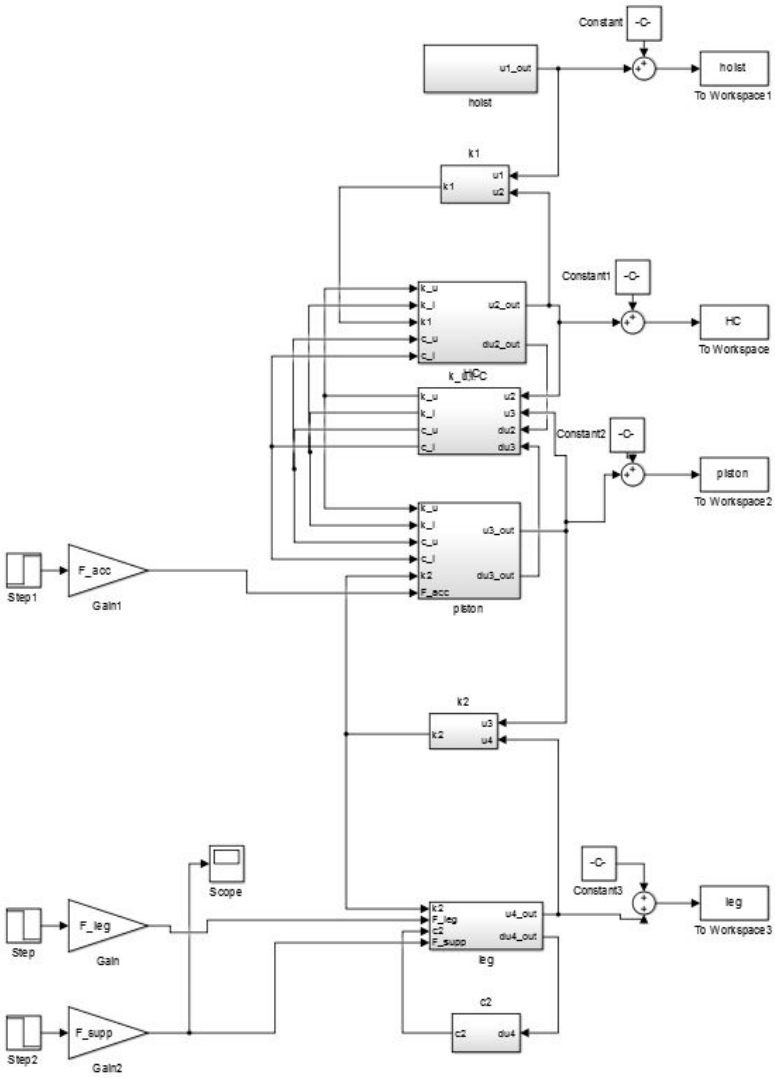

Figure 5-7 - "Simulink model"

The inputs for both models are arbitrarily chosen values for the input parameters.

m_1	10
m_2	1
m_3	10000

k_U	2
k_L	2

k_1	100	c_u	30
k_2	100	cl	30

Table 5-2 - " input for model"

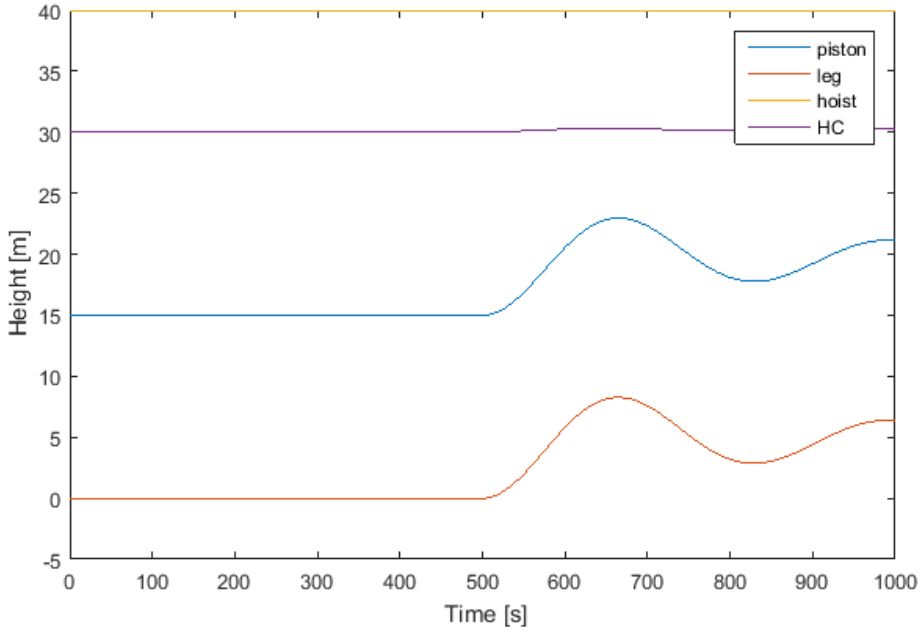

Figure 5-8 –"response of initial model"

At t=500, the cut-off is simulated. This will initiate the fast lift of the leg.
In Maple this is divided into two phases. The phases before and after cut-off.
Or $t<t_{rel}$, showed in Fig. XX and $t>t_{rel}$, showed in Fig. XX

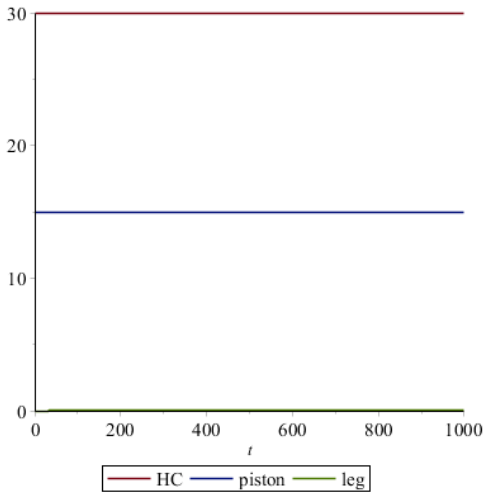

Figure 5-9 "response Maple t<t_release"

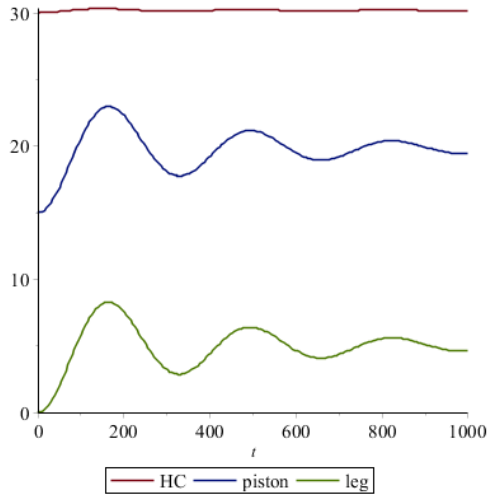

Figure 5-10 "response Maple t>t_release"

In order to compare the results and validate the MATLAB model, both graphs are plotted in the same window. This is done for the phase where $t<t_{rel}$. Fig. 5-11
And done for $t>t_{rel}$ in Fig. 5-12.

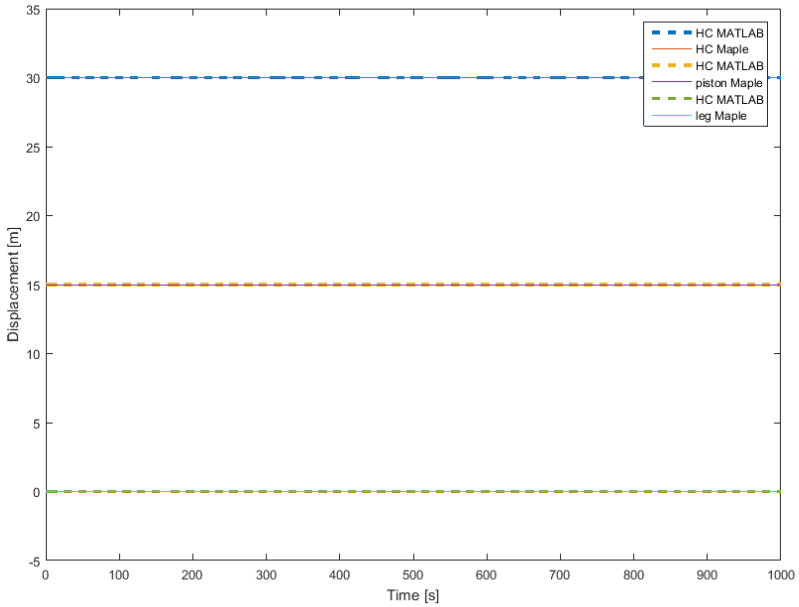

Figure 5-11 -"MATLAB/Maple comparison t<t_release"

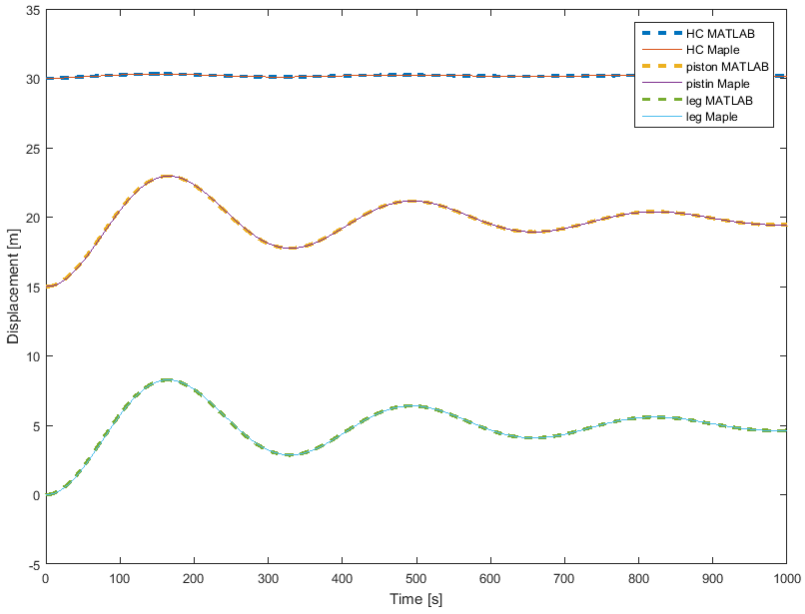

Figure 5-12 -"MATLAB/Maple comparison t>t_release"

At first glance both graphs look perfectly equal. However, when zoomed in a small discrepancy between the graphs is noticeable as shown in Fig. 5-12 and 5-14.

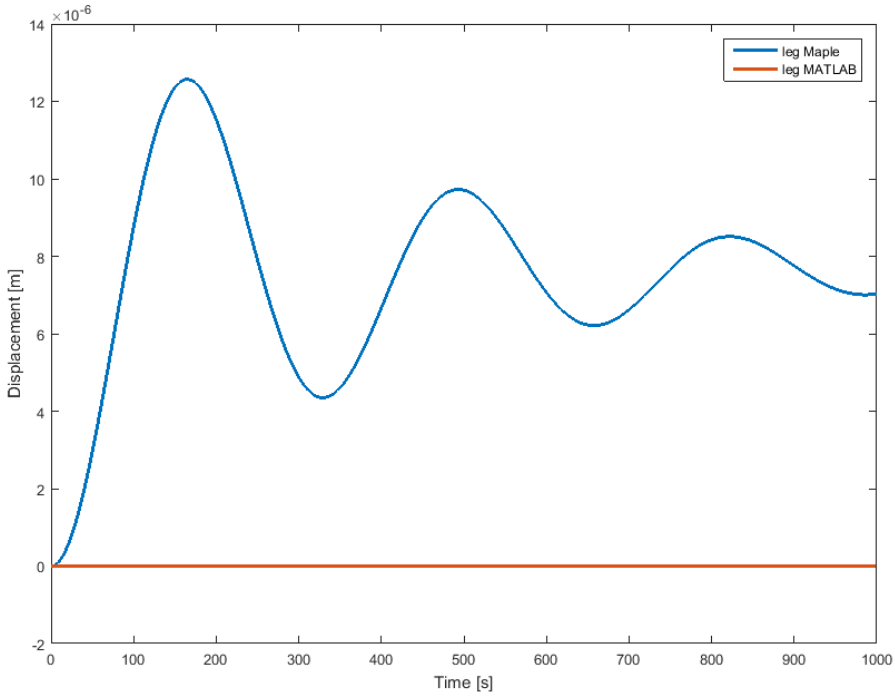

Figure 5-13 “Displacement of the leg”

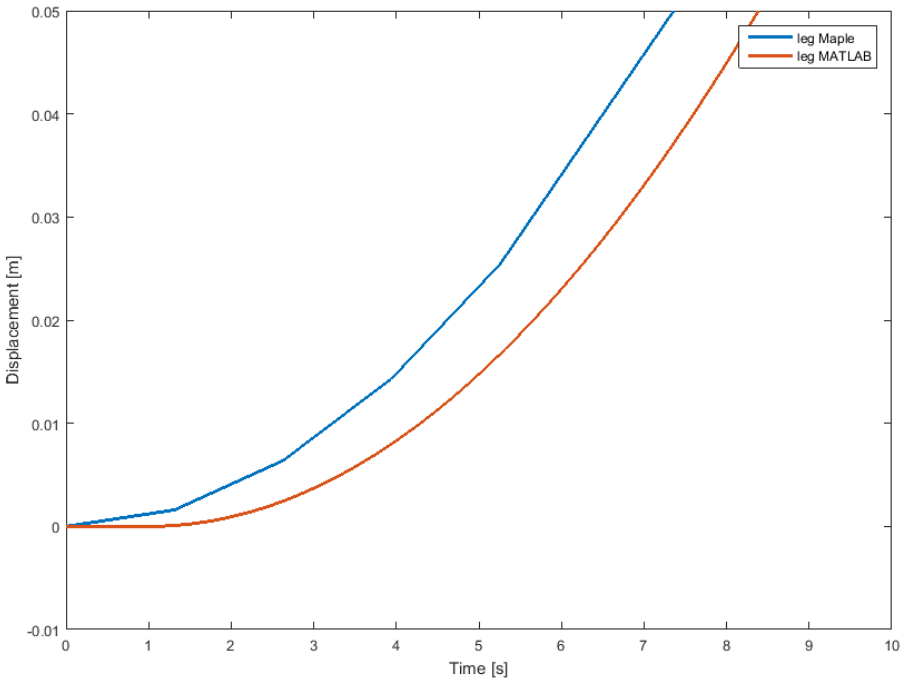

Figure 5-12- "Displacement of the leg t>t_release"

In both of the plots a very small discrepancy between the MATLAB and the Maple model is noticeable.

Both programs do not solve the problems totally analytical. Therefore, rounding errors can occur.
In Figure 5-15 the rounding error in Maple is shown. Both expressions are the same, however, Maple plots them differently. When the input for a Maple model is done in before the calculations are performed, rounding errors can occur.
However, the errors are very in the order of 10^{-8}, which is relative to the motions of the system very small, therefore the model is validated.

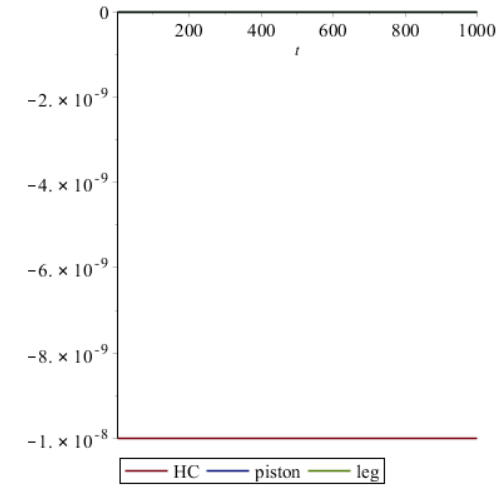

$$ul(t) = \frac{-m1\,k2\,kl\,g - g\,m1\,k\_tot\,kl + g\,kl\,m3\,k\_tot + \frac{g\,kl\,k\_tot^2\,m3}{k2} - g\,k2\,m1\,k\_tot + g\,k\_tot^2\,m3 + kl\,k\_tot^2\,leghoist}{(kl\,k2 + kl\,k\_tot + k2\,k\_tot)\,(kl + k\_tot)}$$

$$ul(t) = 28.30519943$$

$$HC\_init := \frac{-g\,k2\,m1 - g\,k\_tot\,m1 - g\,k\_tot\,m2 + F\_acc\,k\_tot}{kl\,k2 + kl\,k\_tot + k2\,k\_tot}$$

$$HC\_init := 28.30519944$$

Figure 5-13 – "Maple rounding error

5.4 Defining parameters

The hydraulic system for initial lifting is in essence a dynamic power storage device. In this device a relative non-compressible hydraulic fluid is held under pressure by a compressed gas. The fluid has few dynamic power-storage qualities; typical hydraulic fluids can be reduced in volume by only about 1.7% under a pressure of $350*10^5$ N/m^2. In the course of this thesis, this fluid is regarded as incompressible.
However, this relative incompressibility makes it ideal for power transmission, providing quick response to power demand.

Gas, on the other hand, located on the opposite side of the piston in the hydraulic device, can be compressed into small volumes at high pressures. The potential energy in the system can be stored in the compressed gas. In this device tremendous energy of the compressed gas exerts pressure on the piston of the accumulator. The power transmission in the fluid results in the pressure on the piston of the vertical lifting cylinder.

For the modelling of the concept some important parameters in the model have to be defined.

- Spring stiffness of the compress gas in both accumulator and cylinder.
- Damping in the system.
- Initial pressure in the accumulator.
- Hoist wire stiffness.

In this section the methods for obtaining the desired parameters are evaluated.

5.4.1 Compressed gas

The pressure in the accumulator and PHC will define the stiffness of the corresponding spring in the model. This pressure is dependent on the volume of the accumulator or PHC and therefore also dependent on the relative motion of the piston.

Following the statement of Boyle's law [2], the ideal gas law, the absolute pressure exerted by a given mass of an ideal gas is inversely proportional to the volume it occupies, if the temperature and amount of gas remain unchanged within a closed system.
This ideal gas law is the equation of state of a hypothetical ideal gas. It can be characterized by three state variables, namely the pressure, volume, and temperature. The relationship between these state variables is characterized as follows:

$$p \cdot V = n \cdot R \cdot T$$

p = Gas pressure $[N/m^2]$
V = Volume of the gas $[m^3]$
n = Amount of moles of the gas [-]
R = Universal gas constant [-]
T = Temperature $[K]$

Equation 5-4

This is a good approximation of the behaviour of many gases under many conditions, although it has several limitations. It is defined as such that all collisions between atoms or molecules are perfectly elastic and there are no intermolecular attractive forces. In such a gas, all the internal energy is in the form of kinetic energy and any change in internal energy is accompanied by a change in temperature.
The ideal gas law ignores both the volume occupied by the molecules of a gas and all interactions between molecules, whether attractive or repulsive. However, in reality all gases have non-zero molecular volumes. Furthermore, the molecules of real gasses interact with one another in ways that depend on the structure of the molecules and therefore differ for each gaseous substance. While these physics are not included in the ideal gas law, for high temperatures and low pressures the effects of intermolecular interactions and volume discrepancies are negligible. However, due to the high pressures expected in this system, these effects must be included. To account for these effects, real gas equations can be used.
In order to compute the pressures and temperatures related to the volume in the system using real gas equations, several methods can be used. In this study the "empirical κ(P)- value" method is used. In this method it is assumed that the process is adiabatic, i.e. there are no heat losses to the surroundings. This is a valid assumption for periodically changing motions in the PHC [3].

The empirical κ-value method is based on values of the heat capacity ratio κ. The κ-values are directly related to the pressure in the system. Thus, when the pressure is

known at a given time, the κ-value can be derived, with which the new pressure can be calculated according to Poisson relationships [4] for ideal gases in adiabatic processes. What makes this method useful is the ease with which the calculations can be performed.

For the real gas equation in this method the κ is based on pressure only. The κ-properties are derived from [2] for T = 270K.

P_{real} [bar]	κ270
0	1.4
50	1.49
100	1.63
150	1.82
200	2.06
250	2.3
300	2.54
350	2.78
400	3.01
450	3.22
500	3.41

Table 5-3 - "pressure dependent kappa values"

The following equations are used to determine the pressure and temperature.

$$P \cdot V^{\kappa} = \text{Constant}$$
$$T \cdot V^{\kappa-1} = \text{Constant}$$
$$P_1 \cdot V_1^{\kappa_1} = P_2 \cdot V_2^{\kappa_2}$$
$$T_1 \cdot V_1^{\kappa_1-1} = T_2 \cdot V_2^{\kappa_2-1}$$

Equation 5-5

Using these equations the κ-values for real gas from Table X.X, the pressure can be calculated by using:

$$P_1 = P_2 \cdot \frac{V_2^{\kappa_2}}{V_1^{\kappa_1}}$$

Equation 5-6

This equation can be used to determine the pressure to volume relationship for a complete stroke of the cylinder. Using the starting pressure and starting volume at midstroke, the full range of pressure to volume relationship can be obtained by taking adequately small iteration steps, giving $\kappa_1 \approx \kappa_2$.
These Iterations are calculated with use of MATLAB. By acquiring the full range of volume to pressure relationship, these arrays can be used later in combination with lookup tables within the Simulink model to determine the pressure for any given volume. In the figure below, the relationship between pressure and volume for an initial pressure and volume of respectively, 10 bar and 10 m^3, is shown in Fig. 5-17. The non-linear relationship is clearly noticeable.

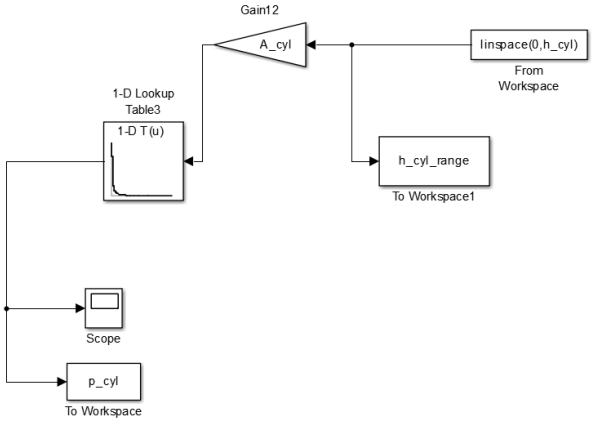

Figure 5-14 - "Lookup table for pressure of cylinder in Simulink"

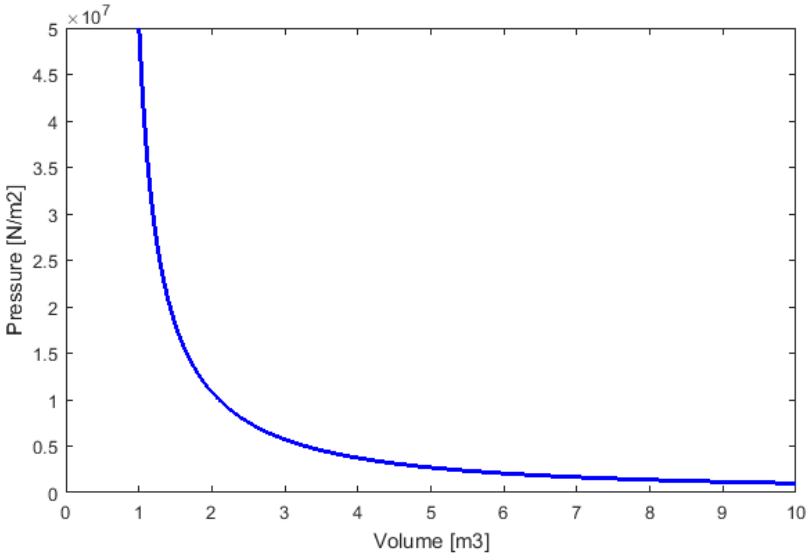

Figure 5-15 – "Non-linear behaviour of pressurized gas"

By knowing the pressure versus the volume of the cylinder and its dimensions, the force acting on the piston for the length of a stroke can be determined. By taking the change of force for a small variation of the displacement of the piston, the spring stiffness of the system can be defined. This non-linear spring stiffness is dependent on the following input parameters: the diameter of the cylinder, its length and the initial pressure.

For a cylinder with the length of 3 meter, a diameter of 0.5 meter and an initial pressure of 10 bar, the following relationship is plotted in Fig. 5-18. The associated spring stiffness is shown in Fig. 5-19.

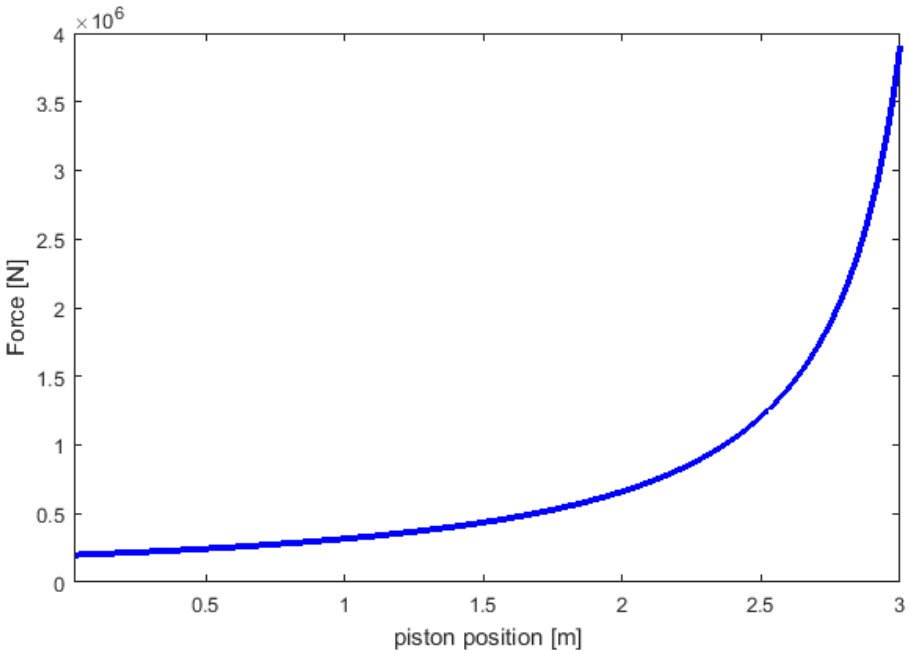

Figure 5-16 – "Force in cylinder"

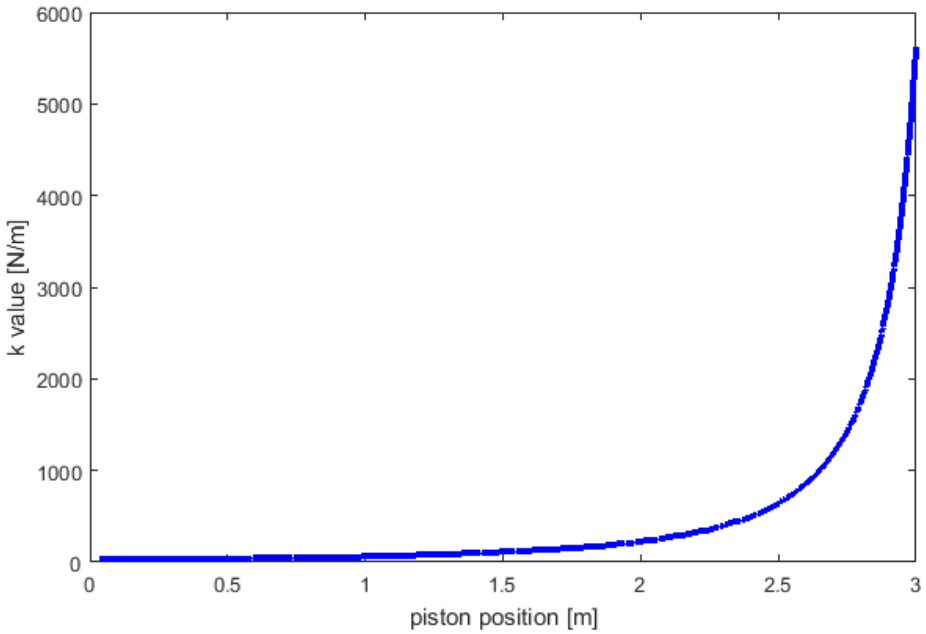

Figure 5-17 – "Spring stiffness in cylinder"

5.4.2 Damping in the system

Viscous friction occurs due to flow through the piping and valves. This system consists of 1 pipeline connecting the accumulator to the PHC and 1 valve controlling the flow of the hydraulic fluid to the PHC.

Pressure drop in piping

The magnitude of the pressure loss due to friction is not only dependent on the length, roughness and diameter of the pipeline, but also on the Reynolds number and flow velocity. Viscous friction could also occur in the accumulator and PHC. However, the pipeline connecting the accumulator with the PHC has a relatively small diameter. Therefore, the flow velocity in this pipe is significantly higher with respect to the accumulator and PHC. This results in a relatively higher friction in the connecting pipeline. The viscous friction in the accumulator and PHC are neglected and only the viscous friction in the pipeline is modelled. The friction in this system can be regarded as a pressure drop through the system.
The pressure drop in piping can be obtained by the following statement [3].

$$\Delta p_w = \lambda \cdot \frac{L}{d_i} \cdot \frac{1}{2} \cdot \rho \cdot V_m{}^2$$

Equation 5-7

Where

Δp_w = Flow resistance [N/m^2]

d_i = Internal diameter [m]

ρ = Density of fluid (+/- 900 kg/m^3)

λ = Friction factor [-]

L = Length of the pipeline [m]

V_m = Flow velocity [m/s]

The internal diameter can be obtained by the following formula:

$$\mathrm{d}_i = \sqrt{\frac{4 \cdot Q}{V_m \cdot \pi}}$$

Q = Flow (m^3/s)

Equation 5-8

Where

$$Q = V_m \cdot A_{pipe}$$

Equation 5-9

With;

$$V_m = \dot{u}_2 - \dot{u}_1 \cdot \frac{A_{cyl}}{A_{pipe}}$$

Equation 5-10

and

$$A_{pipe} = \frac{1}{4} \cdot \pi \cdot D_{pipe}{}^2$$

Equation 5-11

As the velocity increases, the flow transforms from the laminar smooth and steady regime to the fluctuating and unpredictable turbulent regime. The friction factor depends on the flow regime. By calculating the Reynolds number this flow regime can be predicted. Reynold numbers up to 2320 indicate a laminar regime, for higher Reynold numbers a turbulent flow is expected. For both regimes a different method for the calculation of the friction factor is used.

Reynolds number:

$$\mathrm{Re} = V_m \cdot \frac{d_i}{\upsilon}$$

$$\upsilon = \text{ Viscosity (+/- } 5 \cdot 10^{-4} \mathrm{m}^2/\mathrm{s})$$

Equation 5-12

For laminar flow the friction factor can be obtained by:

$$\mathrm{Re} < 2320, \ \lambda = \frac{64}{\mathrm{Re}}$$

Equation 5-13

For a turbulent flow the following formula is used to calculate the friction factor:

$$\mathrm{Re} \geq 2320, \ \lambda = \frac{0.3164}{\sqrt[4]{\mathrm{Re}}}$$

Equation 5-14

The formula of the pressure drop can be re-written to obtain an expression for the friction coefficient of the pipe. This coefficient can be applied in the model.

$$c_{pipe} = \lambda \cdot \frac{L}{d_l} \cdot \frac{1}{2} \cdot \rho \cdot V_m \cdot A_{cyl}$$

Equation 5-15

Where:

c_{pipe} = damping coefficient [kg/s]

d_i = Internal diameter [m]

ρ = Density of fluid (+/- 900 kg/m^3)

λ = Friction factor [-]

L = Length of the pipeline [m]

V_m = Flow velocity [m/s]

A_{cyl} = Surface area piston cylinder[m^2]

The diameter and length of the pipe will determine the friction and are therefore the design parameters. Note that the diameter of the cylinder will have an impact on the flow velocity. Therefore, the damping coefficient will be influenced by the ratio of diameter of the pipe and cylinder.

Pressure drop in valve

A contribution to the total damping is the pressure drop in the valve. This damping is important to the behavior of the system, since it can be controlled. By closing or opening the valve, the damping of the system can be regulated.

The pressure drop in the throttle valve can be obtained by the following formula [5]:

$$\Delta p = \frac{\rho}{2} \cdot \left(\frac{Q}{c * A_{valve}} \right)^2$$

Equation 5-16

Where:

Q = Flow (m^3/s)

ρ = Density of fluid (+/- 900 [kg/m^3])

c = Valve flow coefficient (+/- 1000 [-])

A_{valve} = Surface area of the valve opening (m^2)

To obtain an expression for the friction coefficient of the valve, this formula is re-written into the following form:

$$c_{valve} = \frac{\rho}{2} \cdot \left(\frac{Q}{c^* A_{valve}} \right)^2 \cdot \frac{A_{cyl}}{V_m}$$

Equation 5-17

The design parameter for this friction coefficient is the surface area of the valve opening. This value could be adjusted during the process to enhance the performance of the system. The valve could be closed to realize a higher damping when the excitations of the system become undesirably large. However, in this study the surface area of the valve opening is kept constant.

By adding the friction coefficient of the pipeline to the friction coefficient of the valve, a total friction coefficient can be obtained. In the figure X>X the total damping coefficient is plotted for the following input parameters.

D_{pipe}	0.2	m^2
L	10	m
D_{valve}	0.02	m^2
D_{cyl}	0.5	m^2
υ	0.0005	m^2/s
ρ	900	kg/m^3
c	1000	m/s

Table 5-4 - "Input parameters damping coefficient"

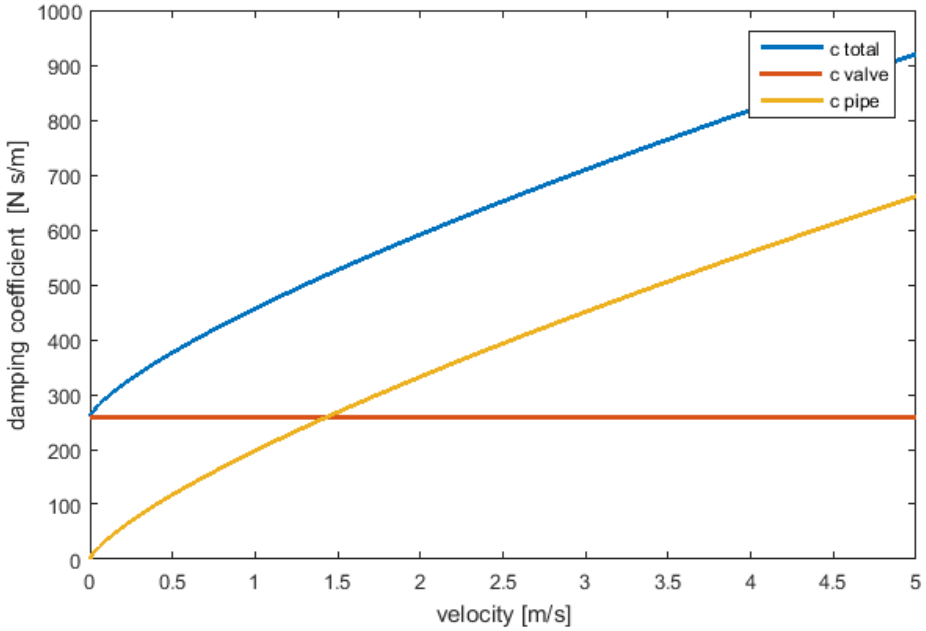

Figure 5-18 - Plot damping coefficient"

5.4.3 Initial pressure

A major design parameter for this fast lift concept is its initial pressure in the accumulator. This pressure is not the pressure just right for the load, but it has to be higher, so that the system actually lifts the load to a higher point.
The fluid pressure has to develop the required push force in the vertical lifting cylinder.
The required push force is of course related to the resulting weight of the leg to be lifted, but also to the stiffness of the compressed air in both the accumulator and the PHC.

It can be noticed in Eq. 5-3 that the initial positions of the piston and the PHC are dependent on the initial pressure in the accumulator, F_{acc}.
The expression for F_{acc} is:

$$F_{acc} = \frac{\begin{array}{l}(m_2 \cdot g + m_3 \cdot g) \cdot (k_1 \cdot k_2) + m_3 \cdot g \cdot k_1 \cdot (k_u + k_l) + \\ (m_1 \cdot g + m_2 \cdot g + m_3 \cdot g) \cdot (k_2 \cdot (k_u + k_l)) + leghoist \cdot (k_1 \cdot k_2 \cdot (k_u + k_l))\end{array}}{(k_2 \cdot (k_1 + (k_u + k_l))}$$

Equation 5-18

Where "*leghoist*" is the desired final position of u_3 for a clearance of the rebound zone.

Modelled as a spring, the compression of the gas will result in the force. When the size of the accumulator is large relatively to the size of the PHC, the volume change in the accumulator will be relatively small resulting in a more constant force. In this way the initial pressure can be modelled as a constant force F_{acc}.

An import parameter for the design is the desired fast lift distance of the leg to prevent a rebounce. In this model this parameter is called "leghoist". This variable must be set larger than the rebound zone in order to achieve a successful lift operation.

5.4.4 Hoist wire stiffness

The stiffness of the hoist cables is dependent on the dimensions of the cable and the material properties of the used steel. The length and consequently the stiffness of the hoist configuration is dependent on the amount of reevings used. Also the stiffness of the hoist wire from the TLB hammerhead to the winch, called dead wire, has to be taken into account. The hoist configuration is shown in Fig.

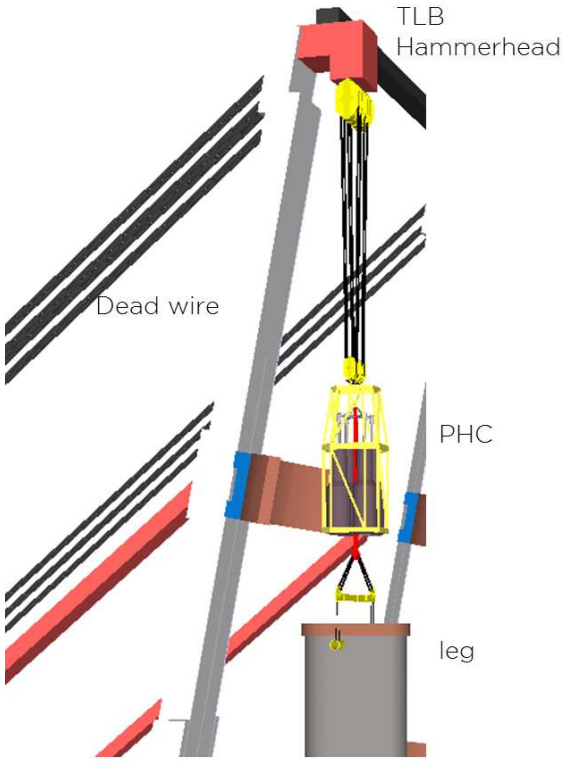

Figure 5-19 - "Hoist configuration'

According to Hooks law the elongation of the dead wire is given as follows:

$$\Delta L_{dead} = \frac{F}{K} = \frac{F_H}{n_H} \cdot \frac{L_{dead}}{EA}$$

Equation 5-19

With:

$$F = \frac{F_H}{n_H}$$

$$k = \frac{EA}{L_{dead}}$$

Equation 5-20

For every hoist wire part the elongation has to be taken including the contribution of the ΔL_{dead} of the dead wires.
A schematic overview of the hoist block wire and sheave configuration is shown in Fig.5-21.

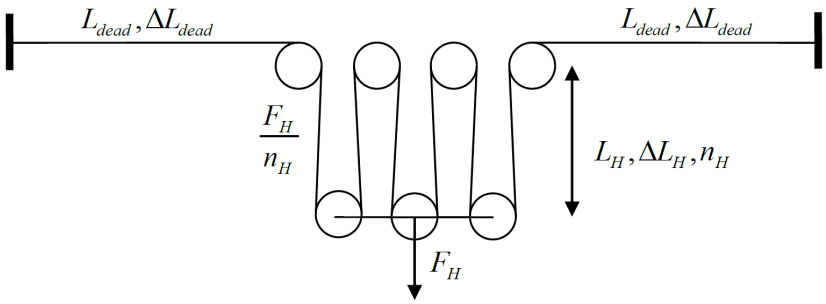

Figure 5-20 - "hoist block and sheave configuration"

$$k_{eq} = \frac{k_H \cdot k_{dead}}{k_H + k_{dead}} = \frac{EA \cdot n_H^2}{n_H \cdot L_H + 2 \cdot L_{dead}}$$

Equation 5-21

With:

k_{eq}, k_H, k_{dead} = Equivalent stiffness, hoist wire, dead wire stiffness $[N/m]$
L_H, L_{dead} = Lenght of hoist wire, dead wire $[m]$
$\Delta L_H, \Delta L_{dead}$ = Elongation of hoist wire, dead wire $[m]$
n_H = Number of reevings of the hoist wire configuration [-]
EA = Effective wire rigidity $[N]$

To calculate the stiffness of the hoist configuration, k_1, the following parameters are used:

EA	2.8 *10^8	[N]
n_H	34	[-]
L_H	110	[m]
L_{dead}	150	[m]

Table 5-5 - "Input parameters hoist stiffness"

This results in a stiffness of 8.01 *10^7 [N/m]

For the hoist wire in the lift configuration connecting the leg and the PHC, the dead wire is excluded. Therefore, the stiffness k_2 can be determined using the following expression.

$$k_{eq} = \frac{EA}{L_H}$$

$$F = p \cdot A$$

Equation 5-22

Using the following parameters:

EA	2.8 *10^8	[N]
n_H	20	[-]
L_H	25	[m]

Table 5-6 - "Input parameters hoist stiffness"

This results in a stiffness of 2.24 *10^8 [N/m]

The parameters mentioned before are related to the selected lift configuration. This shows clearly the coherence between the fast lift concept and the chosen concept for

the lift configuration. The data used for the calculations are obtained from a similar lift project by Allseas [6] and will therefore provide reliable input for the model.

5.5 Requirements

A more advanced model, based on the validated initial model is designed to incorporate the non-linear terms and introduce the heave motions of the PS.
The parameters in this model correspond with the initial model. In this chapter these parameters are obtained. Also the requirements for the model are set.
Summarizing, the following parameters can be determined.

m_1	mass of the PHC	$1*10^4$ [N]
m_2	mass of the piston	$1*10^3$ [N]
m_3	mass of the concrete leg	$4*10^7$ [N]
k_1	spring-stiffness of the hoist cable	$8.01*10^7$ [N/m]
k_2	spring-stiffness of the connecting cable	$2.24*10^8$ [N/m]
k_u	spring-stiffness of the compressed gas in the PHC	Non-linear function dependent on the cylinder diameter, length cylinder, initial pressure.
k_L	spring-stiffness of the compressed gas in the accumulator	Non-linear function dependent on the accumulator diameter, length accumulator, initial pressure.
c	damping coefficient due to the valve and pipeline	Non-linear function dependent on the cylinder/valve opening ratio, length of the pipeline, fluid velocity
F_{sup}	Support force (retaining force)	Can be determined by expression dependent on:
F_{acc}	Pressure force accumulator	Can be determined by expression dependent on:
u_0	motion of the TLB's hammerhead + hoist velocity	Motions are obtained by AQUA-model hoist velocity can be included = 0.0275 [m/s]

Table 5-7 - "overview parameters"

The non-linear terms in this model are calculated for each time step with the lookup functions in Simulink. As illustrated in Table XX, some parameters are dependent on input parameters of the model

D_{cyl}	[m]	Diameter of cylinder (PHC)
h_{cyl}	[m]	Height of cylinder (PHC)
p_{cyl}	[N/m^2]	Initial pressure cylinder
D_{acc}	[m]	Diameter of accumulator
h_{acc}	[m]	Height of accumulator
p_{acc}	[N/m^2]	Initial pressure accumulator
D_{pipe}	[m]	Diameter of the pipe connecting the accumulator tot the PHC
L_{pipe}	[m]	length of the pipeline
D_{valve}	[m]	Diameter of the opening of the valve
leghoist	[m]	proposed clearance of the leg

Table 5-8 - "overview input parameters"

The response of the non-linear components is determined by the input variables. The initial pressure and the volume will have an impact on the properties of the system.
A larger volume will provide a more linear behaviour. A higher initial pressure, contrary, will cause a more non-linear behaviour.
A larger volume can be achieved by increasing the size of the cylinder or accumulator. By enlarging the length, h_{acc} or h_{cyl} the response will be more linear.
The diameter will influence the pressure on the piston. The larger the diameter, the larger the force can be. This can also be obtained from the expression:

$$F = p \cdot A$$

Equation 5-23

The size of the accumulator must be large enough to provide the force required for a fast-lift.

The required force for a fast lift will be in the same order as the gravitational force of the leg to be lifted. For this force must be accounted in the design of the dimensions of the cylinders. Essential for providing this force is the diameter of the accumulators' piston. Force = 4 *10^7 N with an initial pressure of 50 bar, this results in an area of 8 m^2. This corresponds to a diameter of 3.2 m.

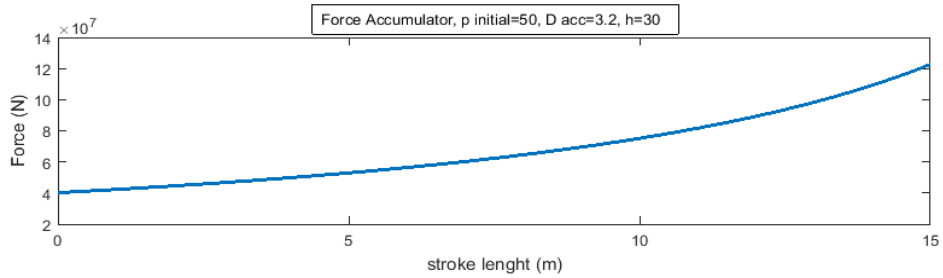

Figure 5-21 - "Accumulator force"

The non-linear behaviour of the damper is caused by the dimensions of the pipeline connecting the accumulator to the PHC. Since the accumulator is located on the deck of the PS, there has to be accounted for a minimal length of 100 meter.
The diameter of the opening of the valve can be adjusted. This will provide the linear part of the damping in the system.
The valve and the dimensions can be adjusted in order to obtain the desired damping value. Since the modelled springs are non-linear, a mean value of the springs stiffnesses can be used to estimate the critical damping value. A damping coefficient around this critical damping value will provide a decent result.

$$c_{crit} = \sqrt{2 \cdot k \cdot m}$$

Equation 5-24

As noticeable in Table XX both the diameter of the PHC as the diameter of the accumulator are input parameters. A variation in diameter between both pistons is accounted for in the model.

The heave response of the PS is obtained from an AQUA-model. With the design conditions of H_s=2.5, T_s=12, heading=0° the heave response of the PS is collected for 200 seconds. In the figures below a focus is laid on the largest heave motion in this timeframe.

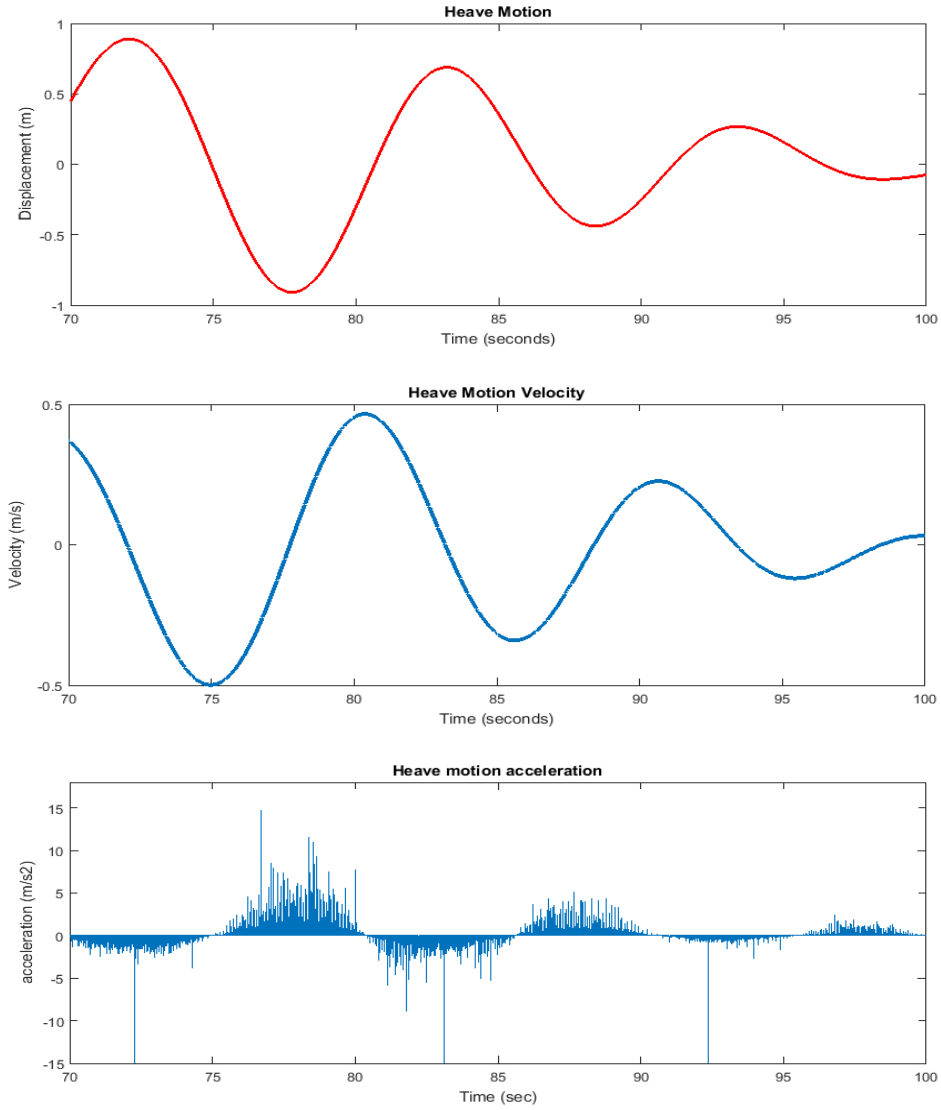

Figure 5-22 - "Response PS"

As illustrated in Fig. 5-23, the expected accelerations of the vessel motions will be around 10 m/s^2. The expected velocity of the motion will be around 0.5 m/s.
In order to prevent a rebound the hoist velocity of the fast lift concept must be larger than the velocity of the leg.

The largest heavemotion observed in the dataset is 0.9m. To prevent a rebound the proposed clearance of the leg must be larger than 0.9 m.

6 FEASIBILITY OF THE LIFTING TOOL

In this chapter the results of the model including the non-linearity in the system are presented. The dimensions of the fast lift concept and its capabilities can be evaluated.

6.1 Weight, size and capabilities

The input parameters of the model can be altered resulting in different responses of the system. The main objective of the fast lift concept is to perform a fast lift with a clearance of 1 meter. The velocity of this fast lift must be larger than the velocity of the heavemotions of the PS in order to prevent a rebound. Therefore, the fast lift velocity must be larger than 0.5 m/s.
The heave compensating capabilities of the concept are a convenient addition to the concept. However, this is not the main objective. Small movements of the leg after the fast lift are allowed. The occurrence of slack wires during the lifting phase must be avoided.

In this study different sets of input will be presented. The resulting motions of the system will be analyzed for different input parameters.
In order to evaluate the effect of the dimensions of the cylinder and accumulator, 6 different concepts are illustrated. For these concepts the responses of the system are presented.
For the last concept an elaboration is made on the non-linear behaviour of the cylinder and accumulator. Moreover, the probability of slack wires will be covered.

The feasibility of the fast lift concept is examined by its dimensions. Conclusions on the dimensions can be drawn from the results of the concepts.

6.1.1 Concept 1

In this concept a relatively small cylinder size is chosen. This is beneficial for the hoist capacity of the PS. The following input parameters are used:

D_{cyl}	[m]	Diameter of cylinder (PHC)	6
h_{cyl}	[m]	Height of cylinder (PHC)	8
p_{cyl}	[N/m^2]	Initial pressure cylinder	2*10^5
D_{acc}	[m]	Diameter of accumulator	3.2
h_{acc}	[m]	Height of accumulator	20
p_{acc}	[N/m^2]	Initial pressure accumulator	50*10^5
D_{pipe}	[m]	Diameter of the pipe connecting the accumulator tot the PHC	0.8
L_{pipe}	[m]	length of the pipeline	100
D_{valve}	[m]	Diameter of the opening of the valve	0.08
leghoist	[m]	proposed clearance of the leg	1.5

Table 6-1 - "input Concept 1"

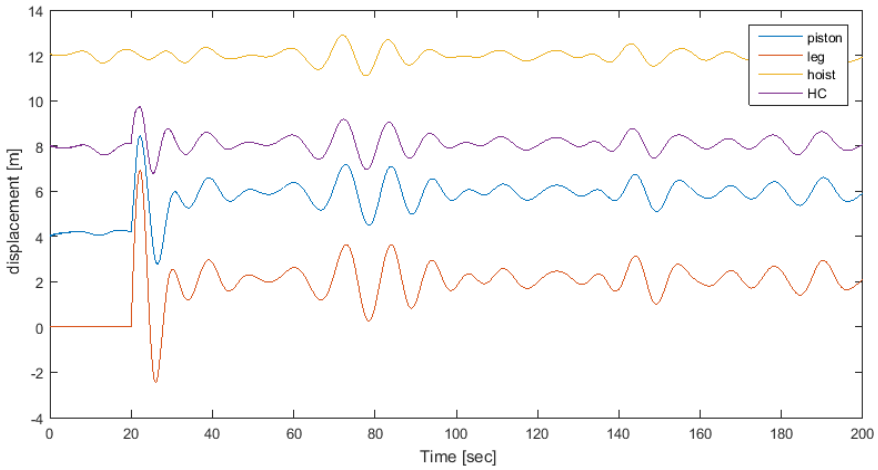

Figure 6-1 " response concept 1"

Due to the small cylinder size the spring stiffness will become larger for relative small motions. This high stiffness will cause peaks in the graph and for the first oscillations an overshoot, as shown in Fig. 6-1. The overshoot can be adjusted by increasing the damping coefficient. However this will result in a direct transfer of the heave motions to the concrete leg.

6.1.2 Concept 2

In this second concept a large cylinder size is chosen. This is beneficial for the heave compensation capabilities of the system. The following input parameters are used:

D_{cyl}	[m]	Diameter of cylinder (PHC)	6
h_{cyl}	[m]	Height of cylinder (PHC)	50
p_{cyl}	[N/m^2]	Initial pressure cylinder	2*10^5
D_{acc}	[m]	Diameter of accumulator	3.2
h_{acc}	[m]	Height of accumulator	20
p_{acc}	[N/m^2]	Initial pressure accumulator	50*10^5
D_{pipe}	[m]	Diameter of the pipe connecting the accumulator tot the PHC	1
L_{pipe}	[m]	length of the pipeline	100
D_{valve}	[m]	Diameter of the opening of the valve	0.15
leghoist	[m]	proposed clearance of the leg	1.5

Table 6-2- "Input Concept 2"

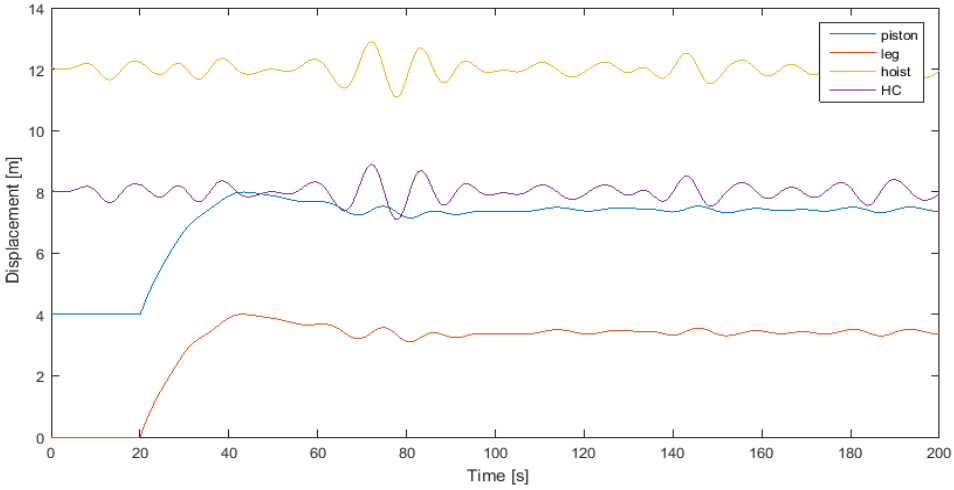

Figure 6-2 - " response concept 2"

"

The responses of the system are presented in Fig. 6-2. Due to the large cylinder and consequently the large volume, the spring behaves very linear and has a relatively low spring stiffness. This results in the nicely compensated heave motions after the fast lift. The response of the system is ideal. However, the size of the PHC is 50 meter. This is too large for a feasible solution.

6.1.3 Concept 3

In this concept is sought for an optimal design for the dimensions of the accumulator. The "optimal" design is dependent on the requirements. These requirements can change if other sub solutions for the total removal procedure are known. At this stage the optimal solution is a concept which provides a fast lift and prevents a rebound. The dimensions of the solutions may not interfere with the feasibility of the concept.

D_{cyl}	[m]	Diameter of cylinder (PHC)	6
h_{cyl}	[m]	Height of cylinder (PHC)	12
p_{cyl}	[N/m^2]	Initial pressure cylinder	2*10^5
D_{acc}	[m]	Diameter of accumulator	3.2
h_{acc}	[m]	Height of accumulator	20
p_{acc}	[N/m^2]	Initial pressure accumulator	50*10^5
D_{pipe}	[m]	Diameter of the pipe connecting the accumulator tot the PHC	1
L_{pipe}	[m]	length of the pipeline	100
D_{valve}	[m]	Diameter of the opening of the valve	0.12
leghoist	[m]	proposed clearance of the leg	1.5

Table 6-3 - "Input Concept 3"

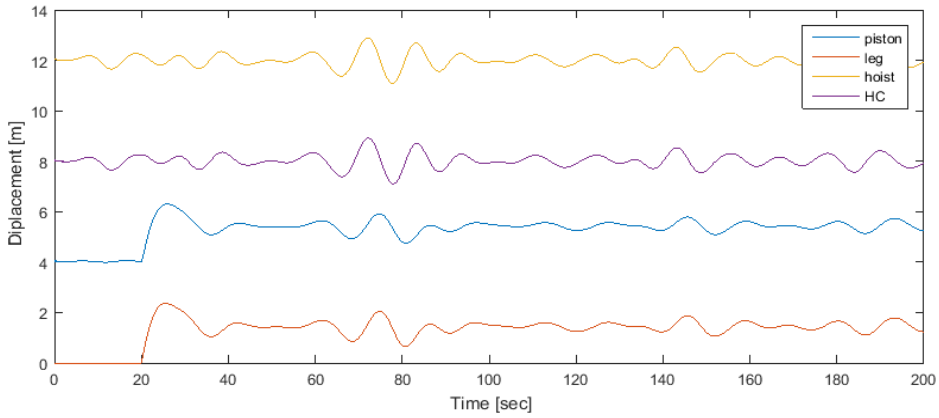

Figure 6-3 - " response concept 3"

At the moment of cut-off, at 20 sec., a fast lift is performed. After this fast lift, the system shows a very small heave compensating capability.
The velocity of the fast lift must be over 0.5 m/s to prevent a rebound. In Fig. 6-4 the velocity of the leg and the hammerhead of the JLS are presented.

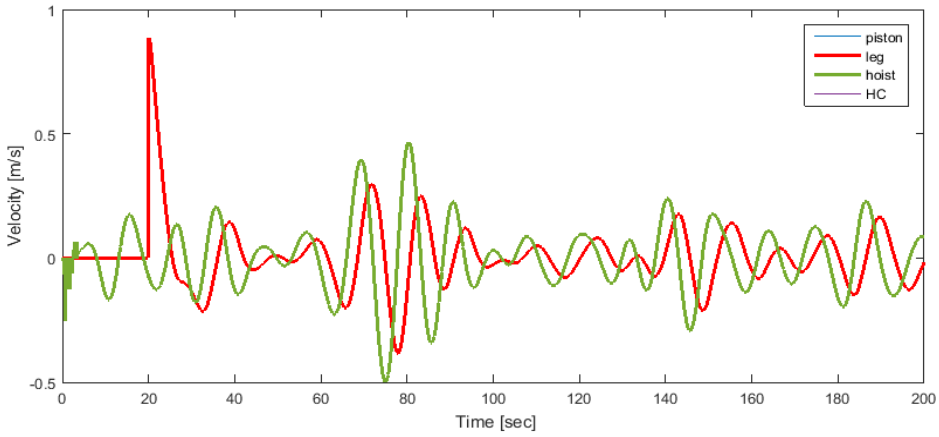

Figure 6-4 - "Velocity of leg / PS"

The velocity of the downward motion of the PS can be 0.5 m/s. In order to compensate for this motion and prevent a rebound, the lifting speed must be at least 0.5 m/s.
The velocity of the leg during the fast lift, at 20 sec., is larger than the maximum velocity of the heave motions. Therefore, there will be no occurrence of a rebound.

6.1.4 Concept 4

In the following 3 concepts the dimensions of the accumulator will be adjusted.
In this concept the volume of the accumulator is increased

D_{cyl}	[m]	Diameter of cylinder (PHC)	6
h_{cyl}	[m]	Height of cylinder (PHC)	12
p_{cyl}	[N/m^2]	Initial pressure cylinder	2*10^5
D_{acc}	[m]	Diameter of accumulator	3.2
h_{acc}	[m]	Height of accumulator	50
p_{acc}	[N/m^2]	Initial pressure accumulator	5*10^5
D_{pipe}	[m]	Diameter of the pipe connecting the accumulator tot the PHC	1
L_{pipe}	[m]	length of the pipeline	100
D_{valve}	[m]	Diameter of the opening of the valve	0.12
leghoist	[m]	proposed clearance of the leg	0.5

Table 6-4- "Input Concept 4"

The larger volume of the accumulator is beneficial for the lifting capabilities, as shown in Fig. 6-5. The larger volume generates a constant lift force. If the dimensions of the accumulator would allow it, a large lift stroke would be possible. However, only a clearance of 1,5 meter is supposed. Therefore the dimensions of this accumulator can be considered as too large.

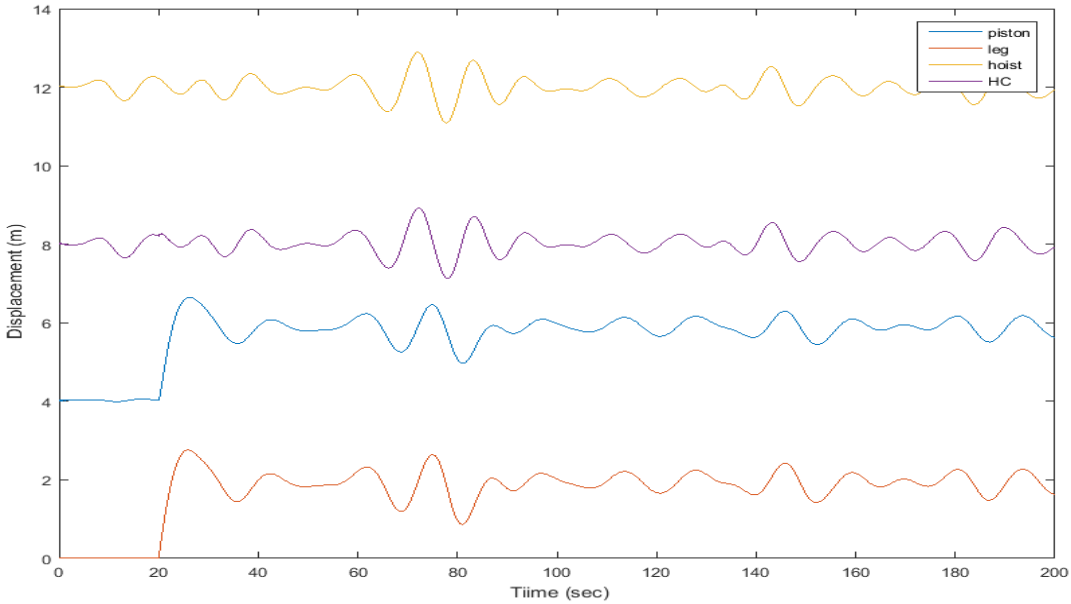

Figure 6-5 - "Response concept 4"

6.1.5 Concept 5

In this concept the volume of the accumulator is decreased. Since the accumulator needs certain dimensions in order to provide the required pressure, as explained in chapter 5.5, the diameter of the piston has to be at least 3.2 meter in order to obtain the required lift force.

D_{cyl}	[m]	Diameter of cylinder (PHC)	6
h_{cyl}	[m]	Height of cylinder (PHC)	12
p_{cyl}	[N/m^2]	Initial pressure cylinder	$2*10^5$
D_{acc}	[m]	Diameter of accumulator	3.2
h_{acc}	[m]	Height of accumulator	5
p_{acc}	[N/m^2]	Initial pressure accumulator	$350*10^5$
D_{pipe}	[m]	Diameter of the pipe connecting the accumulator tot the PHC	1
L_{pipe}	[m]	length of the pipeline	100
D_{valve}	[m]	Diameter of the opening of the valve	0.12
leghoist	[m]	proposed clearance of the leg	4

Table 6-5- "Input Concept 5"

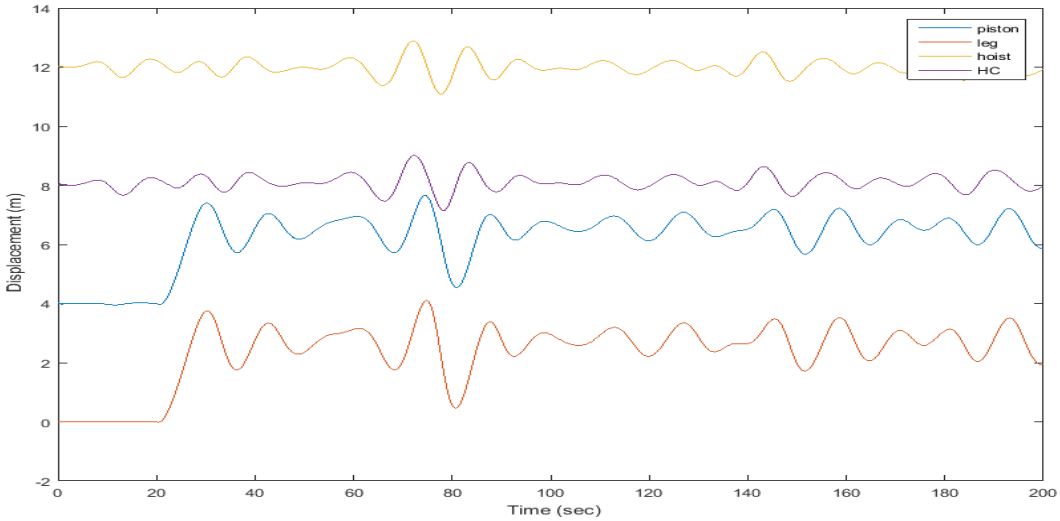

Figure 6-6 - "Response Concept 5"

As shown in Fig. 6-6., the response has larger excitations. The smaller volume of the accumulator will provide a more non-linear behaviour of the spring stiffness. This can be useful for the design of the system, since the force of the accumulator will decrease itself. The volume of the accumulator will also influence the behaviour of the cylinder. This spring stiffness will also become more non-linear and will provide larger variations, as shown in Fig. 6-7.

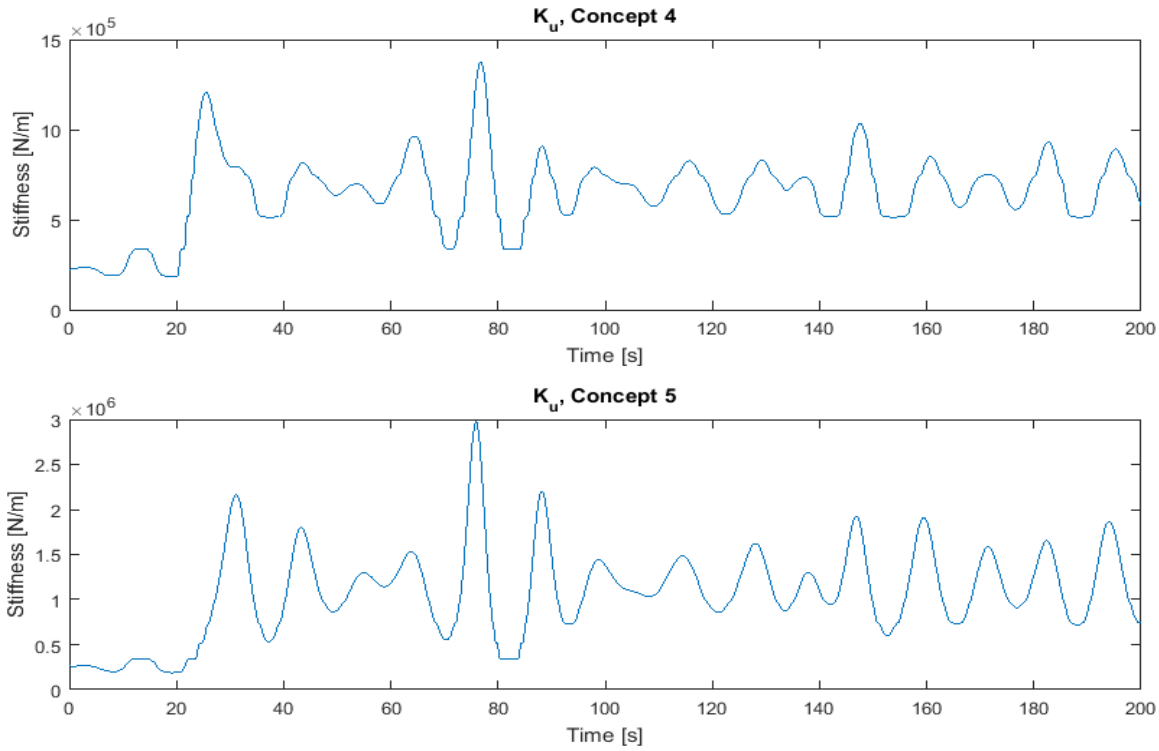

Figure 6-7 - "Difference in k-value cylinder, concept 5/6"

6.1.6 Concept 6

A smaller volume of the accumulator has a positive influence on the behaviour of the system. However, in concept 5 a pressure of 350bar is used. This high pressure could influence the feasibility of the system. In this concept a small accumulator volume with a pressure of 50 bar is sought for.

D_{cyl}	[m]	Diameter of cylinder (PHC)	6
h_{cyl}	[m]	Height of cylinder (PHC)	12
p_{cyl}	[N/m^2]	Initial pressure cylinder	$2*10^5$
D_{acc}	[m]	Diameter of accumulator	3.2
h_{acc}	[m]	Height of accumulator	11
p_{acc}	[N/m^2]	Initial pressure accumulator	$50*10^5$
D_{pipe}	[m]	Diameter of the pipe connecting the accumulator tot the PHC	1
L_{pipe}	[m]	length of the pipeline	100
D_{valve}	[m]	Diameter of the opening of the valve	0.12
leghoist	[m]	proposed clearance of the leg	0.5

Table 6-6- "Input Concept 6"

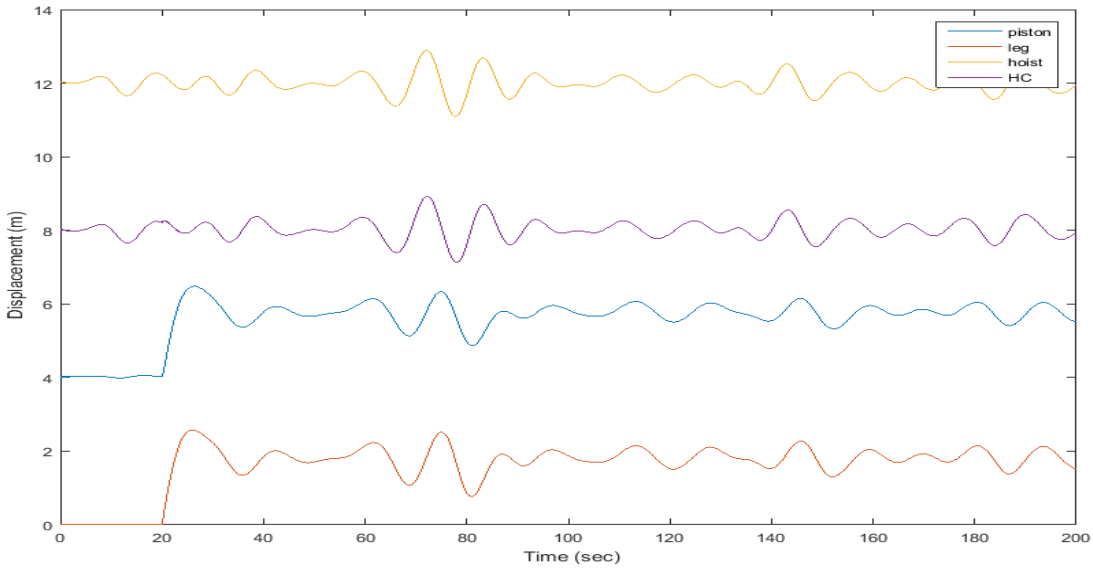

Figure 6-8 - "Response concept 6"

The response of the system, illustrated in Fig 6-8, shows an acceptable clearance of the leg. The compressed gas in the cylinder and accumulator is causing forces acting on the piston. These forces are presented in Fig. 6-9.

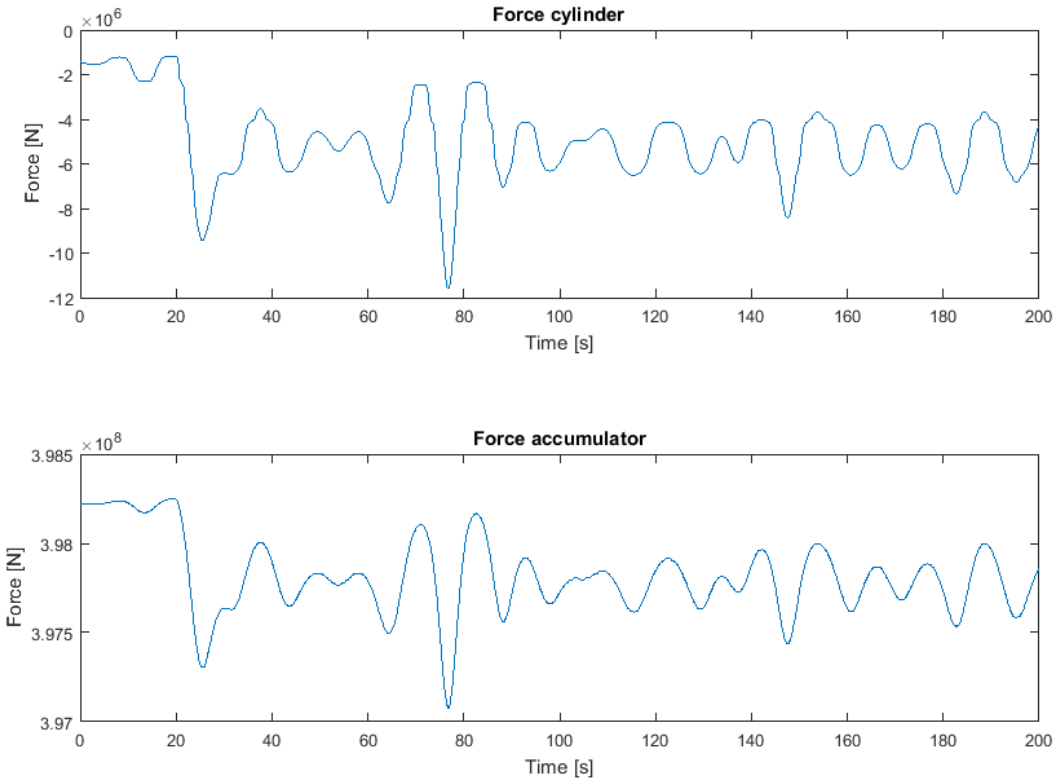

Figure 6-9 - "forces acting on piston"

6.1.7 Slack wires

Since slack wires can be a problem, a focus is laid on the variance in displacement between the TLB hammerhead and the PHC and the variance between the leg and the piston.

A cable is flexible and cannot resist compressive loads. Thus, under any compressive loading conditions a cable becomes slack. While re-tensioning, the buildup of forces in the wires can go too fast, causing high impact or snap loads of the cables [7]. These impact loads can be several orders higher than the normal static and dynamic loading and can cause breaking of the cable. However, even when the tension in the cable does not exceed the specified (static) breaking load, cable failure can occur.
During the lift operation slack wires should be avoided.

The cables connecting the PHC to the TLB and the cables between the leg and the PHC are modelled as springs and the structural damping in these cables is excluded, reliable

quantification on slack wires cannot be given. However, the probability of the occurrence of slack wires can be qualified

As shown in Fig. 6-10 a small discrepancy between the PHC and the hoist just after the moment of cut-off, is noticeable. This may result in slack wires.

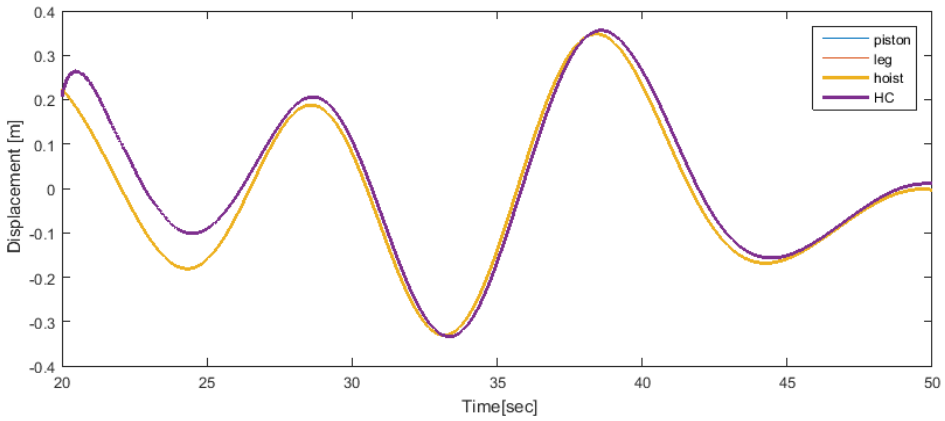

Figure 6-10 - "motion PS and PHC after release"

For an estimation of the occurrence of slack wires the relative displacement is plotted in Fig. 6-11. Noticeable is the larger displacement of the PHC, which can cause slack wires.

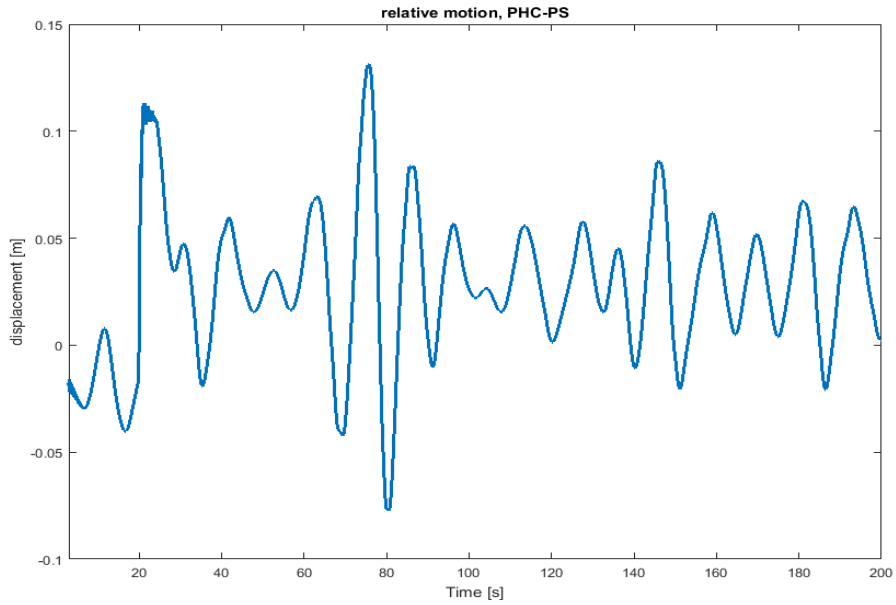

Figure 6-11 - "relative motion, PHC-PS"

In order to give a better qualification on the possibility of occurrence of slack wires, The resulting forces in the cables are plotted. When the forces in the wires become negative, the effect of slack wires will occur. Due to the weight of the system and the pretension before the cut-off, the forces in the cables remain positive, as shown in Fig. 6-12.

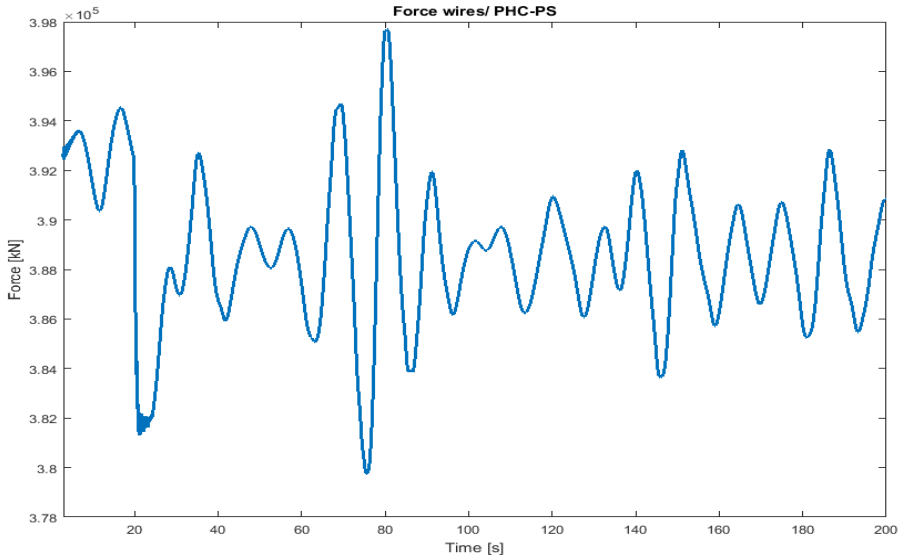

Figure 6-12 - "Force wires, PHC-PS"

The largest response in the system is the displacement of the leg and the piston. In Fig. 6-13 and 6-14 a focus is made on the wires connecting the leg and the piston.

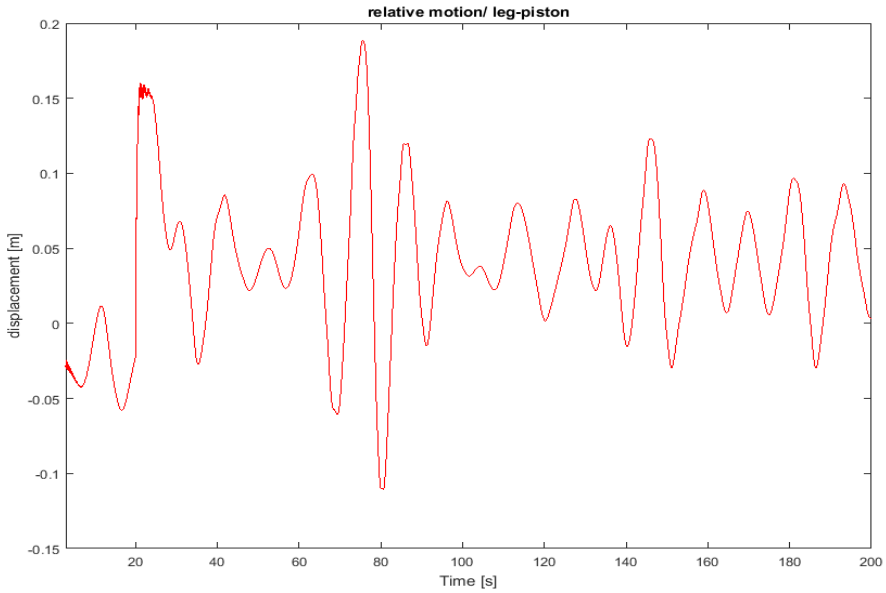

Figure 6-13 - "relative motion, leg-piston"

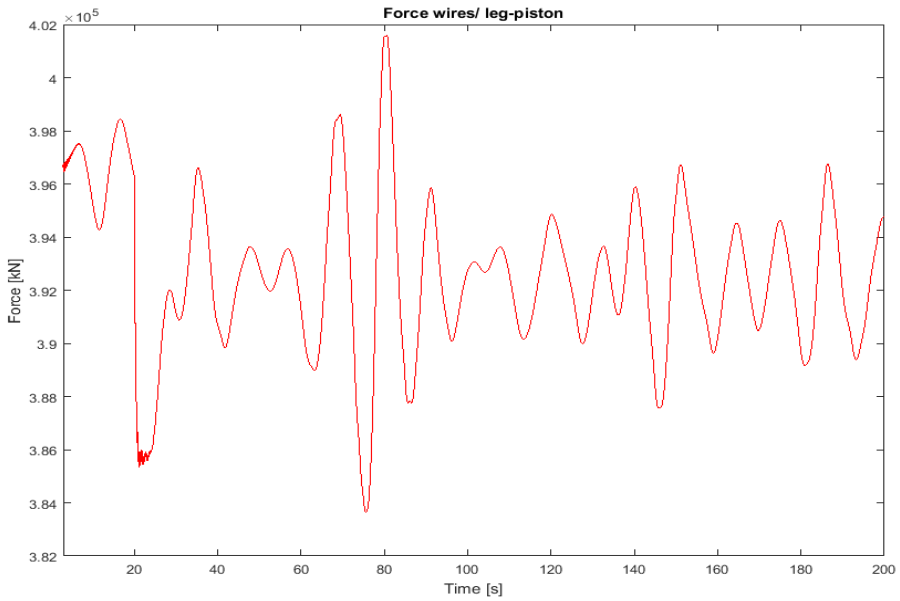

Figure 6-14 - "Force wires, leg-piston"

It can be observed that no slack wires will occur in the system, since the forces in the wires remain positive.

In the wires a large fluctuation of forces can be observed. An adjustment of the parameters could prevent these fluctuations and provide a more heave compensating system. However, the main objective is to perform a safe fastlift to prevent a rebound. Compared to a lift without the fast lift system, the rebound problem disregarded, heave compensating capabilities can already be marked. In Fig. 6-15 and 6-16 the relative motion and the response of the system without the PHC are presented. At t=20, the leg is released. For t<20 the leg is kept still.

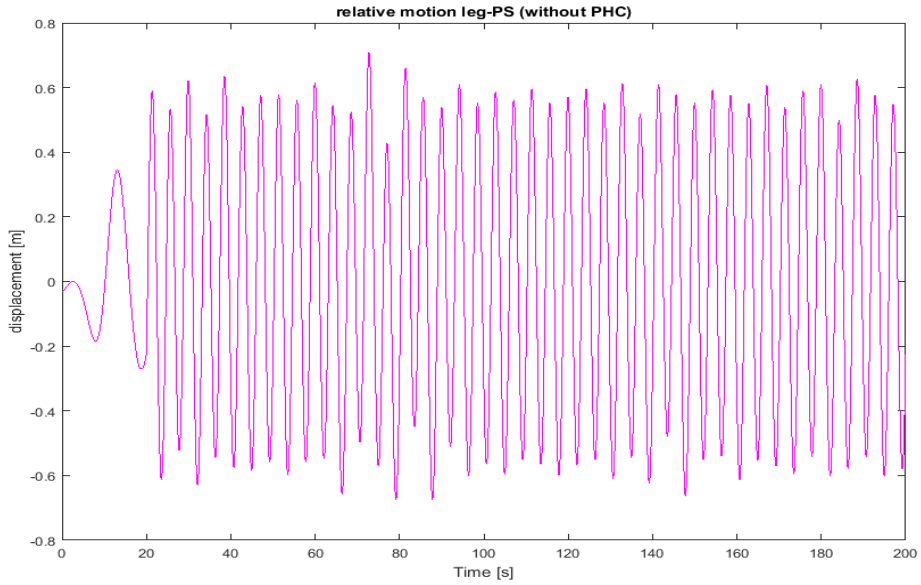

Figure 6-15 - "relative motion, leg-PS (without PHC)"

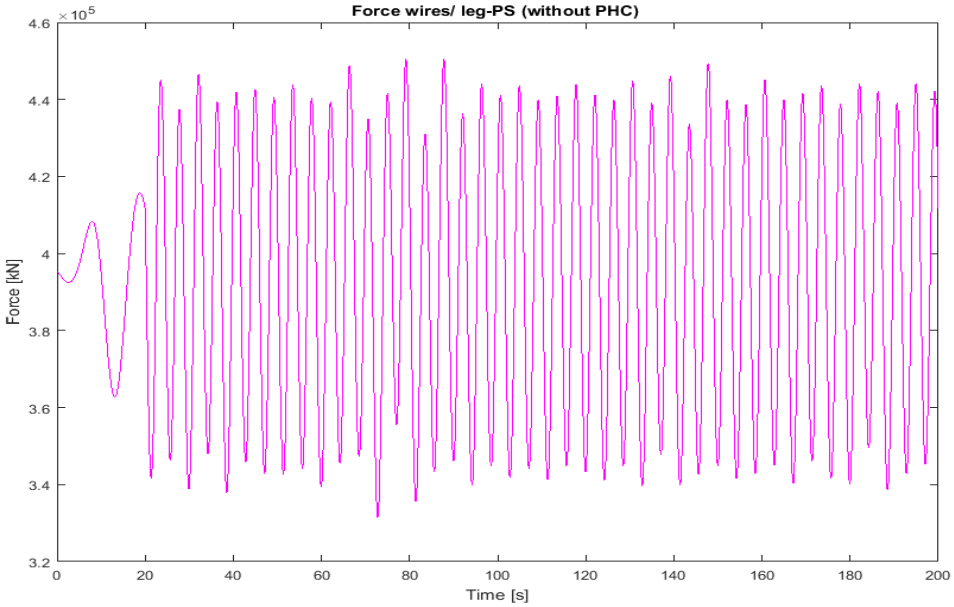

Figure 6-16 - "Force in wires, leg-PS (without PHC)"

6.1.8 Conclusions on concept study

The ideal dimensions of the system are dependent on the requirements.
A cylinder with a diameter of 6 meter with a height of 12 meters will provide satisfying results. By enlarging the volume of the cylinder, a softer spring can be obtained. This will have a positive impact on the heave compensating capabilities of the system.
A high pretension force in the accumulator is required. Therefore, the diameter of the accumulator has to be at least 3.2 meters. This large force is causing a high spring stiffness.The volume of the gas in the accumulator is preferred to be kept relatively small contrary to the volume of the PHC.
The small volume of the accumulator will cause a non-linear spring resulting in a rapid decay of the pretension force. A large cylinder will enhance the heave compensating capabilities of the system.

The responses of the leg and the TLB during the initial lifting phase are displayed in Fig 6-17. In this Figure the hoist velocity is included.

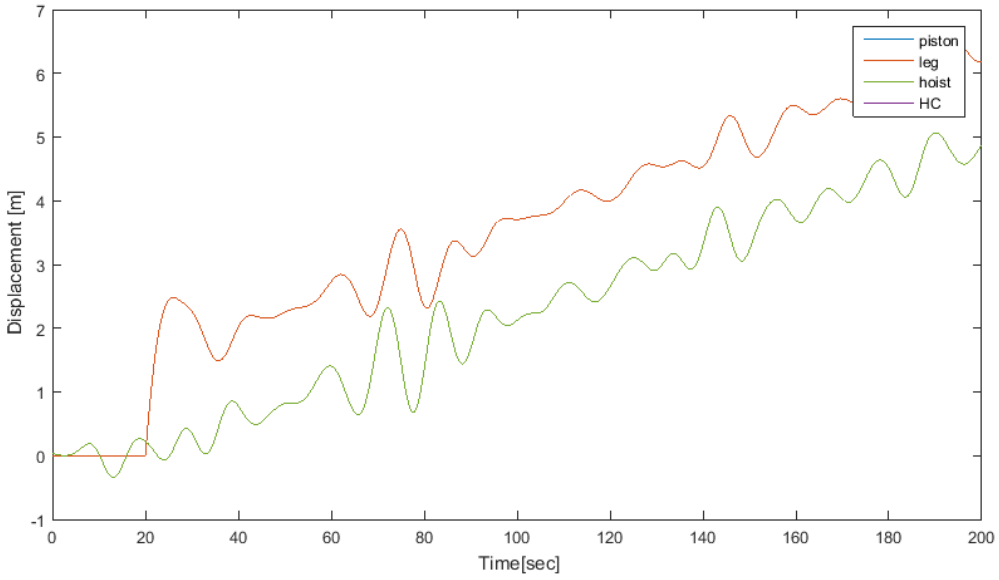

Figure 6-17 - "Leg lift"

6.2 Operational impact

The fast lift concept can produce a fast lift for the concrete leg. However, remarkable is the size of the equipment involved. This would be a challenging project to design a final concept. However, with the use of several smaller cylinders coupled to the same hydraulic system, obtaining a piston area of 6m^2 is possible. With the use of a multi cylinder set-up this can easily be achieved.
As an example 4 cylinders with a diameter of 1.5 m and a length of 12 meter can provide the required properties.
The pistons are modelled downward in this study, for more effective power transmission, the pistons can be reversed. The net cylinder area is the inner surface area of the cylinder minus the rod in the cylinder, connected to the leg. By rotating the pistons this area will be enlarged.
In a multi-cylinder set-up, as shown in Fig. 6-18, the cylinders and piston must be connected to eachother. By designing this concept a better insight into the weight and the lift capacity of the TLB can be obtained.

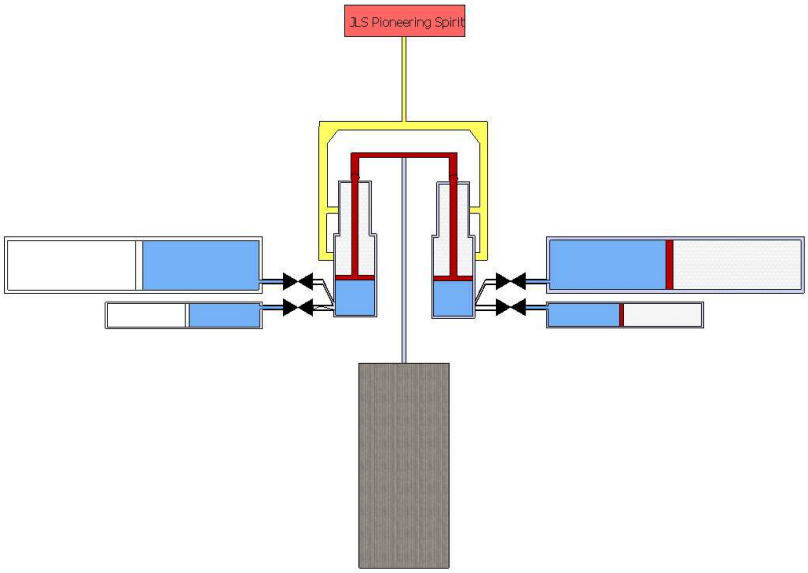

Figure 6-18 - "multi cylinder set-up"

6.2.1 Second accumulator

For the application of this concept a pretension of $1*10^6$ N is required. Therefore a downward force is needed. This will give opportunities for the tie-down concept or the partial cut. In all cases care must be taken for not damaging the structure with this amount of pretension involved.
However, a solution for this pretension problem can be found in the attachment of a second accumulator.

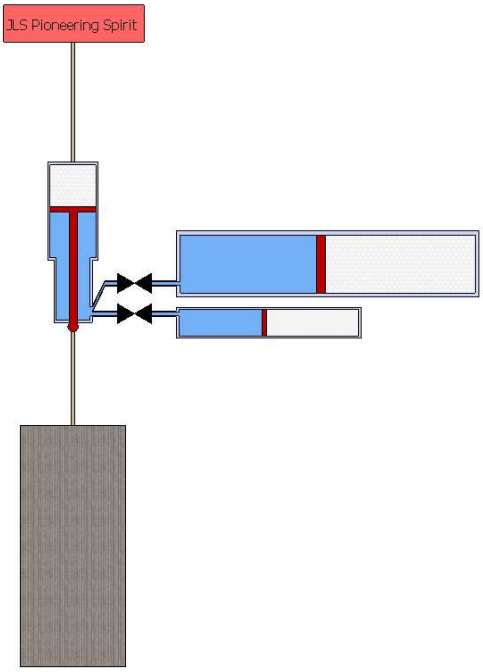

Figure 6-19 - "second accumulator"

After pre tensioning the first accumulator the valve of this accumulator can be closed. All the potential energy, required for a fast lift, is stored inside the accumulator. The valve of the second accumulator can be opened. This second accumulator can act as a PHC, for example during the cutting phase. When the fast lift is required, the valve of the second accumulator can be closed and simultaneously the valve of the first accumulator is opened. This will release all the stored potential energy of the first accumulator, resulting in a fast lift.

6.2.2 External gas volume

As mentioned in chapter 6.1.8., a large cylinder is favourable for the heave compensating capabilities of the concept. The size of the cylinder is limited by the feasibility. A large cylinder will lead to high costs. By relocating the volume of the gas to deck the cylinder size can be kept small and the heave compensating capabilities of a large cylinder can still be experienced. This concept is illustrated in Fig. 6-20. In this case the cylinder size can be determined by the stroke length of the piston. The diameter of the cylinder(s) will not change.

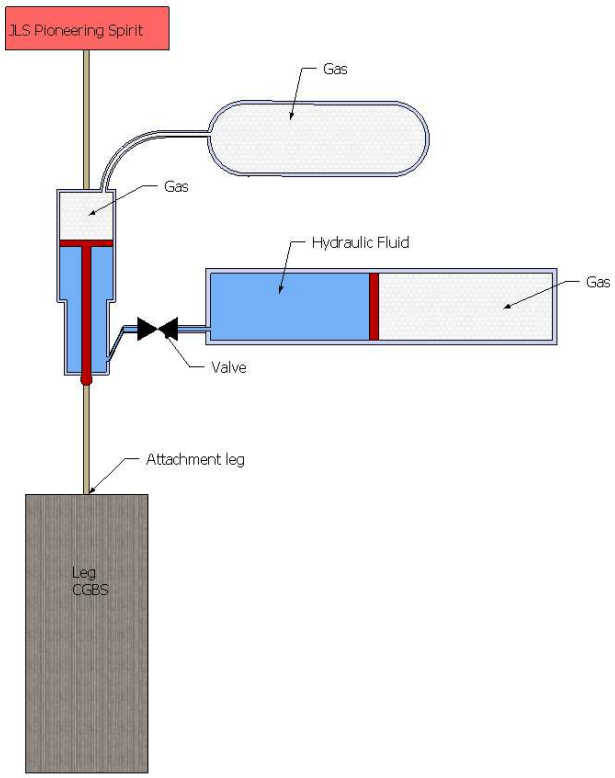

Figure 6-20 - "external gas volume"

7 CONCLUSIONS AND RECOMMENDATIONS

7.1 Conclusions

In the coming decades many oil and gas fields, equipped with large bottom founded structures, approach the end of their lifetime. Those structures have to be decommissioned. Allseas introduced their Pioneering Spirit (PS) and her capabilities offer new possibilities for this decommissioning. The PS is capable of lifting and removing the complete platform topside and subsequently also the legs of the offshore structure. This type of removal has never been carried out before, therefore, uncertainties are present and new concepts have to be developed.

In this thesis a concept for partial removal of the concrete legs with the Jacket Lift System(JLS) of the PS has been analyzed. Regulations allow that the section of the leg of 55 meter below sea level is removed and the remaining part can be left in place. The approach in this thesis, to split up the removal operation into 6 phases, is adequate. Each of these phases has its own technical challenges. Moreover, the components for each phase have their interrelationships.

The most challenging and crucial moment in the removal process is the moment of complete cut-off. At that moment a rebound of the leg with the remaining structure is possible, stability is no longer guaranteed and serious slacking of the lifting wires may occur.

Following the analysis in this thesis, it is concluded that fast lifting, just after cut-off, is the only feasible and practical solution to overcome a rebound, destabilization and slacking. In this thesis a fast lift component, with inherent stability and pretension for the cables has been designed.

As the PS will be involved in lift operations for legs ranging from 1500t to 6500t, the fast lifting component has to cope with this large variety of weight. The solution for the initial fast lift, preventing the leg from a rebound on the remaining bottom founded substructure, has been found in the concept of a sudden release of a pre-tensioned gas loaded spring system.

To perform the fast lift with a massive load like a concrete leg weighing 4000t, a huge amount of energy is required. The solution has been found in a hydraulic system. A passive hydraulic heave compensator type component supports the initial lift, while the temporary demand of huge energy supply has been realized with a hydraulic accumulator as energy storage device. This combination can be regarded as a unique concept.

In order to gain insight into the feasibility of this solution, a model of this concept has been made in MATLAB/Simulink.The extreme demands for the initial lift system requires a non-linear description of the springs in the model. By altering the mechanical dimension parameters and the physical pressure parameters, an estimation of the motion of the leg and hence the feasibility of the concept has been determined.

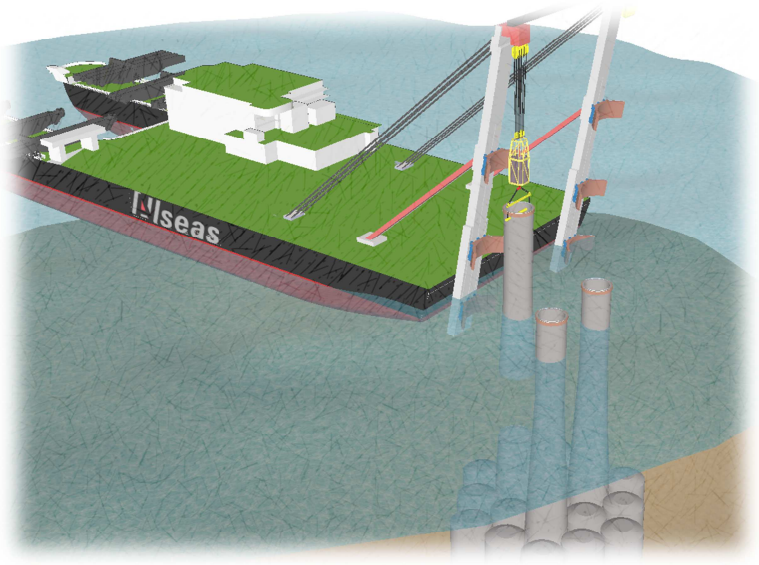

7.2 Recommendations

The forces in the fast lift component, as designed, are extremely high. In this thesis non-linearity in the springs of the simulation model has been introduced. It is recommended to give more extensive attention to the non-linearities of the compressed gas and the related damping in the system.

The fast lifting component is designed and simulated with cylinders, pistons, tubes and valves. In a practical realization all these elements have to be fitted into a sturdy housing construction, especially in a multiple cylinder set-up. During lifting, the dynamic properties of this construction will interact with the other elements. It is recommended to calculate and design this construction.

Since the dimensions of the fast lift solution could become large, the concept with the external gas volume could influence the feasibility of the system. Further study into this concept can be performed.

Horizontal motions and forces were not included since they have a minor influence on the feasibility of this fastlift concept. For the final design of a fastlift system these motions have to be included in the model since they will influence the total lift operation.

The lift operation could influence the motions of the PS, especially during the pretension phase; this influence needs to be determined.

It is also recommended to consider the application of the fast lifting component in the broader context of the removal process, as indicated by the feedback loop in chapter 2. A major challenge in the removal phases is the development of an appropriate cutting method.
At this moment there are several proposals for cutting, but an operational based solution is missing. Furthermore, the condition and the state of integrity of the concrete, after decades in the harsh offshore environment, is unknown. Herewith successful cutting has become a major challenge in the removal operation.

Related to the unsolved cutting challenge, it is recommended to incorporate a second, extra accumulator in the fast lift component. This extra accumulator has to offer heave compensation and a small amount of pretension during the cutting process. In this way, the system possesses the ability to perform a fast lift and simultaneously provides a highly controlled pretension. For a proper design of this concept, it is recommended to incorporate this extra accumulator into the simulation model.

As an initial lift of at least 1.5m is required and a weight of 1500t to 6500t has to be handled, the physical component based on this model will be huge, high demanding and extremely costly. Therefore, it is recommended to develop a physical scale model of the lift component, the lifting device and a scaled leg. A realistic cut-off approach is also required.

It is also recommended to develop an intensive test program in which all variables are carefully tested. The simulation model has to be refined on the basis of these tests and the requirements for a full scale component have to be developed.

In companies, which develop heave compensation type cylinders, a length of 5 m and a diameter of 1m of such a cylinder seems to be the maximum at this moment.
For the realization of the full scale component a number of parallel cylinders are foreseen. It is recommended to start a co-operation with such a company at an early phase. Together a full scale prototype component has to be defined.

Because of the strong interaction between final cut-of and initial lift, it is finally recommended to have one or more cutting companies involved on a project basis.

8 REFERENCES

[1] OSPAR, "OSPAR Decision '98," Oslo-Paris Convention on the protection of the marine environment of the North-East Atlantic, 1998.

[2] A. A. V. a. V. A. T. A. D. Kozlov G. A. Spiridonov V. V. Sychev, "Thermodynamic properties of air," originally published by Standards, Moscow, 1978.

[3] P. Albers, "Motion Control in Offshore and Dredging," Springer, 2010.

[4] H. N. S. D. D. B. a. M. B. Michael J Moran, "Fundamentals of Engineering Thermodynamics," Wiley.com, 2010.

[5] B. Nesbitt, "Handbook of Valves and Actuators: Valves Manual International," Butterworth-Heinemann, 2011.

[6] F. Wasser, "Pieter Schelte Jacket Lift System: Dynamic Analysis of the Initial Lifting Phase".

[7] S. J.M. Niedzwecki, "Snap loading of marine cables," Department of Civil Enghwering, Ocean Enghwerhlg Program, Texas A & M University, College, 1991.

[8] E. Belderbos, "Analysis of the dynamical behaviour of the Jacket Lift System of Pieter Schelte".

[9] I. A. o. O. &. G. Producers, "Decommissioning of offshore concrete gravity based structures (CGBS) in the OSPAR maritime area/other global regions," 2012.

[10] H. H.-A. H.K. Tönshoff, "Diamond tools for wire sawing metal components",," Institute for Production Engineering and Machine Tools, University of Hannover,, 2002.

[11] J. Wang, "Predictive depth of jet penetration models for abrasive waterjet cutting of alumina ceramics," School of Mechanical and Manufacturing Engineering, The University of New South Wales,, 2007.

[12] J. v. B. B. Vrijling, "Manual of hydraulic structure," Technical University Delft, 2011.

9 LIST OF TABLES

10 LIST OF FIGURES

Appendix A

Stability, Weight

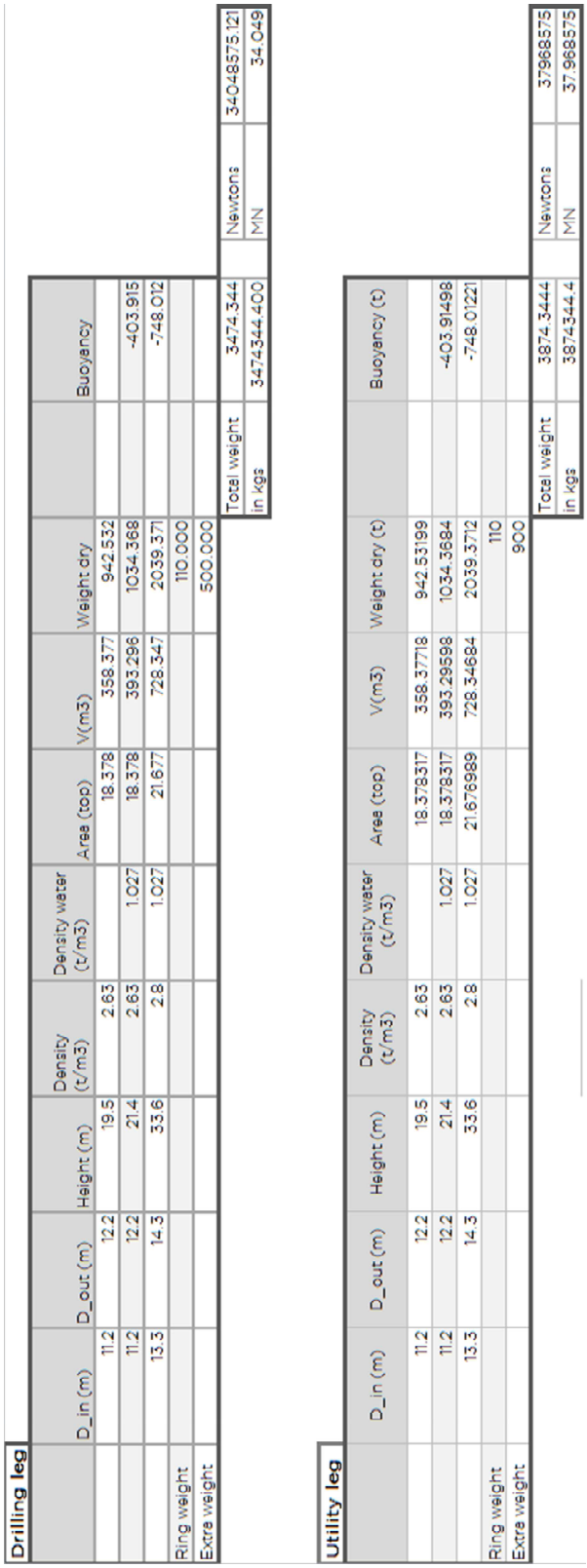

Drilling leg

	D_in (m)	D_out (m)	Height (m)	Density (t/m3)	Density water (t/m3)	Area (top)	V(m3)	Weight dry		Buoyancy
	11.2	12.2	19.5	2.63		18.378	358.377	942.532		
	11.2	12.2	21.4	2.63	1.027	18.378	393.296	1034.368		-403.915
	13.3	14.3	33.6	2.8	1.027	21.677	728.347	2039.371		-748.012
Ring weight								110.000		
Extra weight								500.000		
								Total weight in Kgs	3474.344 3474344.400	Newtons MN	34048575.121 34.049

Utility leg

	D_in (m)	D_out (m)	Height (m)	Density (t/m3)	Density water (t/m3)	Area (top)	V(m3)	Weight dry (t)		Buoyancy (t)
	11.2	12.2	19.5	2.63		18.378317	358.37718	942.53199		
	11.2	12.2	21.4	2.63	1.027	18.378317	393.29598	1034.3684		-403.91498
	13.3	14.3	33.6	2.8	1.027	21.676989	728.34684	2039.3712		-748.01221
Ring weight								110		
Extra weight								900		
								Total weight in Kgs	3874.3444 3874344.4	Newtons MN	37968575 37.968575

Current Forces

Top straight part

$$l_{straight} := 41.07 : \nu := 1.36 \cdot 10^{-6} : Di_{straight} := 12.2 : U := 1 :$$
$$Rey_{straight} := \frac{U \cdot Di_{straight}}{\nu} : \text{rho} := 1027 : c_{w.straight} := 0.9 :$$
$$A_{straight} := l_{straight} \cdot Di_{straight} :$$

$$F_{w.straight} := c_{w.straight} \cdot \text{rho} \cdot U^2 \cdot A_{straight};$$

$$4.631242122\,10^5$$

Lower part

$$Di_{cone} := 14.321 : l_{cone} := 33.6 : Rey_{cone} := \frac{U \cdot Di_{cone}}{\nu} : c_{w.cone} := 0.9 : A_{cone} := l_{cone} \cdot Di_{cone} :$$

$$F_{w.cone} := c_{w.cone} \cdot \text{rho} \cdot U^2 \cdot A_{cone} :$$

Total:

$$F_{w.total} := F_{w.straight} + F_{w.cone};$$

$$9.078840623\,10^5$$

Wave Forces

The wave height is assumed to be 5 meters with a period of 6.5 seconds. The legs are seen as slender structures and the waves are not breaking. Therefore, it is allowed to use Morison's formula.

$$h := 140.2 : g := 9.81 : H_s := 5 : T := 6.5 : L := \frac{g \cdot T^2}{2 \cdot \mathrm{Pi}} : H_b := evalf\left(\frac{1}{7} \cdot L\right) : \mathrm{rho} := 1027 : depth := 55 :$$

Hs/Hb is aproximate .5

$$C_d := 0.7 : K_d := 0.2 : K_i := 0.48 : S_d := 1 : S_i := 0.98 : C_i := 2.0 :$$

Structure specifications

$$l_{straight} := 21.4 : Di_{straight} := 12.2 : l_{cone} := 33.6 : Di_{cone} := 14.321 :$$

Wave Force

$$F_{i.straight} := \frac{C_i \cdot K_i \cdot H_s \cdot \mathrm{rho} \cdot g \cdot evalf(\mathrm{Pi}) \cdot Di_{straight}^2}{4} : F_{d.straight} := \frac{C_d \cdot K_d \cdot H_s^2}{2} \cdot \mathrm{rho} \cdot g \cdot Di_{straight} :$$

$$F_{straight} := F_{i.straight} + F_{d.straight};$$

$$5.868244856\,10^6$$

Resulting Moment

$$M_{straight} := F_{i.straight} \cdot depth \cdot S_i + F_{d.straight} \cdot depth \cdot S_d;$$

$$3.165350061\,10^8$$

Motion Response Calculator - results form

General		
Date	09-Jan-2014	
Project	Brent GBS leg removal	
Specification	TLB angle 106°	
Originator	GRC	
Revision	01	
Vessel	*Pieter Schelte*	[-]
Draft	*17.02*	[m]
AQWA *.lis file	*/IDE_T=17M_COARSEDRIF*	[-]
Water depth	100	[m]
Operational / survival condition	Operational	[-]
Wave spectrum	Jonswap	[-]
Wave directions	150 165 180 195 210 225 2	[deg]
Peakedness factor (γ)	3.3	[-]
Significant wave height	[2.5]	[m]
Wave period	[6]	[s]
Wave period type	Tz	[-]
Wave height reduction applied?	yes	[-]
Wave spreading	no	[-]

Location of interest*	x-Coor [m]	y-Coor [m]	z-Coor [m]
Hammerhead	-47.92	13.50	144.21

Remarks

Heave motions especially for all wave directions matter, since rebound and slack cables are being investigated

*Coordinate system
- positive x-axis points from the APP towards the bow
- positive y-axis points from CL towards PS
- positive z-axis points from the keelline orthogonal upwards
- 0 degree wave direction coming form the stern, positive defined anti-clock wise.

3 hours maximum, single amplitude motions and corresponding environmental conditions

Position**		x	y	z	rx	ry	rz	Hs [m]	Tz [s]	γ [-]	Wave Dir. [deg]
Surge	[m]	**0.37**	0.60	0.53	0.26	0.18	0.10	2.5	6	3.3	75
Sway	[m]	0.29	**1.43**	0.41	0.51	0.14	0.09	2.5	6	3.3	90
Heave	[m]	0.35	0.00	**0.55**	0.00	0.15	0.00	2.5	6	3.3	0
Roll	[deg]	0.29	1.43	0.41	**0.51**	0.14	0.09	2.5	6	3.3	90
Pitch	[deg]	0.37	0.60	0.53	0.26	**0.18**	0.10	2.5	6	3.3	75
Yaw	[deg]	0.33	0.75	0.54	0.26	0.17	**0.12**	2.5	6	3.3	255

Velocity**		x	y	z	rx	ry	rz	Hs [m]	Tz [s]	γ [-]	Wave Dir. [deg]
Surge	[m/s]	**0.26**	0.00	0.40	0.00	0.11	0.00	2.5	6	3.3	0
Sway	[m/s]	0.19	**1.01**	0.28	0.34	0.09	0.08	2.5	6	3.3	270
Heave	[m/s]	0.26	0.00	**0.40**	0.00	0.11	0.00	2.5	6	3.3	0
Roll	[deg/s]	0.19	1.01	0.26	**0.34**	0.09	0.08	2.5	6	3.3	90
Pitch	[deg/s]	0.25	0.55	0.36	0.17	**0.12**	0.08	2.5	6	3.3	75
Yaw	[deg/s]	0.23	0.56	0.37	0.18	0.11	**0.10**	2.5	6	3.3	105

Acceleration**		x	y	z	rx	ry	rz	Hs [m]	Tz [s]	γ [-]	Wave Dir. [deg]
Surge	[m/s^2]	**0.22**	0.00	0.30	0.00	0.08	0.00	2.5	6	3.3	0
Sway	[m/s^2]	0.15	**0.82**	0.17	0.24	0.06	0.07	2.5	6	3.3	90
Heave	[m/s^2]	0.22	0.00	**0.30**	0.00	0.08	0.00	2.5	6	3.3	0
Roll	[deg/s^2]	0.15	0.82	0.17	**0.24**	0.06	0.07	2.5	6	3.3	90
Pitch	[deg/s^2]	0.20	0.44	0.25	0.12	**0.08**	0.06	2.5	6	3.3	75
Yaw	[deg/s^2]	0.19	0.47	0.25	0.13	0.07	**0.08**	2.5	6	3.3	105

**Remarks
- listed values for motions,velocities and accelerations are single amplitudes
- all values are related to 3 hours maxima
- for a complete description of the model and calculation method see the motion report.
- the gravity contribution [g*sin(phi)] is incorporated in all affected values
- Motion analyzer rev. 10c

Appendix B

Appendix C

Year Installed	Operator	Field/Unit	Structure Type	Depth	no. of shafts	diameter shaft	Location		OSPAR region
1973	Phillips	Ekofisk	Tank - DORIS	71 m	1 (caisson)		North Sea (N)	yes	
1989	Phillips	Ekofisk P.B	CGS Protection Ring	75 m	-		North Sea (N)	yes	
1975	Mobil	Beryl A	Condeep 3 shafts	118 m	3		North Sea (UK)	yes	
1975	Shell	Brent B	Condeep 3 shafts	140 m	3		North Sea (UK)	yes	
1975	Elf	Frigg CDPI	CGS 1 shaft, Jarlan Wall	104 m	1 (caisson)		North Sea (UK)	yes	
1976	Shell	Brent D	Condeep 3 shafts	140 m	3		North Sea (UK)	yes	
1976	Elf	Frigg TPI	CGS 2 shafts	104 m	2		North Sea (UK)	yes	
1976	Elf	Frigg MCP-01	CGS 1 shaft, Jarlan Wall	94 m	1		North Sea (N)	yes	
1977	Shell	Dunlin A	CGS 4 shafts	153 m	4		North Sea (UK)	yes	
1977	Elf	Frigg TCP2	Condeep 3 shafts	104 m	3		North Sea (N)	yes	
1977	Mobil	Statfjord A	Condeep 3 shafts	145 m	3		North Sea (N)	yes	
1977	Petrobras	Ubarana-Pub 3	CGS caisson	15 m			Brazil	no	
1978	Petrobras	Ubarana-Pub 2	CGS caisson	15 m			Brazil	no	
1978	Petrobras	Ubarana-Pag 2	CGS caisson	15 m			Brazil	no	
1978	TAQA Bratani	Cormorant A	CGS 4 shafts	149 m	4	16	North Sea (UK)	yes	
1978	Chevron	Ninian Central	CGS 1 shaft, Jarlan Wall	136 m	1		North Sea (UK)	yes	
1978	Shell	Brent C	CGS 4 shafts	141 m	4	15	North Sea (UK)	yes	
1981	Mobil	Statfjord B	Condeep 4 shafts	145 m	4		North Sea (N)	yes	
1981	Amoco Canada	Tarsiut Island	4 hollow caissons	16 m			Beaufort Sea	no	
1982	Phillips	Maureen ALC	Concrete base artic. LC	92 m			North Sea (UK)	yes	
1983	Texaco	Schwedeneck A*	CGS Monotower	25 m	1		North Sea (D)	yes	
1983	Texaco	Schwedeneck B*	CGS Monotower	16 m	1		North Sea (D)	yes	
1984	Mobil	Statfjord C	Condeep 4 shafts	145 m	4		North Sea (N)	yes	
1984	Global Marine	Super CIDS	CGS caisson, Island	16 m			Beaufort Sea	no	
1986	Statoil	Gullfaks A	Condeep 4 shafts	135 m	4		North Sea (N)	yes	
1987	Statoil	Gullfaks B	Condeep 3 shafts	141 m	3		North Sea (N)	yes	
1988	Norsk Hydro]	Oseberg A	Condeep 4 shafts	109 m	4		North Sea (N)	yes	
1989	Statoil	Gullfaks C	Condeep 4 shafts	216 m	4		North Sea (N)	yes	
1989	Hamilton Bros	N. Ravenspurn	CGS 3 shafts	42 m	3		North Sea (UK)	yes	
1993	Shell	NAM F3-FB	CGS 3 shafts	43 m	3		North Sea (NL)	yes	
1993	Statoil	Sleipner A	Condeep 4 shafts	82 m	4		North Sea (N)	yes	
1993	Shell	Draugen	CondeepMonotower	251 m	1		North Sea (N)	yes	
1994	Conoco	Heidrun	Condeep	350 m			North Sea (N)	yes	
1996	BP	Harding	CGS	109 m			North Sea (UK)	yes	
1995	Shell	Troll A	Condeep 4 shafts	303 m	4		North Sea (N)	yes	
1996	Esso	West Tuna	CGS 3 shafts	61 m	3	15.65	Australia	no	
1996	Esso	Bream B	CGS 1 shaft	61 m	1	12	Australia	no	
1996	Ampolex	Wandoo	CGS 4 shafts	54 m	4	16	Australia	no	
1997	Mobil	Hibernia	CGS 4 shafts	80 m	4		Canada	no	
1999	Amerada Hess	South Arne	CGS 1 shaft	60 m	1	17.7	North Sea (DK)	yes	
2000	Shell	Malampaya	CGS 4 shafts	43 m	4	12	Philippines	no	
2005	Sakhalin Energy Investment Company	Lunskoye A	CGS 4 shafts	48 m	4		Sakhalin (R)	no	
2005	Sakhalin Energy Investment Company	Sakhalin PA-B	CGS 4 shafts	30 m	4		Sakhalin (R)	no	
2012	Exxon Neftegas Limited (ENL)	Sakhalin-1 Arkutun Dagi	GBS 4 shafts	33 m	4		Sakhalin-1 (R)	no	
2015	ExxonMobil Canada Properties	Hebron	GBS Monotower	109 m	1		Canada	no	
							Total OSPAR		31

Appendix D

In this Appendix the Equation of Motion of the schematized hydraulic system will be derived in more detail.

The system is modelled as follows:

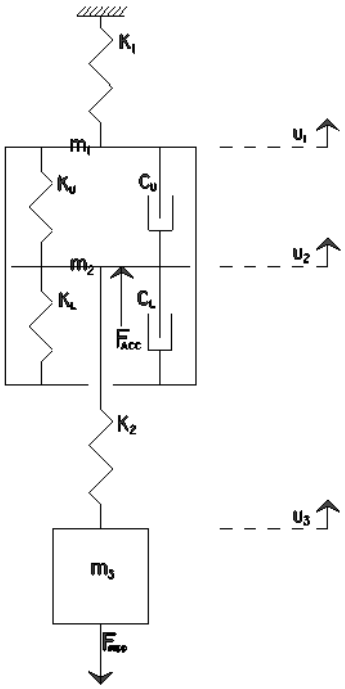

The displacement method is used to determine the equations of motions.

These combined will give the following equations:

This can be written in matrix form:

$u_1 > 0$

$m_1\ddot{u}_1 = -k_1 u_1 - (k_u + k_l)u_1 - (c_u + c_l)\dot{u}_1$

$m_2\ddot{u}_1 = (k_u + k_l)u_1 + (c_u + c_l)\dot{u}_1$

$u_2 > 0$

$m_1\ddot{u}_2 = (k_u + k_l)u_2 + (c_u + c_l)\dot{u}_2$

$m_2\ddot{u}_2 = -(k_u + k_l)u_2 - k_2 u_2 - (c_u + c_l)\dot{u}_2 + F_{acc}$

$m_3\ddot{u}_2 = k_2 u_2$

$u_3 > 0$

$m_3\ddot{u}_3 = k_2 u_3$

$m_3\ddot{u}_3 = -k_2 u_3 - F_{\text{sup}}$

$m_1\ddot{u}_1 = -k_1 u_1 - (k_u + k_l)u_1 - (c_u + c_l)\dot{u}_1 + (k_u + k_l)u_2 + (c_u + c_l)\dot{u}_2$

$m_2\ddot{u}_2 = (k_u + k_l)u_1 + (c_u + c_l)\dot{u}_1 - (k_u + k_l)u_2 - k_2 u_2 - (c_u + c_l)\dot{u}_2 + k_2 u_3 + F_{acc}$

$m_3\ddot{u}_3 = k_2 u_2 - k_2 u_3 - F_{\text{sup}}$

$m_1\ddot{u}_1 + (c_u + c_l)(\dot{u}_1 - \dot{u}_2) + k_1 u_1 + (k_u + k_l)(u_1 - u_2) = 0$

$m_2\ddot{u}_2 + (c_u + c_l)(\dot{u}_2 - \dot{u}_1) + (k_u + k_l)(u_2 - u_1) + k_2(u_2 - u_3) = F_{acc}$

$m_3\ddot{u}_3 + k_2(u_3 - u_2) = -F_{\text{sup}}$

$$\begin{pmatrix} m_1 & 0 & 0 \\ 0 & m_2 & 0 \\ 0 & 0 & m_3 \end{pmatrix}\begin{pmatrix} \ddot{u}_1 \\ \ddot{u}_2 \\ \ddot{u}_3 \end{pmatrix} + \begin{pmatrix} (c_u + c_l) & -(c_u + c_l) & 0 \\ -(c_u + c_l) & (c_u + c_l) & 0 \\ 0 & 0 & 0 \end{pmatrix}\begin{pmatrix} \dot{u}_1 \\ \dot{u}_2 \\ \dot{u}_3 \end{pmatrix} + \begin{pmatrix} k_1 + (k_u + k_l) & -(k_u + k_l) & 0 \\ -(k_u + k_l) & k_2 + (k_u + k_l) & -k_2 \\ 0 & -k_2 & k_2 \end{pmatrix}\begin{pmatrix} u_1 \\ u_2 \\ u_3 \end{pmatrix} = \begin{pmatrix} 0 \\ F_{acc} \\ -F_{\text{sup}} \end{pmatrix}$$

Initial conditions

$$F_{acc} - k_2 \cdot u_3 - (k_u + k_l) \cdot (u_3 - u_2) - (c_u + c_l) \cdot (\dot{u}_3 - \dot{u}_2) = 0$$
$$-(k_u + k_l) \cdot (u_2 - u_3) - (c_u + c_l) \cdot (\dot{u}_2 - \dot{u}_3) - k_1 \cdot u_2 = 0$$
$$\Rightarrow u_2 = \frac{(k_u + k_l) \cdot F_{acc}}{k_1 \cdot k_2 + k_1 \cdot (k_u + k_l) + k_2 \cdot (k_u + k_l)}$$
$$\Rightarrow u_3 = \frac{(k_1 \cdot (k_u + k_l)) \cdot F_{acc}}{k_1 \cdot k_2 + k_1 \cdot (k_u + k_l) + k_2 \cdot (k_u + k_l)} = \frac{u_2 \cdot (k_1 + (k_u + k_l))}{(k_u + k_l)}$$

$$t = 0$$
$$u_2 \rightarrow -(k_u + k_l) \cdot (u_2 - u_3) - k_1 \cdot u_2 - (c_u + c_l) \cdot (\dot{u}_2 - \dot{u}_3) = 0$$
$$\dot{u}_2 = 0; \dot{u}_3 = 0 \Rightarrow -(k_u + k_l) \cdot (u_2 - u_3) - k_1 \cdot u_2 - \cancel{(c_u + c_l) \cdot (\dot{u}_2 - \dot{u}_3)} = 0$$

$$u_3 \rightarrow F_{acc} - k_2 \cdot u_3 - (k_u + k_l) \cdot (u_3 - u_2) - (c_u + c_l) \cdot (\dot{u}_3 - \dot{u}_2) = 0$$
$$\dot{u}_2 = 0; \dot{u}_3 = 0 \Rightarrow F_{acc} - k_2 \cdot u_3 - (k_u + k_l) \cdot (u_3 - u_2) - \cancel{(c_u + c_l) \cdot (\dot{u}_3 - \dot{u}_2)} = 0$$

$$\text{initial condition} \Rightarrow u_2 = \frac{(k_u + k_l) \cdot F_{acc}}{k_1 \cdot k_2 + k_1 \cdot (k_u + k_l) + k_2 \cdot (k_u + k_l)}$$
$$\text{initial condition} \Rightarrow u_3 = \frac{(k_1 \cdot (k_u + k_l)) \cdot F_{acc}}{k_1 \cdot k_2 + k_1 \cdot (k_u + k_l) + k_2 \cdot (k_u + k_l)} = \frac{u_2 \cdot (k_1 + (k_u + k_l))}{(k_u + k_l)}$$

All the Initial Conditions are:

Initial Conditions

$$u_1 = 0$$
$$\dot{u}_1 = 0$$

$$u_2 = \frac{(k_u + k_l) \cdot F_{acc}}{k_1 \cdot k_2 + k_1 \cdot (k_u + k_l) + k_2 \cdot (k_u + k_l)}$$
$$\dot{u}_2 = 0$$

$$u_3 = \frac{u_2 \cdot (k_1 + (k_u + k_l))}{(k_u + k_l)}$$
$$\dot{u}_3 = 0$$

$$u_4 = 0$$
$$\dot{u}_4 = 0$$

Solving the EOM with the initial conditions:

```
F_acc =
(g*k1*k2*m3+g*k1*k2*m4+g*k1*m4*(k_u+k_l)+g*k2*m2*(k_u+k_l)+g*k2*(k_u
+k_l)*m3+g*k2*(k_u+k_l)*m4+k1*k2*leghoist*(k_u+k_l))/(k2*(k1+(k_u+k_
l)));

%old F_acc-
>((g*k1*k2*m4+g*k1*m4*(k_u+k_l)+g*k2*m4*(k_u+k_l)+k1*k2*leghoist*(k_
u+k_l)))/(k2*(k1+(k_u+k_l)))
%F_acc=3988+g*m4; %Force accumulator

F_supp=g*m4-k2*(-g*k1*m3-g*(k_u+k_l)*m2-
g*(k_u+k_l)*m3+F_acc*(k1+(k_u+k_l)))/(k1*k2+k1*(k_u+k_l)+k2*(k_u+k_l
));

% initial deflections
hoist_init=0;
HC_init=(-g*k2*m2-g*(k_u+k_l)*m2-
g*(k_u+k_l)*m3+F_acc*(k_u+k_l))/(k1*k2+k1*(k_u+k_l)+k2*(k_u+k_l));

piston_init=(-g*k1*m3-g*(k_u+k_l)*m2-
g*(k_u+k_l)*m3+F_acc*(k1+(k_u+k_l)))/(k1*k2+k1*(k_u+k_l)+k2*(k_u+k_l
))

leg_init=0
```

Conditions at t>>$t_{release}$

$$t \gg t_{release}$$

$$u_2 \rightarrow -(k_u + k_l)\cdot(u_2 - u_3) - k_1 \cdot u_2 - (c_u + c_l)\cdot(\dot{u}_2 - \dot{u}_3) = 0$$

$$\text{Since } t \gg t_{release}; \dot{u}_2 = 0; \dot{u}_3 = 0$$

$$\Rightarrow -(k_u + k_l)\cdot(u_2 - u_3) - k_1 \cdot u_2 - \cancel{(c_u + c_l)\cdot(\dot{u}_2 - \dot{u}_3)} = 0$$

$$u_3 \rightarrow F_{acc} - k_2 \cdot (u_3 - u_4) - (k_u + k_l)\cdot(u_3 - u_2) - (c_u + c_l)\cdot(\dot{u}_3 - \dot{u}_2) = 0$$

$$\text{Since } t \gg t_{release}; \dot{u}_2 = 0; \dot{u}_3 = 0$$

$$\Rightarrow F_{acc} - k_2 \cdot (u_3 - u_4) - (k_u + k_l)\cdot(u_3 - u_2) - \cancel{(c_u + c_l)\cdot(\dot{u}_3 - \dot{u}_2)} = 0$$

$$-F_z - k_2(u_4 - u_3) = 0$$

$$u_2 = \frac{F_{acc} - F_z}{k_1}$$

$$u_3 = \frac{F_{acc}\cdot(k_1 + (k_u + k_l)) - F_z \cdot (k_1 + (k_u + k_l))}{k_1 \cdot (k_u + k_l)}$$

$$u_4 = \frac{F_{acc}\cdot(k_1 \cdot k_2 + k_2 \cdot (k_u + k_l)) - F_z(k_1 \cdot k_2 + k_1 \cdot (k_u + k_l) - k_2 \cdot (k_u + k_l))}{k_1 \cdot k_2 \cdot (k_u + k_l)}$$

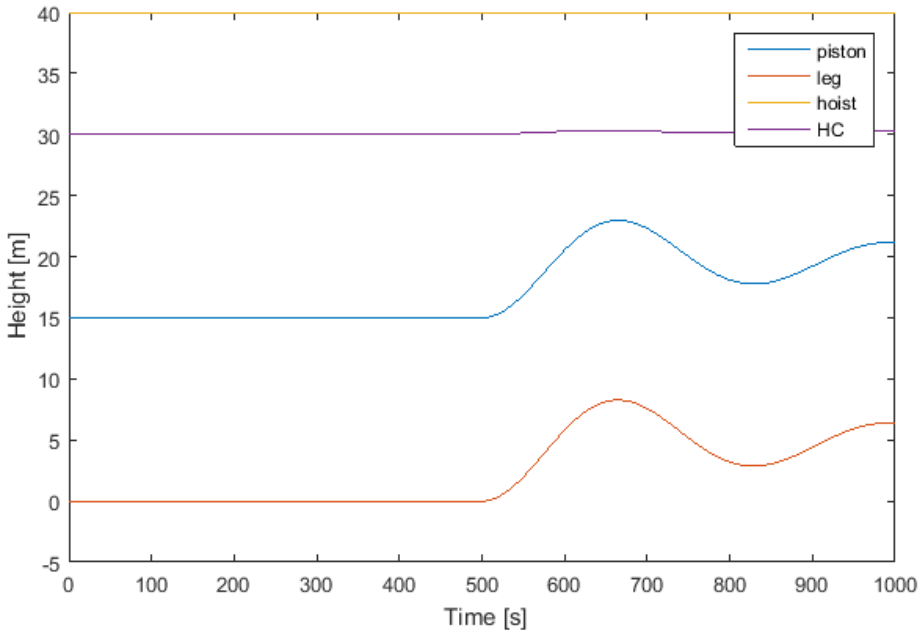
piston
leg
hoist
HC
Height [m]
Time [s]
40
35
30
25
20
15
10
5
0
-5
0
100
200
300
400
500
600
700
800
900
1000

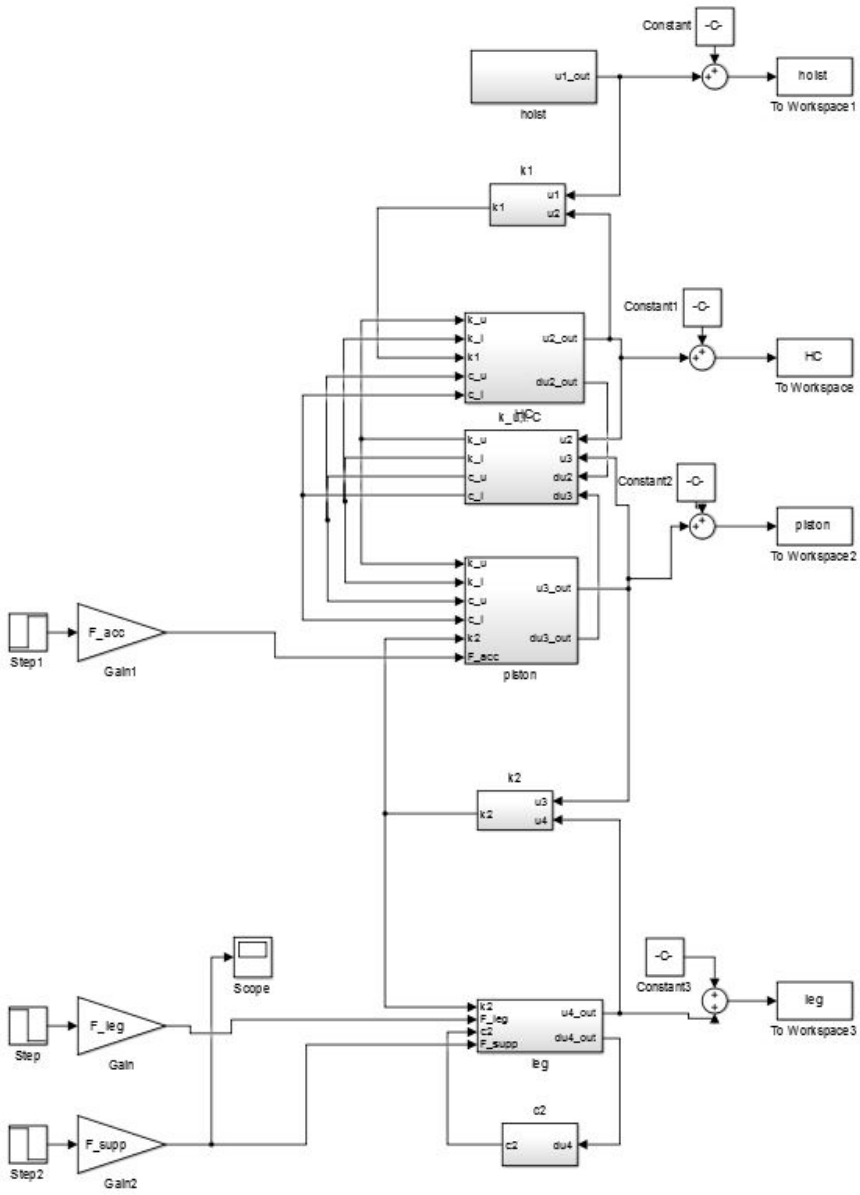

MATLAB script for model

```
clc;
clear all;

%input for test3working5
```

```
k_u=2; %spring in PHC (upper)
k_l=2; %spring in PHC(lower)
c_u=30; %damper in PHC (upper)
c_l=30; %damper in PHC (lower)
k1=100; %cable hoist-PHC
k2=100; %cable PHC-leg
c2=0; %damping leg
m1=0;
m2=10;
m3=1;
m4=10000;
u1=0; %movement hoist t=0
u4_0=0; %movement leg t=0

g=9.81;

leghoist= 5

tf=1000; %final time
ts=0;
t_up=500; %time Force leg --> 0
t_acc=0; %time Force accumulator>0
F_leg=0; %Force in leg
%F_acc = 10000

F_acc =
(g*k1*k2*m3+g*k1*k2*m4+g*k1*m4*(k_u+k_l)+g*k2*m2*(k_u+k_l)+g*k2*(k_u
+k_l)*m3+g*k2*(k_u+k_l)*m4+k1*k2*leghoist*(k_u+k_l))/(k2*(k1+(k_u+k_
l)));

%old F_acc-
>((g*k1*k2*m4+g*k1*m4*(k_u+k_l)+g*k2*m4*(k_u+k_l)+k1*k2*leghoist*(k_
u+k_l)))/(k2*(k1+(k_u+k_l)))
%F_acc=3988+g*m4; %Force accumulator

F_supp=g*m4-k2*(-g*k1*m3-g*(k_u+k_l)*m2-
g*(k_u+k_l)*m3+F_acc*(k1+(k_u+k_l)))/(k1*k2+k1*(k_u+k_l)+k2*(k_u+k_l
));

% initial deflections
hoist_init=0;
HC_init=(-g*k2*m2-g*(k_u+k_l)*m2-
g*(k_u+k_l)*m3+F_acc*(k_u+k_l))/(k1*k2+k1*(k_u+k_l)+k2*(k_u+k_l));

piston_init=(-g*k1*m3-g*(k_u+k_l)*m2-
g*(k_u+k_l)*m3+F_acc*(k1+(k_u+k_l)))/(k1*k2+k1*(k_u+k_l)+k2*(k_u+k_l
))

leg_init=0;


% initial position
```

```
hoist_begin=40;
HC_begin=30-HC_init;
piston_begin=15-piston_init;
leg_begin=0-leg_init;


u_2=(m4*g-F_acc)/k1
u_3=((m4*g)*(k1+(k_u+k_l))-F_acc*(k1+(k_u+k_l)))/k1*(k_u+k_l)
u_4=((m4*g)*(k1*k2+(k1*(k_u+k_l))+(k2*(k_u+k_l)))-
F_acc*(k1*k2+k2*(k_u+k_l)))/(k1*k2*(k_u+k_l))

piston_init

u2_trel=-HC_init-u_2
u3_trel=-piston_init-u_3
u4_trel=-leg_init-u_4


open_system('model_2')
run('model_2')
sim('model_2')

figure(1)

plot(piston,'DisplayName','piston');hold
all;plot(leg,'DisplayName','leg');plot(hoist,'DisplayName','hoist');
plot(HC,'DisplayName','HC');hold off;
legend('piston','leg','hoist','HC')
```

Maple file for validation model

```
> restart;
> g := 9.81; k_u := 2; k_l := 2 ; c_u := 30; c_l := 30; k1 := 100; k2 := 100; m3 := 10000;
      m2 := 1; m1 := 10;
```

$$g := 9.81$$

$$k\_u := 2$$

$$k\_l := 2$$

$$c\_u := 30$$

$$c\_l := 30$$

$$k1 := 100$$

$$k2 := 100$$

$$m3 := 10000$$

$$m2 := 1$$

$$m1 := 10$$

```
> k_tot := k_u + k_l : c_tot := c_u + c_l :
> leghoist := 5 :
> Fz = m3·g
```

$$Fz = 98100.00$$

> $F\_acc := \frac{1}{(k2\cdot(k1 + k\_tot))}(g\cdot k1\cdot k2\cdot m2 + g\cdot k1\cdot k2\cdot m3 + g\cdot k1\cdot m3\cdot k\_tot + g\cdot k2\cdot m1 \cdot k\_tot + g\cdot k2\cdot k\_tot\cdot m2 + g\cdot k2\cdot k\_tot\cdot m3 + k1\cdot k2\cdot leghoist\cdot k\_tot);$

$$F\_acc := 1.019058908\,10^{5}$$

> $F\_ac := 100$

$$F\_ac := 100$$

> $F\_spp := m3\cdot g - k2\cdot \frac{-g\cdot k1\cdot m2 - g\cdot k\_tot\cdot m1 - g\cdot k\_tot\cdot m2 + (F\_acc\cdot(k1 + k\_tot))}{k1\cdot k2 + k1\cdot(k\_tot) + k2\cdot k\_tot};$

$$F\_spp := -18.51852$$

> $F\_supp := 0$

$$F\_supp := 0$$

Equations of motion

> $eq1 := m1\cdot(diff(u1(t), t\$2) + g) + (k1 + (k\_tot))\cdot u1(t) - ((k\_tot)\cdot u2(t)) + (c\_tot)\cdot diff(u1(t), t) - (c\_tot)\cdot diff(u2(t), t);$

$$eq1 := 10\left(\frac{d^2}{dt^2}u1(t)\right) + 98.10 + 104\,u1(t) - 4\,u2(t) + 60\left(\frac{d}{dt}u1(t)\right) - 60\left(\frac{d}{dt}u2(t)\right)$$

> $eq2 := m2\cdot(diff(u2(t), t\$2) + g) - (k\_tot)\cdot u1(t) + ((k\_tot) + k2)\cdot u2(t) - k2\cdot u3(t) - (c\_tot)\cdot diff(u1(t), t) + (c\_tot)\cdot diff(u2(t), t) - F\_acc;$

$$eq2 := \frac{d^2}{dt^2}u2(t) - 1.018960808\,10^{5} - 4\,u1(t) + 104\,u2(t) - 100\,u3(t) - 60\left(\frac{d}{dt}u1(t)\right) + 60\left(\frac{d}{dt}u2(t)\right)$$

> $eq3 := m3\cdot(diff(u3(t), t\$2) + g) - k2\cdot u2(t) + k2\cdot u3(t) - F\_supp;$

$$eq3 := 10000\left(\frac{d^2}{dt^2}u3(t)\right) + 98100.00 - 100\,u2(t) + 100\,u3(t)$$

>

>

Initial conditions

> $HC\_init := \frac{-g\cdot k2\cdot m1 - g\cdot k\_tot\cdot m1 - g\cdot k\_tot\cdot m2 + F\_acc\cdot k\_tot}{k1\cdot k2 + k1\cdot k\_tot + k2\cdot k\_tot}$

$$HC\_init := 36.79462252$$

> $piston\_init := \frac{-g\cdot k1\cdot m2 - g\cdot k\_tot\cdot m1 - g\cdot k\_tot\cdot m2 + (F\_acc\cdot(k1 + k\_tot))}{k1\cdot k2 + k1\cdot(k\_tot) + k2\cdot k\_tot}$

$$piston\_init := 981.1851852$$

> $ics := u1(0) = HC\_init, D(u1)(0) = 0, u2(0) = piston\_init, D(u2)(0) = 0, u3(0) = 0, D(u3)(0) = 0;$

$$ics := u1(0) = 36.79462252, D(u1)(0) = 0, u2(0) = 981.1851852, D(u2)(0) = 0, u3(0) = 0, D(u3)(0) = 0$$

>

```
>
> sys_ode := eq1 = 0, eq2 = 0, eq3 = 0 :
> sol := dsolve({sys_ode, ics}, {u1(t), u2(t), u3(t)}, method = laplace) :
> assign(sol);
>
> plot([u1(t) + 30 - HC_init, u2(t) + 15 - piston_init, u3(t)], t = 0..1000, legend = ["HC",
      "piston", "leg"]);
```

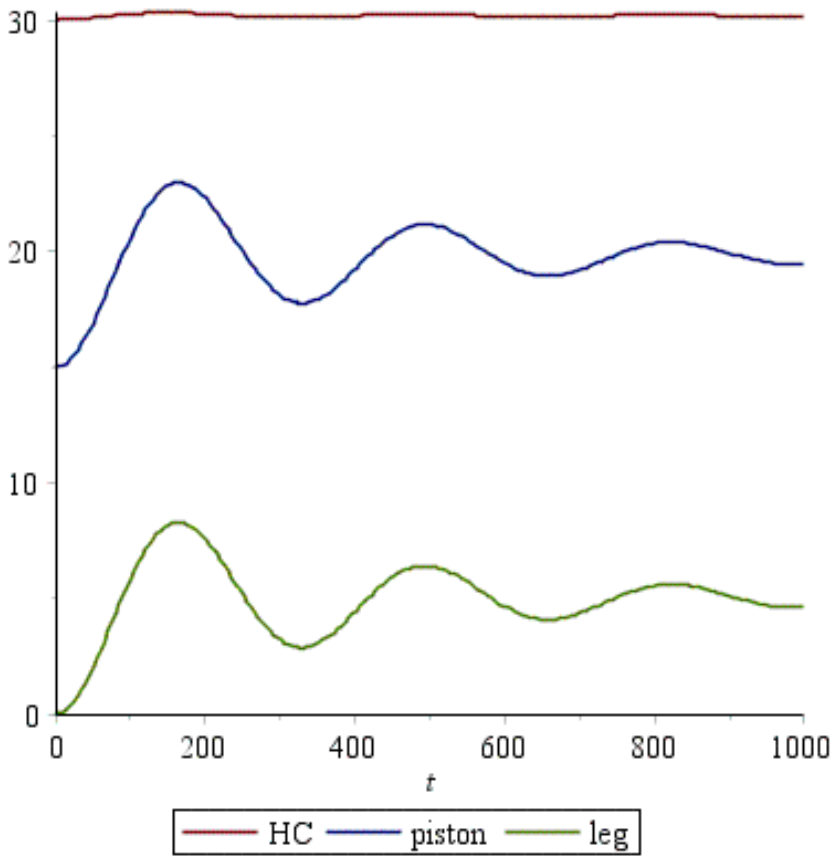


```
>
>
>
```

Appendix E

Compressed gas calculations

Law of Boyle-Gay-Lussac

"Law for ideal gas"

$$\frac{p \cdot V^{\kappa}}{R \cdot T} = C$$

p = Gas pressure (N/m^2)

C = Constant

$$P \cdot V^{\kappa} = \text{Constant}$$

$$T \cdot V^{\kappa - 1} = \text{Constant}$$

$$P_1 \cdot V_1^{\kappa_1} = P_2 \cdot V_2^{\kappa_2}$$

$$T_1 \cdot V_1^{\kappa_1 - 1} = T_2 \cdot V_2^{\kappa_2 - 1}$$

$$P_1 = P_2 \cdot \frac{V_2^{\kappa_2}}{V_1^{\kappa_1}}$$

For very small stepsize $k_1 = k_2$.

The following script is running the Iteration of kappa (in the script: gamma)

```
function [ptb, vtb] = adiabatic_compr_calc(p,V)

ptab=1e5:1e5:500e5;

p_tbv_gamma=[0    5e6   1e7 1.5e7  2e7 2.5e7  3e7  3.5e7 4e7   4.5e7
5e7  1e8  1e15];
gamma_afv_p=[1.4  1.49 1.63 1.82  2.06 2.30  2.54  2.78  3.01  3.22
3.41 4.66 4.66];


for ii = 1:length(p);
    p0 = p(ii);
    V0 = V(ii);

    istart=find(ptab>p0, 1 );
    voltab = zeros(1,length(ptab));
    for i = istart:size(ptab,2)
        if i==istart
            kappa=interp1(p_tbv_gamma,gamma_afv_p,p0);
            voltab(i)=V0*(p0/ptab(i))^(1/kappa);
        else
            kappa=interp1(p_tbv_gamma,gamma_afv_p,ptab(i-1));
            voltab(i)=voltab(i-1)*(ptab(i-1)/ptab(i))^(1/kappa);
        end
    end
    for i = istart-1:-1:1
        if i==istart-1
            kappa=interp1(p_tbv_gamma,gamma_afv_p,p0);
            voltab(i)=V0*(p0/ptab(i))^(1/kappa);
        else
            kappa=interp1(p_tbv_gamma,gamma_afv_p,ptab(i+1));
            voltab(i)=voltab(i+1)*(ptab(i+1)/ptab(i))^(1/kappa);
        end
    end

    vtb(ii,:) = voltab(length(ptab):-1:1);
    ptb(ii,:) = ptab(length(ptab):-1:1);
end


plot(voltab,ptab,'b')
```

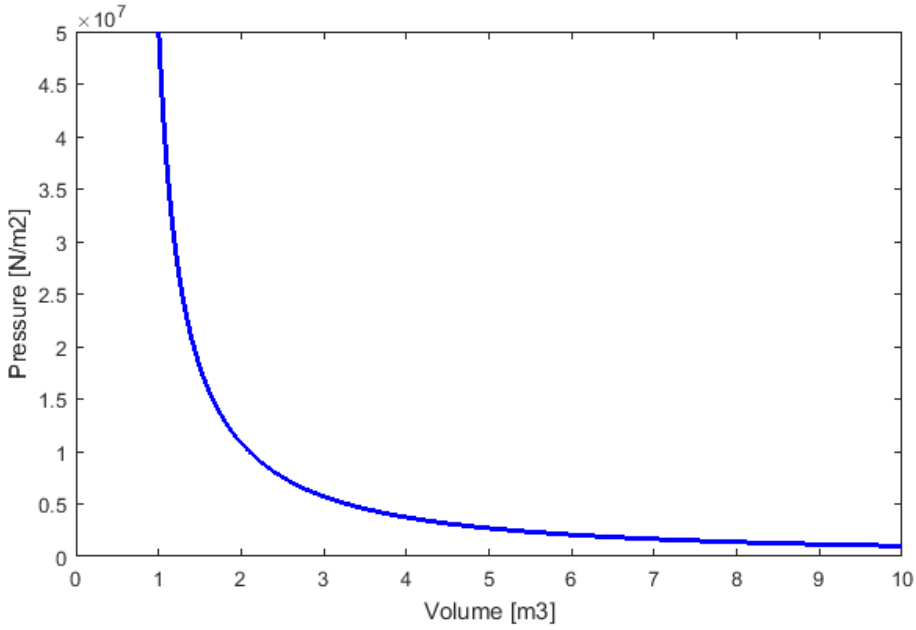


```
clc;
clear all;


%accumulator size
D_acc=0.5;
h_acc=3.5;

dh_acc=10000; %stepsize for p calc
p_acc=10e5 ;%initial pressure in Accumulator

A_acc= pi*(0.5*D_acc)^2;
V_acc=A_acc*h_acc;



% defining stiffness of hydraulic spring

[ptb, vtb] = adiabatic_compr_calc(p_acc,V_acc);


run('P_acc'); %runs P_acc, output is pressure for each heigth of
cylinder
sim('P_acc');
```

```
F_p_acc=p_acc*A_acc;

Fpress_acc=flip(F_p_acc) %pressure increases over height cylinder
%k_pressure = bsxfun(@rdivide, F_p_initial,h_cyl_initial);



h=0.01*h_acc:h_acc/10000:0.9*h_acc; %values of h, of functions (max
= h_acc)
F_press_acc=interp1(h_acc_range,Fpress_acc,h);%function of the
spring Force over height h
k_value_acc=gradient(F_press_acc)%function of k value of spring


figure('name', 'f_press_acc')
plot(h,F_press_acc)
figure('name','k_value_acc')
plot(h,k_value_acc)

k_l_init=mean(k_value_acc) % mean value of k, over height defined in
h
```

Simulink Lookup

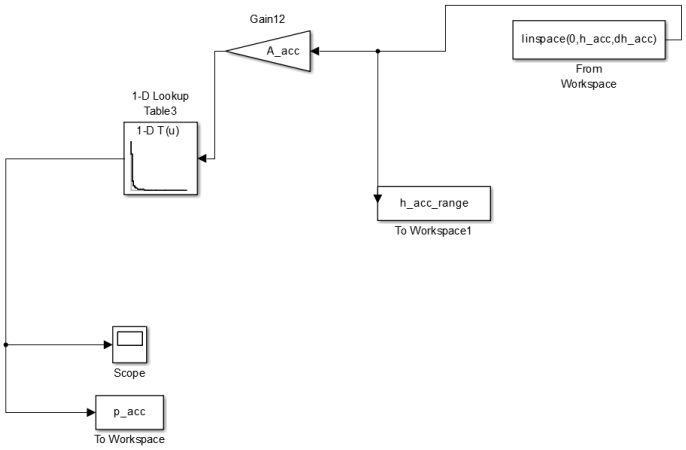

Appendix F

Ccalculation

Pressure drop in piping

$$\Delta p_w = \lambda \cdot \frac{L}{d_i} \cdot \frac{1}{2} \cdot \rho \cdot V_m{}^2$$

Δp_w = Flow resistance

d_i = Internal diameter

ρ = Density of fluid (+/- 900 $\mathrm{kg/m^3}$)

λ = Friction factor

$$\mathrm{d}_i = \sqrt{\frac{4 \cdot Q}{V_m \cdot \pi}}$$

Q = Flow ($\mathrm{m^3/s}$)

$$Q = V_m \cdot A_{pipe}$$

Laminair or turbulent flow

$$\mathrm{Re} = V_m \cdot \frac{d_i}{\upsilon}$$

υ = Viscocity (+/- $5 \cdot 10^{-4} \mathrm{m^2/s}$)

$$\mathrm{Re} < 2320,\ \lambda = \frac{64}{\mathrm{Re}}$$

$$\mathrm{Re} \geq 2320,\ \lambda = \frac{0.3164}{\sqrt[4]{\mathrm{Re}}}$$

Friction coefficient pipe

$$c_{pipe} = \lambda \cdot \frac{L}{d_l} \cdot \frac{1}{2} \cdot \rho \cdot V_m \cdot A_{pipe}$$

$$A_{pipe} = \frac{1}{4} \cdot \pi \cdot D_{pipe}{}^2$$

$$V_m = \dot{u}_2 - \dot{u}_1 \cdot \frac{A_{cyl}}{A_{pipe}}$$

Pressure drop in throttle valve

$$\Delta p = \frac{\rho}{2} \cdot \left(\frac{Q}{c * A_{valve}} \right)^2$$

c = Speed of sound (+/- 1000m/s

ρ = Density of fluid (+/- 900 $\mathrm{kg/m^3}$)

$$A_{valve} = \frac{1}{4} \cdot \pi \cdot D_{valve}{}^2$$

Q = Flow ($\mathrm{m^3/s}$)

$Q = V_m \cdot A$

```
%% input parameters
D_pipe = 0.2;                          %
L = 10;
D_valve = 0.02;
D_cyl = 0.5;

vi = 0.0005;
rho = 900;
c = 1000;

A_pipe = 0.25*D_pipe^2*pi;
A_cyl = pi*(0.5*D_cyl)^2;
A_valve = 0.25*D_valve^2*pi;

%u_vel = 10;
u_vel = linspace(0.001,10,1000); %different velocities
V_m = u_vel.*(A_cyl/A_pipe);
V_m_valve = u_vel.*(A_cyl/A_valve);
Q_pipe = V_m.*A_pipe;
Q_valve = V_m_valve.*A_valve;
d_i = ((4.*Q_pipe)./(V_m.*pi)).^0.5;

%laminair of turbulent
Re= V_m.*(d_i./vi);

if  Re < 2320 , labda = 64./Re  ;
else Re >= 2320 , labda=0.3164./((Re).^0.25);
end

% pressure drop in pipe
c_pipe = labda.*L./d_i*0.5*rho.*V_m.*A_pipe;
%figure('name','c_pipe')
%plot(u_vel,c_pipe)

% pressure drop in valve
c_valve = ((rho/2)*(Q_valve/(c*A_valve)).^2*A_cyl)/u_vel;
C_val=linspace(c_valve,c_valve,1000);
%figure('name','c_valve')
%plot(u_vel,C_val)


c_tot= c_valve+c_pipe;
figure('name','c_tot')
plot(u_vel,c_tot,u_vel,C_val,u_vel,c_pipe)
```

Appendix G

Hoist Cable stiffness calculation

Schematic overview of hoist configuration

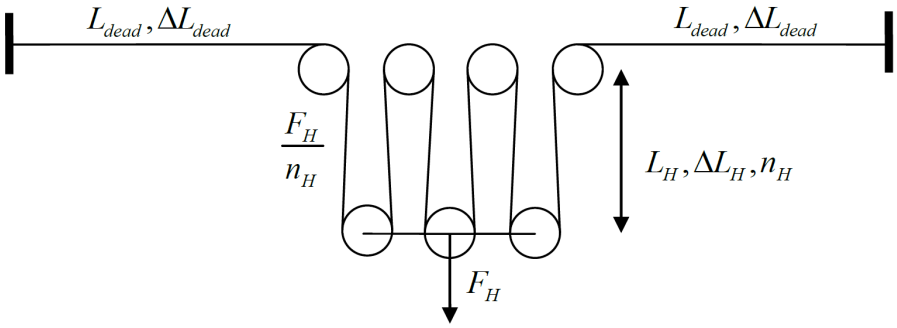

According to Hooks law the elongation of the dead wire is given as follows:

$$\Delta L_{dead} = \frac{F}{K} = \frac{F_H}{n_H} \cdot \frac{L_{dead}}{EA}$$

With:

$$F = \frac{F_H}{n_H}$$

$$k = \frac{EA}{L_{dead}}$$

For every hoist wire part the elongation has to be taken including the contribution of the ΔL_{dead} of the dead wires.

$$\Delta L_H = \frac{F}{k} + \frac{2 \cdot \Delta L_{dead}}{n_H} \text{ with } F = \frac{F_H}{n_H} \text{ and } k = \frac{EA}{L_H}$$

$$\Delta L_H = \frac{F}{n_H}\cdot\frac{L_H}{EA}+\frac{2}{n_H}\cdot\left(\frac{F}{n_H}\cdot\frac{L_{dead}}{EA}\right)$$
$$=F_H\cdot\left(\frac{L_H}{n_H\cdot EA}+\frac{2\cdot L_{dead}}{n_H^2\cdot EA}\right)$$
$$=F_H\cdot\left(\frac{1}{k_H}+\frac{1}{k_{dead}}\right)$$
$$=F_H\cdot\left(\frac{1}{k_{eq}}\right)$$

The equivalent stiffness of the total system then yields in:

$$k_{eq}=\frac{k_H\cdot k_{dead}}{k_H+k_{dead}}=\frac{\frac{n_H\cdot EA}{L_H}\cdot\frac{n_H^2\cdot EA}{2\cdot L_{dead}}}{\frac{n_H\cdot EA}{L_H}+\frac{n_H^2\cdot EA}{2\cdot L_{dead}}}=\frac{EA\cdot n_H^2}{n_H\cdot L_H+2\cdot L_{dead}}$$

With:

k_{eq}, k_H, k_{dead} = Equivalent stiffness, hoist wire, dead wire stiffness $[N/m]$
L_H, L_{dead} = Lenght of hoist wire, dead wire $[m]$
$\Delta L_H, \Delta L_{dead}$ = Elongation of hoist wire, dead wire $[m]$
n_H = Number of reevings of the hoist wire configuration [-]
EA = Effective wire rigidity $[N]$

To calculate the stiffness of the hoist configuration k_1 the following parameters are used:

EA	$2.8 * 10^8$	[N]
n_H	34	[-]
L_H	110	[m]
L_{dead}	150	[m]

This results in a stiffness $k_1 = 8.01 * 10^7$ [N/m]

Calculation of k_2

$$k_{eq} = \frac{EA}{L_H}$$

EA	2.8 *10^8	[N]
n_H	20	[-]
L_H	25	[m]

This results in a stiffness of k_2 = 2.24 *10^8 [N/m]